UNIVERSITÀ
DEGLI STUDI
DI PADOVA

Administrative unit: **University of Padova**

Department: **Land, Environment, Agriculture and Forestry (TESAF)**

PHD PROGRAM: **Land, Environment, Resources and Health (LERH)**

Batch: **XXX**

HYDROLOGICAL AND GEOMORPHOLOGICAL ANALYSIS OF HEADWATER BASINS CAUSING THE DEBRIS FLOW TRIGGERING

PhD Program Coordinator: Prof. Davide Matteo Pettenella

Supervisor: Prof. Vincenzo D'Agostino

PhD candidate: Roberta Pastorello

UNIVERSITÀ
DEGLI STUDI
DI PADOVA

Sede Amministrativa: **Università degli Studi di Padova**

Dipartimento: **Territorio e Sistemi Agro-Forestali (TESAF)**

CORSO DI DOTTORATO: **Territorio, Ambiente, Risorse e Salute (TARS)**

Ciclo: **XXX**

ANALISI IDROLOGICA E GEOMORFOLOGICA DEI BACINI DI TESTATA IN CUI AVVIENE L'INNESCO DI COLATE DETRITICHE

Coordinatore: Prof. Davide Matteo Pettenella

Supervisore: Prof. Vincenzo D'Agostino

Dottoranda: Roberta Pastorello

Summary

List of figures

List of tables

Abstract

The main subject of the present thesis is the triggering of debris flows, which has been studied from a geomorphological and from a hydrological point of view. The thesis is a compilation of three papers, each one focused on a specific part of the triggering mechanism. In fact, debris flows are dangerous events, typical of mountain territories all over the world and they necessitate the concurrence of many variables to be triggered. In the last decades, different studies stated that the main variables involved in the initiation of a debris flow are: terrain slope, water input and sediment availability. If these factors exceed some specific critical thresholds, the probability of a debris flow triggering can be very high. However, the fact that so many variables are involved makes these events difficult to forecast.

In the present study, we analysed different aspects related to the triggering probability. For this reason, the thesis is composed of three different papers: (1) Chapter 2, titled "On the criteria to create a susceptibility map to debris flow at a regional scale"; (2) Chapter 3, titled "Correlation between the rainfall, sediment recharge and triggering of torrential flows in the Rebaixader catchment (Pyrenees, Spain); (3) Chapter 4, titled "Rainfall durations and corresponding dominant mechanism for the initiation of debris flows in three basins characterized by different geomorphological settings".

In Chapter 2, we analysed the geomorphological variables of the catchments that have the most important role in the triggering of debris flows. We used a model named Flow-R that works at a regional scale (allowing to analyse an entire valley) to study the potential triggering areas, neglecting the hydrological part of the mechanism. In fact, starting from a real case study (event of 4th August 2012), we used the collected data regarding the triggering and deposition areas to model the debris flow event. We analysed the morphological parameters that had better discriminate the potential triggering areas from the zones in which the erosion and slope failure are highly improbable.

In Chapter 3, we studied the two triggering variables related to water input and sediment recharge. In this case, we focused on: (1) rainfall, investigating its influence on the triggering of debris flows and on the accumulation and mobilization of sediments; (2) sediment availability, considering the registered debris flow volumes as the previously available sediment quantity inside the triggering area, in the period before the triggering of the event. The analysed catchment is in the Spanish Pyrenees and it is a good case study because since summer

2009 it has been equipped with a monitoring station (rain gauges, piezometers, video cameras, geo-phones). Therefore, the rainfall datasets registered with a time interval of 5 minutes inside the catchment are relatively long and allows to study potential correlations between the water input and the sediment mobilization. We searched if there are any correlations between the volume of the triggered event and the total precipitation of the recharge period (the period between the considered debris flow and the previous one). We then analysed the correlations between the maximum rainfall intensities of the triggering rainfall events and the volume of the debris flows. Finally, we used a parameter called "rainfall erosivity" that, calculated for each rainfall event, considers at the same time the total precipitation, the maximum intensity and the kinetic energy of the rain. This parameter has been calculated using two different time scales: (1) for the single triggering rainfall event; (2) as the sum of all the rainfall events happened during every recharge period. The results are interesting because it is clear that rainfall scarcely influences the quantity of the mobilized sediment, evidencing that there are other important variables involved in this mechanism. Whereas, the triggering or non-triggering of a debris flow is strongly dependent on the rainfall erosivity of the triggering rainfall event.

After these two analyses, made at the regional scale and at the basin scale, in Chapter 4 we went more in the detail, focusing on the headwater basins (the upper parts of debris flow catchments). We analysed three study areas: (1) the headwater basin of Rio Rudan, located in the south side of Mount Antelao (Italian Dolomites); (2) the headwater basin of Rio Chiesa, located in the south side of Col di Lana (that is also located inside the dolomitic region, but it is characterized by a different geology, mainly composed of volcanic and sedimentary rocks); (3) the headwater basin of Rio Rebaixader, located in the Spanish Pyrenees (mainly composed of metamorphic rocks). In each headwater basin, we extracted three control cross sections along the channel network. For every cross section we calculated the critical triggering discharge for the debris flow initiation using the formulas of Gregoretti and Dalla Fontana (2008) and of Whittaker and Jaggi (1986). Then, we made some hydrological simulations using the software FLO-2D, using as water input different hyetographs created using the Intensity-Duration equations of Gregoretti and Dalla Fontana (2007) and of Cannon and Ellen (1985). These simulations allowed us to verify which is the minimum rainfall duration (related to the corresponding rainfall intensity) needed to reach the critical discharge in the control cross sections. To test also the possible shallow slope failure triggering mechanism, we also made a slope stability analysis in the three initiation areas, using the geotechnical parameters derived from the analysis

of terrain samples collected inside the headwater basins. These two different analysis gave an overall view on the mechanism of mobilization of sediments in the analysed areas. The results show that the critical discharges in the three basins are comparable, whereas the slope stability analysis evidences some differences between the basins. In fact, Rio Rudan resulted generally more stable than the two other basins, even with high saturation conditions of the terrain. This can mean that in this basin the principal triggering mechanism is the “channel-bed failure”, whereas in the two other basins mechanisms of “shallow slope failure” are also probable.

Riassunto

La seguente tesi è stata sviluppata in forma compilativa, come raccolta di articoli. Il filo conduttore di tutto il manoscritto è l'analisi del fenomeno di innesco di colate detritiche. Questo tipo di eventi, tipico di zone montane di tutto il mondo, necessita della concomitanza di particolari fattori per poter accadere. Negli ultimi decenni, differenti studi a riguardo, hanno dimostrato che tra le principali variabili in gioco nel determinare l'innesco di una colata, ci sono: la pendenza del terreno, una sufficiente quantità d'acqua e una certa disponibilità di sedimento nell'area sorgente che possa venire mobilizzata. Questi fattori, quando concomitanti sopra ad una certa soglia limite, determinano una elevata probabilità di innesco di un fenomeno di colata detritica. Il fatto però che ci siano in gioco molte differenti variabili, rende questi meccanismi molto difficili da comprendere e predire con estrema esattezza.

In questo studio, si è cercato di analizzare tutti gli aspetti legati alla probabilità di innesco per dare un quadro complessivo del fenomeno, prendendo in considerazione differenti variabili in differenti aree di studio. Per questo motivo la tesi è strutturata in tre parti distinte: ad un primo capitolo introduttivo in cui viene presentato il fenomeno di colata detritica nella sua interezza, segue il Capitolo 2, intitolato "On the criteria to create a susceptibility map to debris flow at a regional scale". In questa parte della tesi, vengono analizzate le variabili geomorfologiche del terreno che incidono maggiormente nel possibile innesco di una colata detritica. Utilizzando un modello chiamato Flow-R che lavora a scala regionale (permettendo di analizzare un'intera vallata e non solamente singoli bacini), si è trascurata la parte idrologica del fenomeno concentrandosi sulla morfologia del terreno. Partendo infatti dai dati reali (dati di pioggia, volumi di colate, mappatura delle aree di innesco e delle aree di deposito) misurati durante e successivamente l'evento del 4 agosto 2012 che ha interessato l'intera Val di Vizze (Provincia di Bolzano) si è cercato di ricostruire nel modo più verosimile l'innesco e la propagazione di colate nel territorio analizzato, cercando di trovare i parametri morfologici che permettessero di discriminare accuratamente le possibili aree sorgenti dalle zone in cui invece l'erosione e l'innesco sono altamente improbabili.

Proseguendo con il Capitolo 3 della tesi, denominato "Correlation between the rainfall, sediment recharge and triggering of torrential flows in the Rebaixader catchment (Pyrenees, Spain)" si è invece passati ad analizzare le due variabili pioggia e quantità di sediment, legate all'innesco di colata detritica. In questo caso, a differenza della precedente analisi, ci si è

concentrati: (1) sulla pioggia, analizzando se questa influisca non solo nel determinare lo switch innesco si/innesco no, ma provochi degli effetti anche sull'accumulo e/o mobilizzazione dei sedimenti nelle aree di innesco; (2) sulla quantità di sedimento disponibile per un eventuale innesco di colata, considerando i volumi detritici registrati come il sedimento disponibile, nell'area di innesco, durante il periodo pre-colata. Il bacino analizzato in questa seconda parte della tesi, si trova nei Pirenei spagnoli ed è un ottimo caso studio in quanto fin dall'estate 2009 è stato equipaggiato con una stazione di monitoraggio che comprende pluviometri, geofoni, piezometri e videocamere. La serie storica dei dati di pioggia, che viene registrata con un intervallo temporale di 5 minuti, è quindi relativamente ampia. Inoltre, essendo questo un bacino caratterizzato da un'elevata frequenza di fenomeni di colata detritica e di correnti iperconcentrate, si è avuta a disposizione una serie di una ventina di eventi (con relativo volume di detriti) registrati sempre a partire dall'estate 2009. Una serie di dati di questo tipo, permette quindi di effettuare analisi molto più approfondite rispetto a quelle che si possono fare in singoli bacini non costantemente monitorati in cui ci si limita a prendere in considerazione le giornate caratterizzate da eventi di colata. Si è quindi studiato se ci fosse correlazione tra il volume dell'evento innescato e la quantità di pioggia caduta nel periodo trascorso tra l'evento di colata stesso e il precedente (questo viene denominato in letteratura "periodo di ricarica"). Si sono successivamente verificate le eventuali correlazioni tra l'intensità massima degli eventi di pioggia del periodo di ricarica e il volume del successivo evento innescato. Per fare uno studio più complesso si è deciso di utilizzare una variabile denominata "rainfall erosivity", questo parametro calcolato per ogni evento di pioggia registrato, mette insieme la quantità totale di precipitazione misurata con l'energia cinetica della pioggia stessa, calcolata utilizzando la massima intensità media nella mezz'ora. Con questo parametro si è differenziato tra la pioggia totale caduta durante il periodo di ricarica e la pioggia del singolo evento innescante. I risultati ottenuti sono molto interessanti, infatti risulta chiaro come la pioggia abbia un'influenza relativamente scarsa sull'accumulo di sedimenti e sulle quantità mobilizzate, dimostrando come queste quantità siano influenzate da altre variabili in gioco, mentre l'innesco o il non innesco di una colata è fortemente dipendente dall'energia dell'evento di pioggia che si verifica sul bacino.

Dopo aver svolto una prima analisi a scala regionale e una seconda a scala di singolo bacino, nel Capitolo 4 si è entrati ancora più nel dettaglio, prendendo in considerazione solamente il sottobacino di testata. In questo capitolo, intitolato "Rainfall durations and corresponding

dominant mechanism for the initiation of debris flows in three basins characterized by different geomorphological settings", sono state analizzate tre differenti aree studio: (1) il sottobacino del Rio Rudan, che si trova nel versante meridionale del Monte Antelao, in pieno territorio dolomitico; (2) il sottobacino del Rio Chiesa, posto sul versante meridionale del Col di Lana, caratterizzato da una geologia differente rispetto al primo, composta da una mescolanza di rocce vulcaniche e sedimentarie; (3) il sottobacino del Rio Rebaixader, che si trova nei Pirenei spagnoli ed è composto principalmente da rocce metamorfiche.

In ognuno dei tre sottobacini, sono state estratte tre sezioni di controllo, lungo la rete idrografica, e per ognuna di esse sono state calcolate le relative portate critiche di innesco di colata detritica utilizzando le due formule di Gregoretti e Dalla Fontana (2008) e Whittaker e Jaggi (1986). Successivamente in ciascuno dei sottobacini, utilizzando il software di modellazione FLO-2D, sono state effettuate diverse modellazioni idrologiche utilizzando come input di pioggia, differenti pluviogrammi creati utilizzando le equazioni di Intensità-Durata sviluppate da Gregoretti e Dalla Fontana (2007) e da Cannon e Ellen (1985). Queste indagini hanno permesso di verificare quale sia la durata minima di pioggia (legata alla corrispondente Intensità soglia) necessaria per raggiungere la portata critica di innesco nelle sezioni di controllo analizzate. Per completare lo studio sul meccanismo d'innesco nei tre sottobacini analizzati, è stata fatta anche un'analisi di stabilità di versante, utilizzando i parametri geotecnici derivanti da campioni di suolo prelevati nelle aree di innesco. Queste due analisi danno insieme una visione complessiva del modo in cui le colate detritiche si sviluppino nelle aree analizzate. I risultati mostrano infatti come, in tutti e tre i sottobacini, le portate critiche di innesco siano comparabili come grandezza, mentre le analisi si stabilità di versante evidenziano come il bacino del Rio Rudan sia mediamente più stabile rispetto alle altre due aree, anche in condizioni di elevata saturazione del suolo. Questo fa pensare che in questo bacino il meccanismo di innesco più probabile sia il cosiddetto "channel bed failure", mentre negli altri due bacini ci sono sicuramente anche fenomeni di "shallow slope failure" che avvengono nelle aree dissestate di versante portando grandi quantità di detriti all'interno del reticolo idrologico.

1 Introduction

Hungr et al. (2013, p. 183) describe a debris flow like "a very rapid to extremely rapid surging of saturated non-plastic debris in a steep channel". Because of the increasing expansion of human settlements in unstable mountainous areas, due to the economic development of the last century (Fuchs et al. 2008), this type of mass movement, formed by water, air and sediment, has become one of the most dangerous threats for alpine valleys (Cavalli and Grisotto 2006).

In the last decades, many studies about the characteristics of the deposition area and about the behaviour of the flow in the alluvial fan have been published (Bardou et al. 2007; Scheidl and Rickenmann 2010), but lesser attention has been given to the initiation zone and to the triggering mechanism. Although the deposition process of the phenomenon is the one that causes the principal damages, it is of primary importance to study the upper part of catchments to understand the triggering mechanism in order to be able to predict this type of events (D'Agostino and Bertoldi 2014).

There are two main types of debris flow triggering: (1) shallow slope failure, when a shallow landslide, after a rapid infiltration of water in the superficial soil layers, develops in a debris flow; (2) channel-bed failure, when the debris flow generates from the erosion of the channel bed and of the channel banks, caused by the superficial runoff. This last type of debris flow is less studied and understood compared to the first one (Tognacca and Bezzola 1997; Cannon et al. 2004; Berti and Simoni 2005; Gregoretti and Dalla Fontana 2008). In both cases, precipitations play an important role. Berti and Simoni (2005) argue that a debris flow can be triggered by three different types of meteorological conditions: (1) short and intense thunderstorms following a relatively long dry period; (2) less intense thunderstorms following a sustained period of weak rainfall; or (3) thunderstorms of low intensity following a long period of rainfall.

According to Takahashi (1981) and Rickenmann and Zimmermann (1993) the triggering of a debris flow depends on the combination of three principal conditions: water input, terrain slope and sediment availability (Horton et al. 2013). The first one depends on the characteristics of rainfalls that generate the surface runoff and in the last years different studies have focused on this subject (Bacchini and Zannoni 2003; Berti and Simoni 2005; Guzzetti et al. 2007; Floris et al. 2010; Gregoretti and Degetto 2012). The second and the third are related to the topographical

and morphological characteristics of the catchment area and are much less studied. Different authors (Imaizumi et al. 2006; Marchi et al. 2008) point out that few studies are focused on the morphology of rock headwater basins and particularly on the shape and extension of the channel network in the initiation zones. In a recent study, Legg et al. (2014) found significant differences in the morphology of the channel network between debris flow basins and non-debris flow basins. This confirms the importance of a topographic and morphological analysis of the headwater basins to understand the debris flow genesis.

The tendency of the superficial runoff to mobilize the debris located in channels and the consequent debris flow triggering depends also on the characteristics of the sediments (Gregoretti and Dalla Fontana 2008). In fact, sediment availability is one of the most important factors related to the triggering mechanism. The catchments prone to debris flows are tipically distinguished in two types: transport-limited systems (supply-unlimited) influenced by the sediment transport capacity; weathering-limited system (supply-limited) influenced by sediment availability (Bovis and Jakob 1999). In this last type, between two debris flow events, there is usually a longer time interval compared to the first type of basins. The supply-limited systems, after every event, need to "recharge" the sediments up to a specific threshold. For this reason, the same rainfall conditions can trigger a debris flow only if the sediment quantity exceedes the recharge threshold. Brayshaw and Hassan (2009) recently proposed a new version of the weathering-limited system. They analyzed the sediment recharge in gullies and from their results it seems that the recharge threshold is not constant. It increases with the increasing of the sediment quantity in the channel. This means that small shallow landslides can easily trigger a debris flow when the debris recharge in channel is low. On the contrary, if the sediment recharge is high, the initial failure that could trigger the debris flow has to be larger.

1.1 Definition and classification of debris flow

Debris flows are among the most dangerous natural hazards in mountainous areas. They are a specific type of mass flow that can be distinguished from other types of landslides for some peculiar characteristics. Debris flows are mixed masses formed by rocks, mud, water and air. Their movement depends on channel slope, flow characteristics, channel shape and volumetric concentration. This last is higher than that of debris flood or bedload transport events, and for this reason their behaviour cannot be compared to that of clear water. Different volumetric

concentration ranges have been proposed for debris flows (Beverage and Culbertson 1964; Takahashi 1981; Costa 1984). The most common range is between 20% and 70%.

Debris flows have a typical wave form with a front, a body and a tail (Figure 1.1). Granular debris flows, characterized by the presence of large debris, have a specific wave form with the front higher than the rest of the body. This happens because larger boulders and woody debris are usually located in the front. Ancey (2001, p. 533) stated that "in some cases no front is observed because either it has been overtaken by the body or the materials are well sorted […]". Muddy debris flows have a typical wedge front shape without a real selection of sediments. Finally, in muddy debris flows that move on a smoothed channel, the front develops a typical form with a raised crest higher than the following body.

The body is the larger part of the debris flow wave and it transports debris of any size, from boulders to little mud particles. Finally, the tail has a lower solid concentration than the rest of the wave. It is characterized by small particles and has a flowing behaviour more similar to that of debris floods.

A debris flow event can last from several minutes to about an hour. During this period, it is common to observe different pulses. In fact, usually an entire event is constituted of several debris flow waves. The velocities that the flow can reach depend on the characteristics and on the morphology of the channel. A typical range is between 1-2 m/s to 10-12 m/s. The fastest observed debris flows reached velocities of about 20 m/s.

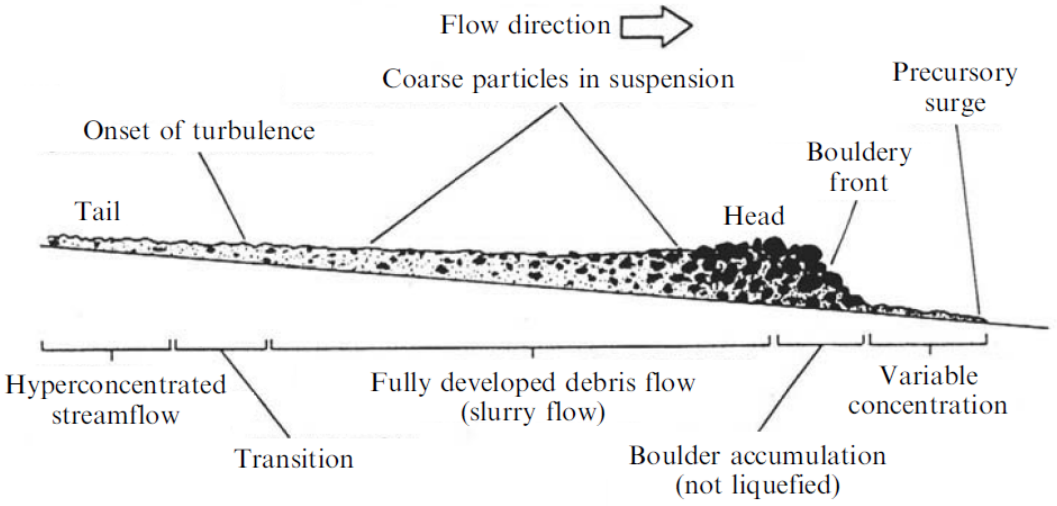

Figure 1.1: Shape of a typical debris flow wave (from Pierson 1986).

To clarify the distinction among the different types of torrential flows affecting mountain torrents and to use a common terminology, many classifications have been proposed in the last decades.

Among the first proposed classifications, one of the most important and widely used is that of Varnes (Varnes 1954, 1978; Cruden and Varnes 1996). He defines a debris flow like a rapid mass movement formed by solid granular material, water and air that behaves like a viscous fluid. Also Pierson and Costa (1987) proposed a well-known classification based on the rheological characteristics of the flow. Whereas, another important classification is that of Coussot and Meunier (1996) that developed a classification based on the solid fraction and on the material type distinguishing between: stream flows, hyper-concentrated flows, mudflows, debris flows, granular flows, debris avalanches and landslides.

Hungr et al. (2013) recently proposed a revised and updated version of this classification, posing particular attention to the terminology. They distinguish the different types of movements: fall, topple, slide, spread and flow (Cruden and Varnes 1996) and also the type of material involved in the landslide: rock, clay, mud, silt sand gravel and boulders, debris, peat and ice. A summary of all the types of mass movements described in this classification is given in Table *1.1*.

Another classification extensively used and cited is that of Ancey (2001). This is simpler than the previous one and concerns only with the different types of debris flows. It is based on the mechanical behaviour and on the rheological characteristics of the flow. The author distinguishes three debris flow types:

- Muddy debris flows: they are fluxes of the viscous-plastic type, and their behaviour is well represented by the Bingham model or by the pseudo-plastic model, in the case of higher clay content. This type of debris flow is formed by a great quantity of sediment of unsorted dimensions, and the matrix is formed by clay material. They stop with slopes about 5-6% and the deposits are lobate with well defined margins.
- Granular debris flows: they are characterized by a collisional- frictional behaviour. They have low quantity of matrix and many sediments of great dimensions. This type of debris flows stops at higher slopes than the previous type, about 15-20%. The deposit shape is irregular, without well defined margins.
- Lahar-like debris flows: they are also called fluid debris flows and exhibit a frictional-viscous behaviour. At low velocities, they have higher friction stresses between

particles. Whereas, at higher velocities they behave similarly to a Newtonian fluid. They are composed by a high content of matrix with great silt quantity and low gravel and clay quantity. These types of debris flow are very dangerous because they stop only at slopes about 1% and form flat deposits.

Table 1.1: Summary of the new version of the classification system, proposed by Hungr et al. (2013).

Type of movement	Rock	Soil
Fall	1. Rock/ice fall	2. Boulder/debris/silt fall
Topple	3. Rock block topple 4. Rock flexural topple	5. Gravel/sand/silt topple
Slide	6. Rock rotational slide 7. Rock planar slide 8. Rock wedge slide 9. Rock compound slide 10. Rock irregular slide	11. Clay/silt rotational slide 12. Clay/silt planar slide 13. Gravel/sand/debris slide 14. Clay/silt compound slide
Spread	15. Rock slope spread	16. Sand/silt liquefaction spread 17. Sensitive clay spread
Flow	18. Rock/ice avalanche	19. Sand/silt/debris dry flow 20. Sand/silt/debris flowslide 21. Sensitive clay flowslide **22. Debris flow** 23. Mud flow 24. Debris flood 25. Debris avalanche 26. Earthflow 27. Peat flow
Slope deformation	28. Mountain slope deformation 29. Rock slope deformation	30. Soil slope deformation 31. Soil creep 32. Solifluction

1.2 Morphology of debris flow catchments

A debris flow cachment is charaterized by some specific morphometric variables. Marchi and D'Agostino (2004), using data collected from 127 basins, showed three important variables that can be used to discriminate debris flow catchments from non-debris flow catchments. (1) The area of the basin is usually lower than 15 km^2 and (2) the channel length does not exceed 8 km. In fact, the more the catchment is large, the more the material is diluted along the channel and it becomes very difficult to observe the formation of an alluvial fan. (3) The third important

indicator is the channel slope: usually the slope range for the mobilization of a debris flow is between 20-70%.

Another important discriminating variable is the Melton number. This is the ratio between the elevation difference from the higher point to the lower point of the catchment and the square root of the catchment area. This index gives a good overview on the type of flow dominating the basin (D'Agostino 1996).

A debris flow basin is tipically divided in three parts: initiation zone, transport zone and deposition zone (Figure 1.2).

- The initiation zone (Figure 1.2) is usually characterized by a very high slope gradient and by the presence of loose debris that can be easily mobilized by a water runoff. The sediment recharge depends on the rock type and on the topography of the slope. The erosional processes that cause the recharge of material can be slow but continuous, causing a great annual accumulation, or in other cases there can be old non-consolidated deposits (Ancey 2001). In the initiation area are located also the channel heads. The usual point in which it can be observed the starting of a gully is on the scree slopes at the base of steep rock faces (Gregoretti and Dalla Fontana 2008). Initiation areas characterized by a steep slope gradient have a smaller superficial extent than areas with lower slope gradient. For this reason, the first type of areas are characterized by a more dissected morphology, with a greater number of gullies (Montgomery and Dietrich 1988).
- The transport zone (Figure 1.2) is the central part of the catchment. It is characterized by the presence of the main channel and other secondary channels. This can be a very active part of the catchment. In fact during a debris flow event, the channel can be eroded by the flow, contributing to increase the total sediment volume. The channel can be incised to several meters during intense debris flow events. The most stable parts of the transport zones are the reaches incised until the bedrock. This part of the catchment is usually characterized by steep slopes. In fact, the flow does not stop here but it is transported to the next part of the catchment. In some cases, there can be the formation of lateral deposits on the channel banks.
- The deposition zone (Figure 1.2) usually corresponds to the alluvial fan. This part of the catchment is characterized by a different morphology than the previous ones. In fact, it has lower slope gradients and for this reason the flow normally stops here. On the fan,

the flow is no longer confinated, but spreads on a wider area and reaches a certain runout distance. The sudden stop of the debris flow front can cause an increase of the flow depth in the debris flow body (Ancey 2001). The morphology of the deposits varies with the different types of flows: muddy debris flows usually show lobate deposites. Whereas, granular debris flows are more eterogeneous, with the presence of big boulders (VanDine 1996). The deposit of the flow is influenced by the slope gradient: Barbolini (2008) suggested a threshold value of 10-15° for non-confinated debris flows and 4-8° for confinated debris flows.

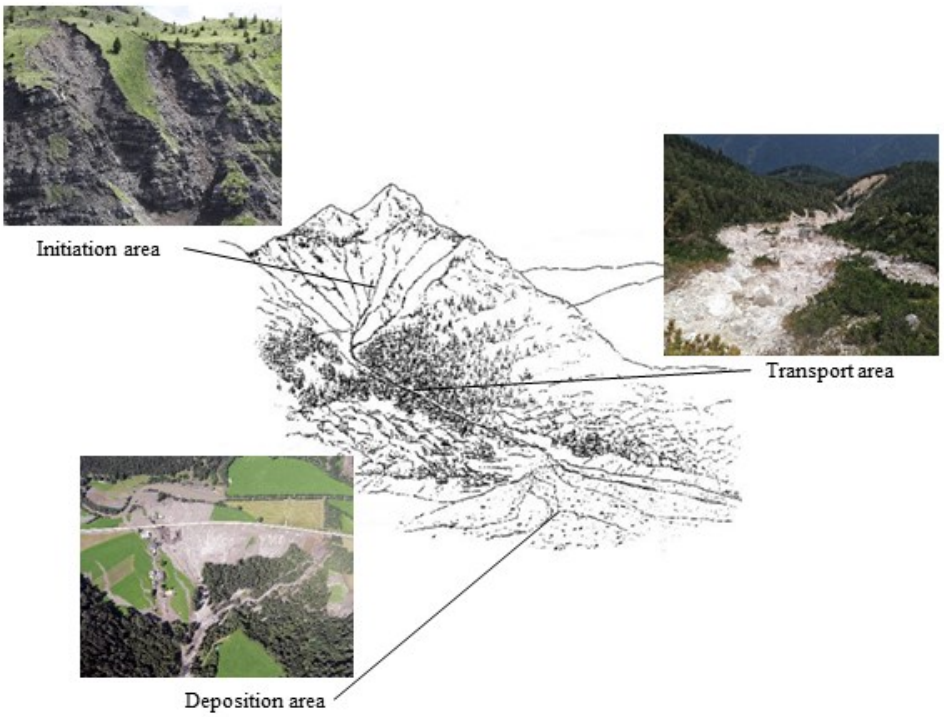

Figure 1.2: A Typical debris flow basin (from Ancey 2001).

1.3 The triggering mechanism

The triggering areas are located in the upper parts of the headwater basins. These areas are characterized by a high slope gradient and are usually covered by deposits of loose debris that can be easily mobilized by a certain water discharge because they are in a state close to their critical friction angle.

The triggering areas can be located below the intersection between two or more sub-surficial flows (rills or little gullies) in where the water input is usually higher. The triggering areas can be also located in the scree slopes located below the rock faces (typical of the dolomitic region). These great debris deposits, during intense meteoric events, can be mobilized by water flows coming from the overhead couloirs incised in the rock faces.

Rickenmann and Zimmermann (1993) and Takahashi (1981) stated that there are three critical factors that combined together lead to the triggering of a debris flow. These are: (1) sediment availability, (2) slope gradient and (3) water input.

(1) Sediment availability is of course an important variable. Bovis and Jakob (1999) distinguish two types of debris flow catchments: transport-limited basins in which the triggering is influenced by water content. In fact, the morphological characteristics of these basins lead to an unlimited sediment recharge. The second type of catchments is called weathering-limited system. In this case, the basin is not characterized by an unlimited sediment availability, but the triggering happens only if, with the same water discharge, the sediment volume exceeds a specific threshold value. These type of basins have a certain sediment recharge, that depends on different variables related to the characteristics of the triggering areas: geology, dimension (usually larger basins have higher sediment quantities) and also vegetation (Jakob et al. 2005). In fact, forested watersheds show a higher recharge because the presence of woody debris contribute to form log-jams that facilitate sediment accumulation. The sediment recharge increases rapidly right after a debris flow event, but after some years (8-10) the sediment recharge abruptly decreases. Dhakal and Sidle (2003) Guthrie (2002) and Swanston and Swanson (1976) found that failures that cause the triggering of debris flows are more frequent after a forest cut. In fact, recently logged basins are characterized by more frequent but less strong debris flows.

   Studying many supply-limited systems Brayshaw and Hassan (2009) observed that gullies that experienced recent debris flows, having for this reason a lower sediment quantity, have a higher probability of a new debris flow triggering, if compared to gullies that already accumulated a high sediment recharge. This behaviour causes a “cycle-mechanism” in which stability favours stability and viceversa. The sediment threshold value to be reached for the debris flow triggering is not constant, but increases in time (Figure 1.3).

   Comparing the sediment volume of the source areas with the volume effectively transported downstream, it can be seen that generally, catchments have a low sediment transport

capacity (Fryirs 2013). For this reason, it is important to study the sediment volume of the source areas (D'Agostino and Bertoldi 2014), but also the connectivity of these zones with the channel network. A debris talus with a high sediment volume can be of "no use" if it is totally disconnected from the channels. Cavalli et al. (2013) proposed a topographic index that shows the potential sediment transport inside the catchment from the triggering areas to the channel network. This index does not take into account of processes such as rock falls, landslides ore snow avalanches, and it neglects the role of vegetation and the extension/location of the source areas. However, it is a relatively simple method to characterize the attitude of the different parts of the catchment to mobilize the sediments.

(2) The slope gradient is the second important triggering factor. This characteristic involves the triggering areas and the channel network. In fact, some reaches of the channel can often behave like source areas because the water flow erodes the bed and the banks mobilizing a large sediment quantity. A channel can be eroded to the bedrock, critically varying its morphology. Legg et al. (2014) suggested that channels with a loose sediment bed become more stable through time. In fact, their slope tends to decrease, and so a higher discharge is needed to mobilize the sediments of the channel bed.

(3) The water input is the third critical triggering factor. This is one of the most studied variables, in fact many studies focus on the rainfall thresholds linked to the debris flow triggering (Bacchini and Zannoni 2003; Berti and Simoni 2005; Gregoretti and Degetto 2012). Sidle et al. (1985) related Caine's (1980) critical triggering threshold with the cumulated rainfall curve necessary to saturate soil. The result shows that intense cumulative rainfalls not close to the ones needed to saturate soil, can trigger a debris flow for a duration lower than 24 hours. Whereas, for rainfall durations longer than 24 hours the triggering mechanisms derives by terrain saturation.

The water input that triggers a debris flow usually derives from heavy summer storms. The meteorological factors can be distinguished in primary (e.g. storms or snow melt) and secondary (e.g. antecedent rainfalls) (Wieczorek and Glade 2005). However, also other types of phenomena like for example a natural dam-break or the break of a hydraulic pipe can trigger a debris flow.

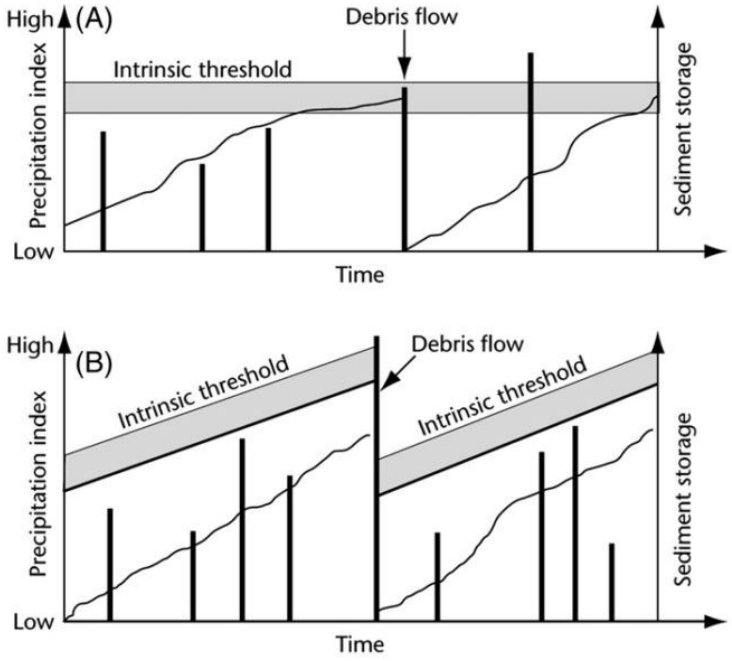

Figure 1.3: Revision of the sediment volume threshold proposed by Bovis and Jakob (1999) (A) revised by Brayshaw and Hassan (2009) (B) from Brayshaw and Hassan (2009).

1.4 The different types of debris flow triggering

There are two main triggering mechanisms for the initiation of a debris flow: shallow slope failure and channel bed failure.

- SHALLOW SLOPE FAILURE

  This is a common type of debris flow triggering. The sediments start to move as a landslide that subsequently develops into a debris flow. The transformation to a mature debris flow happens when the initial failure enters in the channel and there is a sudden increase in the water content of the mass (Johnson and Rodine 1984; Ellen and Fleming 1987; Iverson et al. 1997; Sassa and Wang 2005). While moving to the channel, the initial failure can erode other superficial deposits, increasing the debris flow volume (Costa and Williams 1984; Santi and Mathewson 1988).
- CHANNEL BED FAILURE

  This second type of triggering mechanism is less studied and understood than the previous one (Tognacca and Bezzola 1997; Cannon et al. 2004). It is the typical triggering mechanism of the dolomitic region (Berti and Simoni 2005).

Berti and Simoni (2005) stated that this triggering mechanism is typical of small catchments characterized by steep slopes, with no vegetation and exposed bedrock. This particular morphology of the catchment favours the water to flow into channels, entraining a large sediment quantity from the bed and the banks. So, the flow usually starts as an intense bedload transport and gradually transforms into a debris flow (Takahashi 2000; Tognacca et al. 2000).

Different authors have described other types of triggering: These other types can be connected to one of the two main triggering mechanisms, but show some distinctive characteristics that can be used to set a classification.

1. Debris flow triggering on a talus cone at the footage of a rock face

   This is a typical triggering mechanism that can be observed in the Dolomites. During heavy rainfalls, the water flows on the rock faces originating a high discharge that hit the loose debris of the scree slope. This water flow destabilises the talus, starting the sediment transport (D'Agostino et al. 2004).

2. Dam Break

   This type of triggering happens when a natural dam located in the upper part of a channel, suddenly breaks releasing downstream a high and extremely rapid water discharge. Usually, at the beginning of the event there is the formation of a debris flood. With the entraining of loose sediment material, it develops into a debris flow wave (Capart et al. 2001).

3. GLOF (Glacial Lake Outburst)

   This is a particular type of the previous one triggering mechanism. The glacial lakes are often dammed by ice and debris. If this natural dam breaks, the lake rapidly flows downstream, producing a high water discharge that erodes the loose debris forming the broken dam and also other erodible material located on the flow path (Petrakov and Krylenko 2007). These debris flows can be very dangerous because are always characterized by great volumes and long runout distances (Breien et al. 2008).

4. Earthquake

   This is an indirect cause of debris flow triggering. In fact, Lin et al. (2004) associated the Chi-Chi earthquake of 1999 to the increasing of debris flow events in the following period. The earthquake caused important morphological changes in the catchments like the opening of abundant fractures that contributed to increase the sediment availability.

The water easily infiltrated in these fractures, causing the destabilisation of the bedrock and the release of a high volume of loose debris.

The consequent increasing of landslides associated to heavy rainfall events caused the triggering of several debris flows. The morphological changes caused a lowering of the rainfall triggering threshold, leading to a higher number of events.

5. Post-fire debris flow

   In recently burned basins, the soil erosion is very high. Consequently, the sediment volume of the source areas is higher than before the fire. Debris flows triggered in these areas are usually initiated as landslides originated for the erosion of the superficial deposits (Cannon et al. 2001, 2004; Santi et al. 2008). The soil changes caused by the fire play an important role in fact, the increasing of soil moisture (Klock and Helvey 1976; Helvey 1980; Swanson 1981; Megahan 1983) and the lack of roots that help in stabilising the terrain (Swanson 1981; DeGraff 1997) contribute to the increasing of debris flow triggering.

1.5 Research questions and objectives of the thesis

To cover up all the main variables involved in the triggering mechanism, we divided the research questions of the thesis into three main groups, each one referring to the corresponding chapter of the thesis. The main research questions are:

1. Which are the best morphological parameters to identify the debris flow triggering areas in the case of a regional study?
2. Do rainfalls influence the sediment availability during the recharge period? Is there any correlation between rainfalls during the recharge period and debris flow volume? Is there any correlation between the rainfall erosivity power and the triggering of torrential flows?
3. How does the headwater basin respond to rainfalls? How much time is needed in these upper parts of the catchments to have a water runoff capable of mobilizing sediments inside the channels? Are the hillslopes of the headwater basins unstable due to their morphological and geotechnical characteristics?

1.6 The thesis structure

The triggering mechanism of debris flows is very complex because it comprises many different variables both hydrological and geological. For this reason, we decided to divide the work in three different parts, each one focusing on a different aspect of the triggering phenomenon.

In the second chapter of the thesis, we analyse some morphological parameters related to the susceptibility to debris flows. In this case, we worked at a regional scale taking the Vizze Valley (South Tyrol, Italy) as case study. This chapter is an edited version of the article titled "On the criteria to create a susceptibility map to debris flow at a regional scale using Flow-R", published on Journal of Mountain Science in 2017.

In the third chapter of the thesis, we focused on rainfall that is one of the most important variables influencing the triggering mechanism. In this case, we chose the catchment of the Rebaixader torrent (Axial Pyrenees, Spain) as case study. This chapter corresponds to the paper titled "Correlation between the rainfall, sediment recharge and triggering of torrential flows in the Rebaixader catchment (Pyrenees, Spain)", which is currently under revision in Landslides.

In the last chapter of the thesis, we moved from rainfall to the corresponding generated water runoff, analysing the potential formation of debris flows by the two main studied triggering mechanisms: channel bed failure and shallow slope failure. For this analysis, we used empirical equations and field data collected in the three chosen study areas (Rio Rudan and Rio Chiesa catchments, Dolomites, Italy; and Rio Rebaixader catchment, Pyrenees, Spain). This last chapter refers to the article titled "Rainfall durations and corresponding dominant mechanism for the initiation of debris flows in three basins characterized by different geomorphological settings" that will be soon submitted to a peer-review journal.

2 On the criteria to create a susceptibility map to debris flow at a regional scale

2.1 Abstract

Studies on susceptibility to debris flows at regional scale (100-1000 km^2) are very important for the protection and management of mountain areas. To reach this objective, routing models, mainly based on land topography, can be used because they can predict susceptible areas rapidly and necessitate few input data. In this research, Flow-R model is implemented to create the susceptibility map to debris flow of the Vizze Valley (BZ, North-Eastern Italy; 134 km^2). The analysis considers the model application at local scale for three sub-catchments and then it explores the model upscaling at the regional scale by verifying two methods to generate the source areas of debris flow initiation. Using data of an extreme event occurred in the Vizze Valley (4th August 2012) and historical information, the modelling verification highlights that the propagation parameters are relatively simple to set in order to obtain correct runout distances. Furthermore, a double DTM filtering - using a threshold for the upslope contributing area (0.1 km^2) and a threshold for the terrain-slope angle (15°) - provides a satisfactory prediction of source areas and susceptibility map within the geological conditions of the Vizze Valley.

This chapter is an edited version of Pastorello R, Michelini T, D'Agostino V (2017). On the criteria to create a susceptibility map to debris flow at a regional scale using Flow-R. Journal of Mountain Science 14(4). DOI: 10.1007/s11629-016-4077-1.

2.2 Introduction

Among the different types of landslides affecting alpine areas all over the world, debris flows are one of the most dangerous. In fact, they cause every year loss of human lives and huge damages to infrastructures (Dowling and Santi 2014).

A debris flow is a "very rapid to extremely rapid surging flow of saturated debris in a steep channel, [with] strong entrainment of material and water from the flow path" (Hungr et al. 2013). Debris flows are usually characterized by a higher peak discharge than water flows and for this reason, they often overflow the channel banks, spreading over the alluvial fan (Rickenmann 1999). Unfortunately, the most suitable areas for human activities in a mountain environment are mainly located near the rivers and over the alluvial fans (Hürlimann et al. 2006). For this reason, the expansion of settlements in alpine valleys during the last century contributed to increase the risk for human lives and infrastructures (Cavalli and Grisotto 2006; Fuchs et al. 2008).

To identify the risk caused by debris flows to human settlements, it is of primary importance to detect the areas susceptible to this phenomenon. Studies of susceptibility to debris flow at a regional scale have become of primary importance nowadays because the increasing severe summer storms, observed in the last years, can easily trigger several debris flows in the same valley, causing widespread damages in a vast territory (Park et al. 2013). Susceptibility maps help to identify areas with the greatest probability to be interested by the natural hazard, and that deserve to be carefully analysed for the redaction of a more detailed hazard map (Horton et al. 2011).

To this purpose, scientists have developed different methods in the last decades (e.g. O'Brien et al. 1993; Ghilardi et al. 2001; Crosta and Frattini 2003; Rickenmann et al. 2006). The main methodologies that can be used for studies of susceptibility comprise historical researches or the use of modelling software. They differ according to the analysis scale. D'Agostino (2013) studied the relationship between time scale and area scale. It results that the most detailed studies involve micro-areas (single catchments) and are carried on especially for single events. Whereas, more general studies are carried on at macro-area level, considering more than one catchment at a time, and also entire valleys with extension between 100 and 1000 km^2 (regional scale). In this case, the research is usually more generic and instead of focusing only on a single event, it involves all the historical events recorded in the area.

Historical information are always important because they help to identify the type of event (debris flow, debris flood, bed-load transport, fluvial flood, large-wood/or not large-wood conditioned event), they give information about the magnitude and of the consequences for human activities.

The modelling software are important instruments that can be used for the back-analysis of past events: they help to reconstruct the behaviour of the flow of a specific event. Moreover, they can be used to simulate potential events, estimating the damage that infrastructures and other human facilities could suffer from a debris flow.

For the regional scale studies, models are usually empirical, and are based on the morphological and topographic characteristics of the analysed area. On such a large scale, it is impossible to account for specific variables such as flow velocity or rheological characteristics.

The topographic models are simpler than the physically based ones. In fact, they need few input data like terrain slope, geology, drainage network. This simplicity is a specific choice because the triggering factors are different and complex. However, at the regional scale, some of the specific triggering factors can differ from a catchment to another. Therefore, it is better to use a more generic approach. Moreover, it would be time consuming, to analyse in detail large areas (such as a valley). Whereas, the parameters needed by a topographic model can be easily extrapolated by the Digital Terrain Model and few other thematic maps. This approach strongly reduces the time to be spent for the analysis.

These topographic models have also the advantage to identify the priority areas of analysis, with a minimum need of input data. In the last decade, experts have proposed several models (e.g. Fannin and Wise 2001; Cavalli and Grisotto 2006; Miller and Burnett 2008). Among these, Horton et al. (2013) developed Flow-R (Flow path assessment at a Regional scale), a model for susceptibility mapping at a regional scale. Many studies have applied this model (e.g. Blahut et al. 2010; Kappes et al. 2011; Michoud et al. 2012) for different natural hazards (debris flow, rock fall and snow avalanche).

Flow-R does not give information about flow velocity or deposition volume because these values cannot be easily estimated at a regional scale (Iverson and Denlinger 2001; Horton et al. 2008). The resulting simulations include all the possible inundated areas, and so the simulated propagations are usually wider than the real ones.

Flow-R shows good potential on the identification of the most susceptible areas, but one of the most important phases of the simulation, the identification of the source areas, can be improved.

In fact, it is difficult to set parameters capable of fitting on the regional scale of analysis (>100 km^2). Other authors working with the same model (e.g. Blahut et al. 2010; Kappes et al. 2011; Park et al. 2013) used the standard method implemented in Flow-R, using different thematic maps analysed with specific thresholds. One purpose of this work is to improve the methodological path to be used for the identification of these initiation areas. Therefore, we also tried another approach, specifically calibrated in our analysed area. With this second methodology, we identify the source areas using two simple parameters (terrain slope and flow accumulation), already recognized as key parameters for the identification of the most susceptible areas by Carrara et al. (2008).

To reach this objective, the methodology has been tested on a real case study. We used data about the triggering and deposition areas from a debris flow event occurred on 4th August 2012 in the Vizze valley (Pfitschertal) (Bz, North-Eastern Italy). We investigated for the best simulation parameters in terms of flow propagation and deposition at a local scale. After the identification of these parameters at a local scale, we moved to the regional scale, analysing the whole valley and testing the two different methods to identify the source areas. The information on exceptional debris flows, which affected many tributaries of the Vizze valley on the August 2012 event and in the past, was used to verify the reliability of the two methods

2.3 Study area

2.3.1 Geographical and meteorological characteristics of the valley

The Vizze valley (Pfitschertal) (geographical coordinates: 46°54' N, 11°28' E) is an Alpine valley located in the northern part of Alto Adige-Südtirol (Italy), near Austria boundary (Figure 2.1). The valley has an area of 134 km^2 and has the classic geomorphological characteristics of alpine valleys (high slope gradient, high sediment availability). Moreover, severe summer storms, that are the typical triggering phenomena of debris flows, hit this region every year.

Vizze Valley is a secondary valley of the Isarco Valley (Eisacktal) that begins from Passo di Vizze (Pfitscherjoch) (2248 m a.s.l.) and ends near Vipiteno (Sterzing) (948 m a.s.l.), and so it has a NE-SW orientation. The higher peak of the area is Gran Pilastro (Hochfeiler) (3510 m a.s.l.), located at the eastern limit of the valley. The lateral sides of the valley are mainly covered by forests. On the valley bottom, there are fields, pastures, communities, buildings and roads. Whereas, the upper part of the valley is composed by rock outcrops, talus cones, snowfields

and glaciers. The different communities displaced along the valley are all part of the municipality of Val di Vizze (Pfitsch). This municipality has a population of 2800 inhabitants and an area of 142 km^2.

The main river of the valley is Rio Vizze (Pfitscherbach), a left tributary of the Isarco River (Eisack). It begins on Mount Lavizza (Haupenhöhe) (3040 m a.s.l.) and flows into the Isarco River near Vipiteno (Vanzetta 1987). It has several tributary creeks. Among these, the most dangerous ones are Rio Piazza (Platzbach), Rio Aiga (Aigerbach), Rio di Riva (Rainbach) and Rio Avenes (Afenserbach) on the right valley side; and Rio Transacqua (Ueberwasserwaldbach), Rio di Borgo (Burgumerbach), Rio di Montegrande (Grossbergbach) and Rio Tulve (Tulferbach) on the left of the valley.

The geological area that comprises the Vizze valley is located within the Pennidic domain, mainly formed by metamorphic rocks. In the sides of the valley, different types of rocks can be observed: schists, marbles, paragneiss, Zentralgneiss, migmatites and few paraschist pre-granitic (Astori and Venturini 2012).

The surface glacial deposits along the valley (quaternary formations) are more recent. They can be found in the great part of the valley bottom, and their origin dates back to the last ice age of the Würmian, about 12000 years ago. These formations are usually located on the valley sides, characterized by gentle slopes, and in the glacier cirques.

The study area is characterized by an alpine climate, with mean annual rainfalls between 700 and 800 mm, concentrated particularly during summer and autumn. On 4th August 2012, an extreme summer storm stroke the valley causing the triggering of several debris flows. The rain gauge of Vipiteno registered 72.8 mm of rainfall in 6 hours, with a return period between 200 and 300 years (Macconi et al. 2012). The dangerousness of this event has been also amplified because of the already saturated soil. In fact, in June and July, 143.6 mm and 202.4 mm of rain respectively were recorded.

This powerful storm triggered various landslides along the valley (Macconi et al. 2012). There were 45 landslide events and, among these, 37 were debris flows. Moreover, 14 debris flow events occurred in small gullies not included in the digital channel network of the Autonomous Province of Bolzano. These flows damaged the road system, railways, and residential areas. Two communities, Avenes and Tulve, were the most damaged, with each one suffering a fatality.

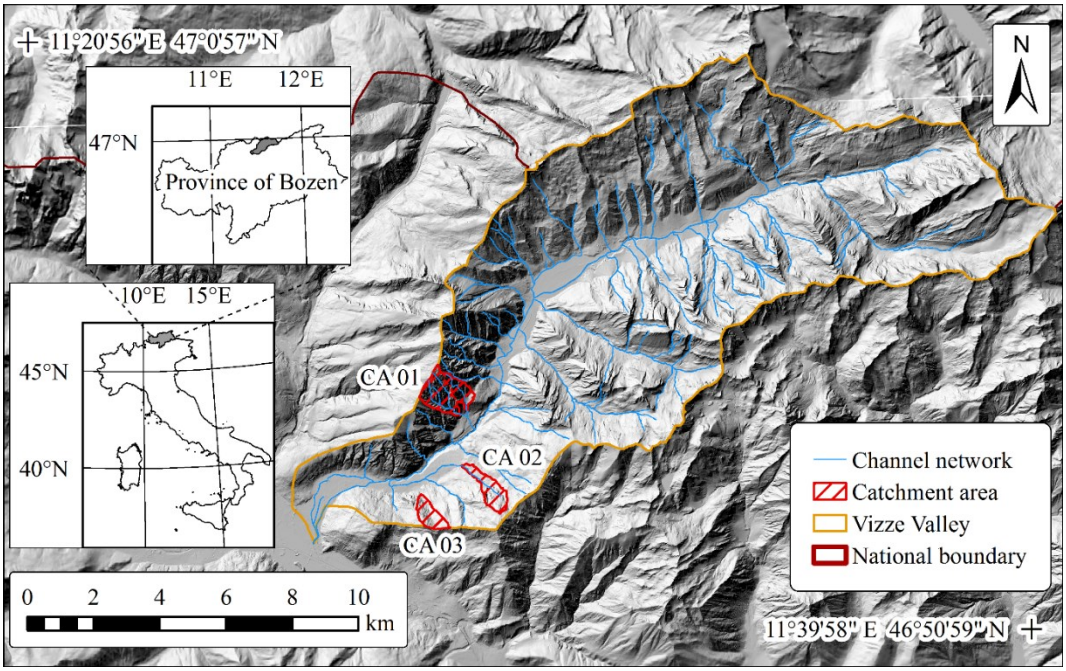

Figure 2.1: Map of the Vizze Valley and location of the three local case studies

2.3.2 The local case studies

The calibration of the Flow-R parameters for the propagation has been conducted through a back analysis at a local scale in three case studies: CA01, CA02 and CA03 (Figure 2.1). The catchments exhibit different morphological characteristics (Table 2.1).

Table 2.1: Morphological characteristics of the three catchments.

	CA01	CA02	CA03
Area (km^2)	1.40	0.98	1.06
Min elevation (m)	1330	1257	1060
Mean elevation (m)	1949	1815	1540
Max elevation (m)	2563	2323	1950
Mean slope (°)	44.56	35.19	34.32
Max slope (°)	82.79	79.48	75.93

The real event of 2012 has a return period close to 300 years. This is also the maximum return period used for the redaction of the hazard maps in the Autonomous Province of Bolzano. Therefore, we used the real deposition areas from this event as the comparison term for the modelling results.

CA01: We selected the first study area in correspondence of Rio Avenes, in the right bank of Rio Vizze (Figure 2.2). This catchment exhibits a semi-natural flow path, with the presence of few buildings of the Avenes community on the alluvial fan. The stream, in the upper and central part, is divided in two branches that merge just below the fan apex. However, the morphology of the alluvial fan suggests that the two branches would continue to flow on separated paths until their insertion in Rio Vizze. This change from the natural course could derive from some hydraulic control structures built in the last decades. In fact, just above the alluvial fan, there are eleven check dams.

CA02: We selected the second case study in correspondence of Rio Tulve (Figure 2.3). This is a more "anthropic" stream; in fact, in the central and lower part of the channel there are lateral walls, twenty-nine check dams and one filter-retention check dam with a storage basin. Just downstream of the fan apex, the stream crosses the Tulve community and sharply changes direction flowing toward west, parallel to the Rio Vizze for about 1.5 km. However, based on the natural morphology of the terrain, it seems that in reaching the Tulve community, the natural flow direction would continue along a straight path, in direction of Rio Vizze. This path is confirmed by the deposition area of the August 2012 event: the debris flow overflowed the right bank, flooding over the buildings of the Tulve community and reaching Rio Vizze just below the community, ignoring the channel track that flows toward west (Figure 2.3).

CA03: We selected the third case study in correspondence of a catchment near CA02 (Figure 2.3). This is the most natural area, with two little gullies that flow downstream, merging with Rio Tulve, just before its junction with Rio Vizze. The deposition area of this catchment is located over forests and grasslands. There are no buildings over the alluvial fan.

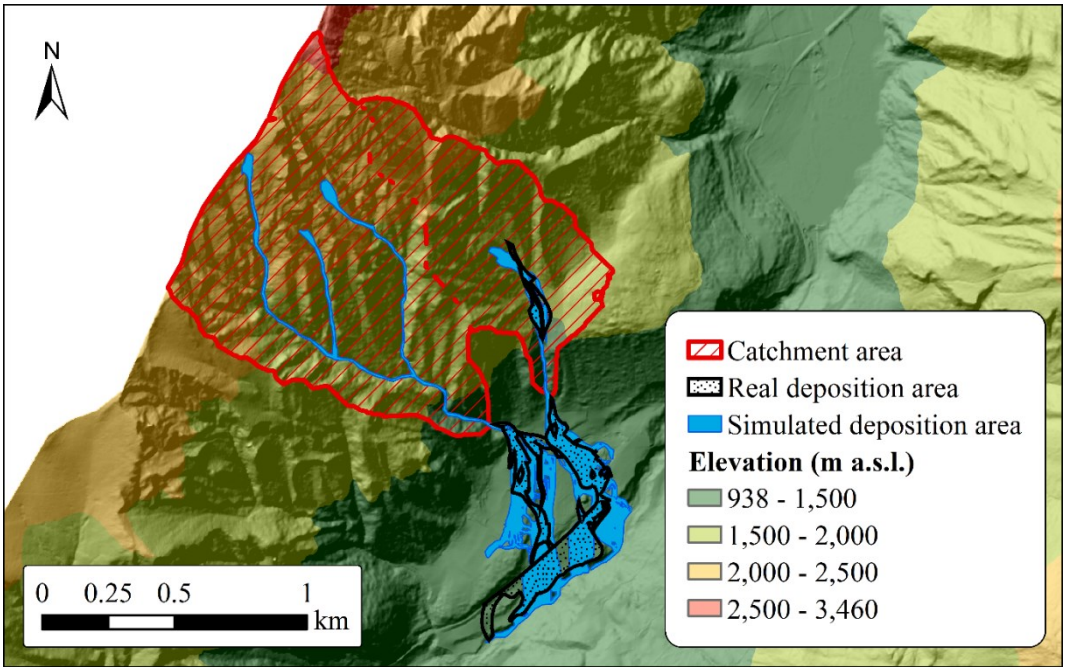

Figure 2.2: Result of the best simulation on the CA01 area compared to the real deposition area of the August 2012 event.

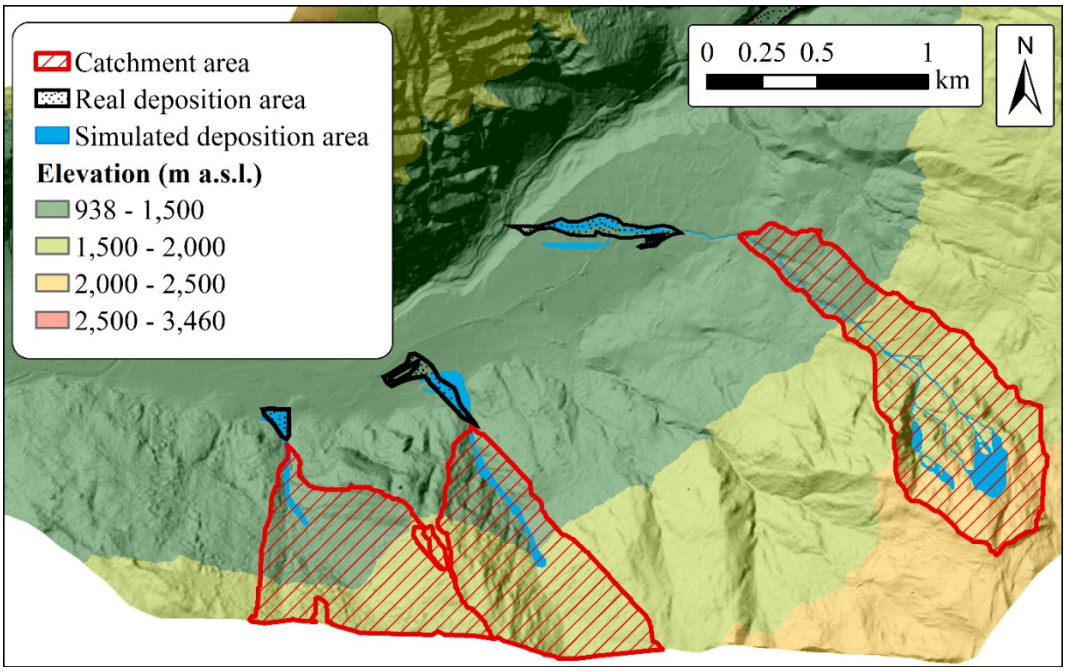

Figure 2.3: Result of the best simulations on the CA02 and CA03 areas compared to the real deposition areas of the August 2012 event.

2.4 Materials and methods

2.4.1 Data

We used DTM maps with different resolutions and debris flow data derived from the August 2012 event. The Autonomous Province of Bolzano provided both types of datasets. At a local scale, we used DTM maps with a resolution of 2.5 m. Whereas, at a regional scale, we used a grid resolution of 10 m, as suggested by different authors (Blahut et al. 2010; e.g. Horton et al. 2013). The extent of the triggering and deposition areas of the real event have been used at a local scale (CA01, CA02 and CA03) to identify the best simulation parameters.
To verify if the final susceptibility map of the Vizze Valley was consistent, we compared it with data about historical debris flow events. We collected this last dataset from the ED30 archive of the Province of Bolzano (Macconi et al. 2012).

2.4.2 Flow-R model

For the creation of the susceptibility map, we used Flow-R model "Flow path assessment of gravitational hazard at a regional scale". This model works through MATLAB® and can simulate different types of natural hazards (debris flow, snow avalanche, rock fall) at a regional scale. The results are probabilistic and they do not provide information about the volume or the velocity of the flow (Horton et al. 2013).
The computation process consists of two phases:

- Identification of the source cells;
- Modelling of the potential path and deposition area reached by the flow.

For the identification of the source cells, the model uses a standard procedure, hereafter called *Method 1* (Table 2.2). The software can read thematic maps, in the ASCII raster format. According to Takahashi (1981) and Rickenmann & Zimmermann (1993) the three critical factors for the triggering of a debris flow are sediment availability, slope gradient, and water input. For this reason, we initially used three input maps: flow accumulation (a proxy of the water input), terrain slope and plan curvature (that is an indirect measure of sediment availability) (Horton et al. 2013).
The program elaborates these maps using different threshold values and classifies every property as excluded, or favourable or ignored. The last one comprises cells a priori eliminated

(e.g. sub-areas from the classification analysis). In the final source area map, the program recognises as source cells only those classified as favourable at least once and never excluded.

Table 2.2: Input maps (and corresponding criteria chosen for the Flow-R computation), used in the two methods to identify the source areas.

	Input	Criteria
Method 1	Flow accumulation	Heinimann (1998)
	Slope	>15°
	Plan curvature	< -2/100 m^{-1}
Method 2	Predefined sources from Flow accumulation	>10 ha
	Predefined sources from Slope	>15°

Flow-R analyses the flow accumulation raster using one of the two different threshold curves for the triggering of debris flow. The first one has been created from data collected by Rickenmann & Zimmermann (1993) after the extraordinary 1987 debris flow happened in Switzerland; the second one is based on the study of Heinimann (1998). These curves relates flow accumulation with channel slope gradient. For our computations, with *Method 1*, we used the equation from Heinimann (1998), denominated as "Rare events" in Flow-R:

$$\begin{cases} \tan\beta_{thres} = 0.32\, S_{uca}^{-0.2} & if\ S_{uca} < 2.5\ km^2 \\ \tan\beta_{thres} = 0.26 & if\ S_{uca} \geq 2.5\ km^2 \end{cases} \quad (2.1)$$

Where $tan\beta_{thres}$ is the slope threshold and S_{uca} is the upslope contributing area.

The terrain slope raster has been processed choosing a threshold value of 15°, as suggested by different authors (Takahashi 1981; Rickenmann and Zimmermann 1993; Bathurst et al. 1997; Huggel et al. 2002). Whereas, the triggering value chosen for the plan curvature is -2/100 m^{-1} (Horton et al. 2013). In fact, a negative value of the curvature indicates a concave morphology of the terrain, and so it helps localising hollows, gullies and channels (Carrara et al. 2008).

Flow-R estimates the propagation of the flow through an expansion probability and an energetic balance. These criteria control respectively the lateral spreading and the runout (Michoud et al. 2012).

Different flow direction algorithms are available for the first computation. In this study, a modified version of the Holmgren (1994) algorithm, proposed by Horton et al. (2013), is used:

$$p_i^{fd} = \frac{(\tan\beta_i)^x}{\sum_{j=1}^{8}(\tan\beta_j)^x} \; \forall \begin{cases} \tan\beta > 0 \\ x \in [1; +\infty[\end{cases} \quad (2.2)$$

Where i, j are the flow directions, p_i^{fd} is the susceptibility proportion in the direction i, $\tan\beta_i$ is the slope gradient between the central cell and the cell in the direction i, and x is the variable exponent. Equation (2.2) is a development of the previous multiple flow direction algorithm proposed by Quinn et al. (1991). The authors considered "the spreading over every downward cell in a continuous and not random way" (Lari et al. 2011, p. 935). The development proposed by Holmgren (1994) is the introduction of the x exponent, which allows to consider different spreading scenarios. If x=1 the algorithm matches the one proposed by Quinn et al. (1991), showing a large expansion. For higher values of x the flow tends to converge up to a single direction in case $x \to \infty$ (O'Callaghan & Mark 1984 from Kappes et al. 2011). The innovation proposed by Horton et al. (2013) is the *dh* variable, very useful if the DTM has a high resolution. The *dh* variable enables to raise up from 1 to 70 meters the central cell of the computational window (3×3 matrix) , and so it allows the flow to be guided by the general topography and not by the great details of the DTM (Horton et al. 2013). Therefore, it indirectly takes into account of flow height, an important parameter not considered in the computation. In addition to this algorithm, there is also an inertial parameter, called persistence function. It accounts for the change in the flow direction angle between two consecutive cells. For its computation, three different functions are proposed: *proportional*, *Gamma (2000)* and *cosine*. The persistence function used by the program is the following:

$$p_i^p = w_{\alpha(i)} \quad (2.3)$$

Where p_i^p is the flow proportion in the direction i, and $\alpha(i)$ is the angle between the previous direction and the direction from the central cell to the cell i. The parameter w assumes a different value depending on the chosen function. For example, if $\alpha = 45°$, the value of w will be 0.8 for the proportional function, of 0.707 for the cosine and of 1 for Gamma (2000). Therefore, the three functions weight differently the direction followed by the flow from a cell to the next one. Finally, the overall susceptibility is:

$$p_i = \frac{p_i^{fd} p_i^p}{\sum_{j=1}^{8} p_j^{fd} p_j^p} \quad (2.4)$$

Where i, j are the flow directions, p_i is the susceptibility value in the direction i, p_i^{fd} is the flow proportion according to the persistence and p_0 is the susceptibility value of the central cell previously estimated.

Flow-R calculates the runout as an energetic balance between a cell and the next one, without considering the volume or the flow mass. In the model, two different formulas are implemented: the two-parameter frictional model proposed by Perla et al. (1980), and the simplified Friction-Limited model (SFLM).

The first one was initially developed for snow avalanche but has been used also for debris flows (Zimmermann et al. 1997). It calculates the runout distance as a function of the coefficient of friction μ and the mass-to-drag-ratio (ω).

The SFLM model uses as main parameter the *travel angle*, also named *fahrböschung angle* (Heim 1932). This is the angle between the horizontal plane and the line linking the highest triggering point with the farthest deposition point. This approach may result in improbable runout distances if the catchment area is very steep because unrealistic energetic values could be reached during the propagation (Horton et al. 2013). For this reason, it is possible to set a velocity limit of the flow, avoiding erroneous results. In both cases, the program computes the runout distance as the kinetic energy produced from a cell to the next one, along the debris flow path. The used equation is the following:

$$E_{kin}^i = E_{kin}^0 + \Delta E_{pot}^i - E_f^i \quad (2.5)$$

Where E_{kin}^i is the kinetic energy of the cell in the direction i, E_{kin}^0 is the kinetic energy of the central cell, ΔE_{pot}^i is the change in the potential energy to the cell in the direction i and E_f^i is the loss of frictional energy to the cell in the direction i.

The result of the model is a raster file showing all the propagations obtained as sum or maximization of the susceptibility values (Michelini et al. 2014).

2.4.3 Simulation methodology

When analysing the three case study simulations (local scale), we used input maps with a resolution of 2.5 m. Then, we assumed the real source areas, mapped after the 2012 event, as predefined sources. In this way, the program simply started the propagations from these zones. This method was convenient because allowed us to concentrate only on the propagation parameters. We tested a very large set of simulation parameters (empirical trial and error approach), which resulted in a total number of 75 runs for the three catchments. The following model setting, and routing parameter combinations were considered:

- Spreading function:
  - *x* exponent from 4 to 25
  - *dh* value from 0 to 2 m;
- Runout function:
  - Travel angle from 10° to 12°
  - Perla model: M/D (ω) from 20 to 200 and μ from 0.02 to 0.25
  - Velocity limit from 15 m/s to 20 m/s.

Finally, we chose the settings for each catchment that better reproduced the real deposition area of the 2012 event. More precisely, we evaluated the accuracy of each simulation comparing the real deposition area with the simulated deposition area. The followed method was proposed by Scheidl and Rickenmann (2010), and has been used also in other studies (e.g. Bettella and D'Agostino 2012). From the overlapping between the predicted deposition areas and the real ones, we obtained three sub-areas: *X*, *Y* and *Z*. The *X* area is that part of "flooded" (deposition) terrain correctly predicted by the modelling (true positive). *Y* is that part of the "flooded" area predicted by the model but not affected by the debris flow in the reality (false positive). *Z* is that portion of the area hit by the real event but completely ignored by the modelling (false negative). From the relationship between these three sub-areas and the observed routing and deposition zones (*Z*+*X*), we calculated the accuracy indicators proposed by Scheidl and Rickenmann (2010). These are the followings: the α indicator (positive accuracy), being $\alpha = X/(Z+X)$; the β indicator (loss of accuracy due to area excess), being $\beta = Y/(Z+X)$, and the γ indicator (loss of accuracy due to area lack), being $\gamma = Z/(Z+X) = 1 - \alpha$. Since the best accuracy rating between the predicted area and the real area is characterized by high values of α (close to 1) and low values of β and γ (close to a null value), we introduced a new index δ that rates

an overall accuracy resulting from the ratio between the correctly predicted area proportion (α) and wrongly predicted area proportion (β and γ):

$$\delta = \frac{\alpha}{\beta+\gamma} = \frac{\alpha}{1+\beta-\alpha} \quad (2.6)$$

The more δ is higher, the more the simulation is accurate. Values of δ greater or equal than 2.5 indicate a very accurate modelling (e.g., $\alpha = 0.75; \beta = 0.05; \gamma = 0.25$), while values lower than 0.25 (e.g., $\alpha = 0.20; \beta = 0.20; \gamma = 0.80$) express poor and very far from the reality model results. Intermediate δ values within the range 0.5-1.0 correspond to a region of model-result acceptability.

To conduct the simulations on the Vizze valley (regional scale), we used different input maps and different parameter settings. First of all, we used a grid size of 10 m, as suggested by different authors (e.g. Blahut et al. 2010; Fischer et al. 2012; Horton et al. 2013). This resolution allows to maintain a good compromise between the computation time and the resulting simulations. For the identification of the source areas, we used two different methods: *Method 1* (Table 2.2), already implemented in Flow-R. To try to improve the identification of the initiation areas we introduced *Method 2*. In this case, we selected the source cells with a GIS analysis, creating two different maps of predefined sources: one from the flow accumulation and one from the terrain slope analysis. Also Montgomery & Dietrich (1994) indicated both the slope gradient and the upslope contributing area as discriminating factors for debris flow susceptibility.

Flow-R considers as sources all the cells that have a value of one, and automatically excludes the ones that have a value of zero. Therefore, the first map used as predefined sources, has been created from the flow accumulation raster, assigning a value of one to all the cells that drain at least an area of 0.1 km^2. This value is based on the threshold area that was highlighted by Montgomery & Foufoula-Georgiou (1993) and it separates debris-flow dominated channels from alluvial channels. Santos & Menéndez Duarte (2006) have also confirmed this value (Cantabrian Cordillera, Spain). For the creation of the second predefined source map, all the cells that have a slope angle higher than 15° have been selected as source areas. Takahashi

(2007) reconfirmed this value as necessary for debris-flow initiation, being critical for processes of channel bed failure.

To set the propagation parameters of the simulation at regional scale, we used the parameter combination resulting from the best fitting of the three local case studies (CA01, CA02, and CA03). In detail, we adopted that combination providing the highest mean (δ_m) of the three accuracy values (δ_i, Equation 2.6).

Finally, we verified the simulated maps using three informative layers: fans affected by historical debris-flow, the map of the valley cones hit by the 4th August 2012 event, the susceptibility map provided by the Bolzano Province. Because of the lack of detailed flooding maps, the accuracy verification at regional scale was simplified with respect to that at local scale cross-checking the number and the position of the involved areas (deposition and triggering zones). A sensitivity analysis was also carried out to show at which extent this choice on the routing/deposition parameters influences the results in case different generation of source areas (*Method 1* or *Method 2*) are adopted.

2.5 Results

2.5.1 Results at a local scale

Table 2.3: Parameters of the best simulation obtained in each case study.

Case study	Source	Propagation				Computational time
	Input	Spreading		Runout		
		Algorithm	Value	Model	Value	
CA01	Predefined sources	Holmgren weights	*dh*=1m *x*=07 default	SFLM velocity	11° 20 m/s	113 s
CA02	Predefined sources	Holmgren weights	*dh*=1m *x*=20 default	SFLM velocity	10° 20 m/s	92 s
CA03	Predefined sources	Holmgren weights	*dh*=1m *x*=06 default	Perla velocity	*M/D*=30 μ=0,10 20 m/s	133 s

CA01: Rio Avenes catchment

The parameters that gave the best accuracy rate in the first study area are the following: the modified version of the Holmgren (1994) algorithm with x=07 and dh=1 m, for the assessment of the spreading width. The SFLM method using a travel angle of 11° and a velocity limit of 20 m/s, for the assessment of the runout (Table 2.3). The resulting propagation is shown in Figure 2.2.

CA02: Rio Tulve catchment

This area is different from CA01. In fact, the real debris flow followed a thin path spreading over the right bank of the stream. For this reason, the parameters for the assessment of the spreading extent with the highest accuracy value are different from the previous case study (Table 2.4). The exponent of the Holmgren (1994) algorithm is higher than the one used in the previous catchment (x=20 and dh=1 m) because the flow is better represented by a single flow direction. For the assessment of the runout, the SFLM model resulted as the best algorithm also in this case, but using a travel angle with a value of 10° (Figure 2.3).

CA03: near CA02 catchment

The parameters that gave the highest accuracy values (Table 2.4) were different from both the previous case studies. For the assessment of the spreading, we used x=06 as exponent of the Holmgren (1994) algorithm. Whereas, the algorithm for the assessment of the runout is the one from Perla et al. (1980), with M/D=30 and μ=0.1, and a velocity limit of 20 m/s (Table 2.3 and Figure 2.3).

In Table 2.3 are illustrated the parameters used in the best simulations for the three case studies. In the last column is shown the time taken by the program computations using an Intel Core i7 CPU (12.0 GB RAM).

Table 2.4: Values of partial accuracy indicators (α and β) and overall accuracy (δ) obtained from the simulation run in each catchment (row), using the best set of parameters from each case study (column).

Analysed catchment	Modelling parameters								
	CA01			CA02			CA03		
	α	β	δ	α	β	δ	α	β	δ
CA01	0.78	0.86	0.72	0.40	0.64	0.42	0.63	0.54	0.68
CA02	0.45	0.36	0.49	0.51	0.26	0.69	0.26	0.18	0.28
CA03	0.74	1.14	0.53	0.25	0.70	0.17	0.58	0.41	0.70
δ_m			**0.58**			0.43			0.55

The accuracy value (δ) obtained from the CA01 back analysis is the highest between the three case studies (0.72 on Table 2.4). The simulation parameters from the CA01 back analysis gave an overall accuracy (δ) of 0.53 if used on CA03. This is the second-best accuracy value obtained among the CA03 simulations. Moreover, the mean of the accuracy values (δ_m) obtained from the three case studies, using the CA01 modelling parameters, is the highest (0.58 on Table 2.4). This confirms the quite satisfactory goodness of this set of parameters. Even the parameters obtained from the CA03 back analysis gave good values of accuracy both on CA03 and CA01 (0.68 and 0.70 respectively), but both these values are lower than the 0.72 obtained with the parameters of CA01 (Table 2.4). CA02 is a completely different case study. In fact, its back-analysis parameters are dissimilar if compared to the two other basins. The parameters obtained from CA01 and CA03 provide a deposition area wider than the real one, if used on CA02. For the same reason, also the accuracy values obtained on CA01 and CA03, using the best set of parameters from CA02, are low (0.49 and 0.28 respectively, on Table 2.4). The explanation of these results is the artificial morphology of Rio Tulve channel (CA02). The presence of hydraulic control structures, in particular a filter check dam located along the main channel, strongly influences the debris flow spreading. Consequently, these structures affect the best fitting parameters obtained by the Flow-R back analysis simulations. In fact, this model works only on a topographical and morphological base, without considering the presence of anthropic structures that, changing the channel bed morphology, strongly influence the debris flow propagation. The deposition areas obtained on CA02, using the parameters from CA01 and CA03 back analyses, could correspond to the deposition area that would have been flooded without the presence of the debris flow control structures.

2.5.2 Results at a regional scale

2.5.2.1 Source cells identification

To compute the potential propagation, Flow-R starts by identifying the source cells. In Table 2.2 are highlighted the maps used in the two methods and the correspondent threshold chosen for each computation. The source cells have been distinguished in different elevation classes (Figure 2.4) and in different slope classes (Figure 2.5). With *Method 1*, the identified sources are more than with *Method 2*. In Figure 2.4 the identified cells from the two methods are separated in eight classes of elevation.

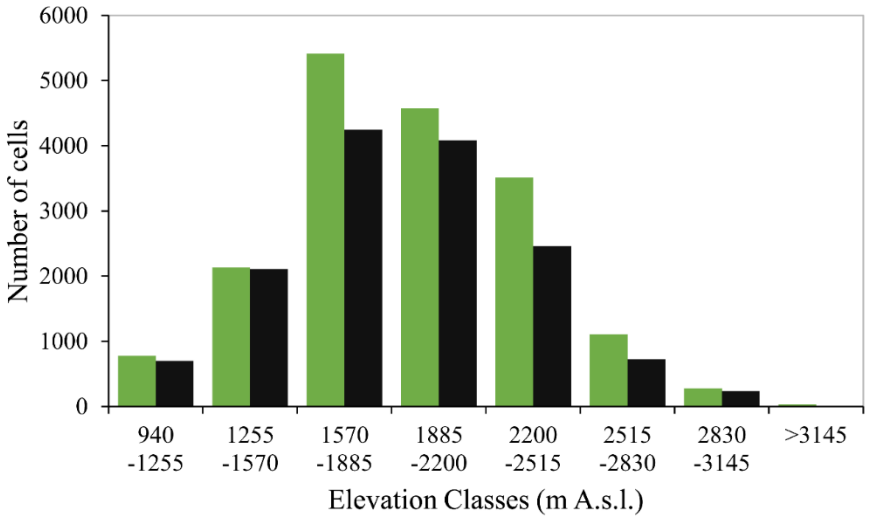

Figure 2.4: Number of source cells identified with *Method 1* (green) and *Method 2* (black) defined by eight different elevation classes.

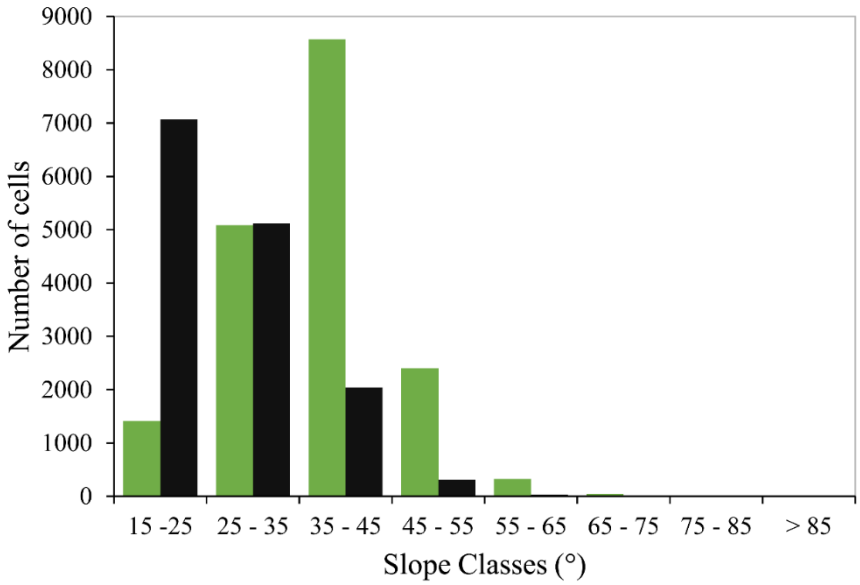

Figure 2.5: Number of source cells identified with *Method 1* (green) and *Method 2* (black) defined by eight different slope angle classes.

The resulting debris flows simulated from the source areas of *Method 1* (Figure 2.6) affect the most part of the gullies, even the smaller ones. Moreover, the corresponding propagation shows many potential debris flows on the lateral sides of the valley, relatively far from the channel network (Figure 2.7).

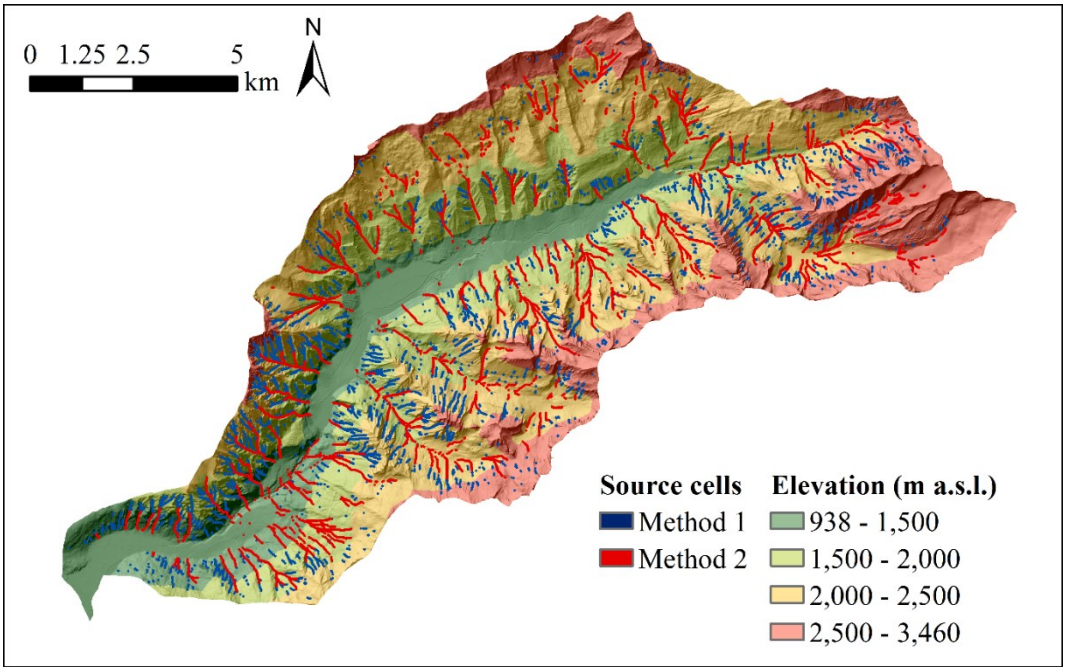

Figure 2.6: Result of the source cells identification obtained from Flow-R with the two different methods.

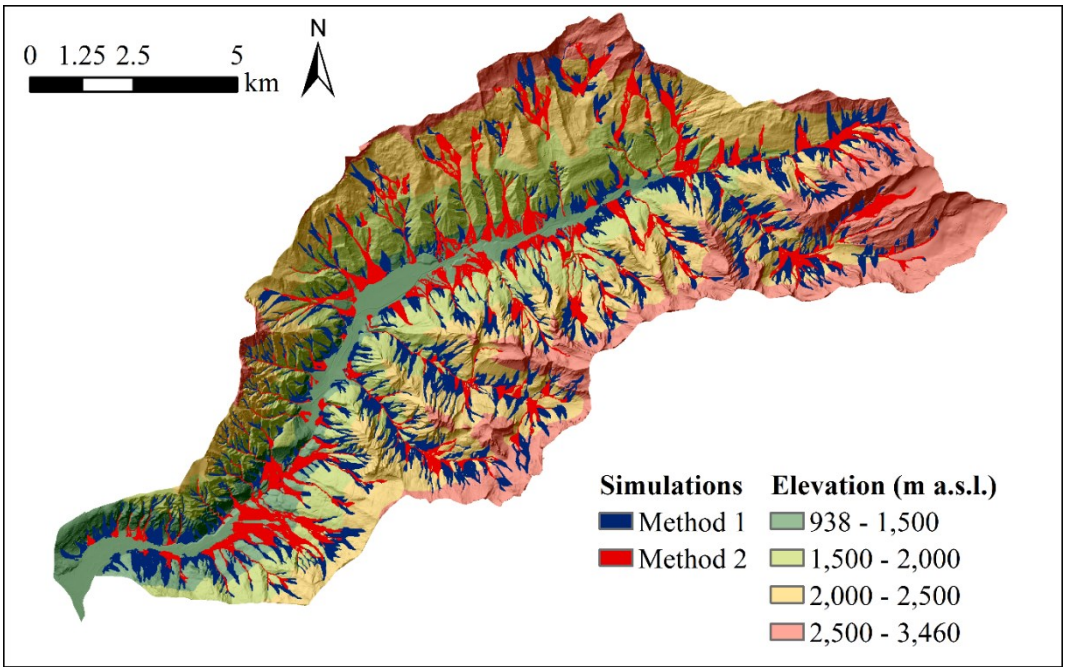

Figure 2.7: Result of the propagations obtained using the same propagation parameters starting from the two different sets of source areas (Method 1 and *2* in Figure 2.6).

Working directly on the flow accumulation and on the slope raster with a GIS analysis, as we made with *Method 2*, we could exclude from the computation, a large number of non-significant cells that are located in rills and small gullies (Figure 2.6). The source cells identified with

Method 2 are located above the main channels of the valley, and the corresponding spreading simulation is in agreement with the geomorphological features of the valley (Rio Vizze), showing a more realistic scenario (Figure 2.7). In fact, the number of cones identified as susceptible with *Method 2* (56 cases) is close to the real number of flooded cones of the August 2012 event (Table 2.5) and also agrees with the susceptibility Map of the Province of Bozen (Table 2.5). On the contrary, the number of cones resulted to be involved using *Method 1* was 3.5 times greater than that of the reference event (August 2012).

Using *Method 2*, the model identified 85 susceptible channel heads of debris flow initiation. Among these, 44 are not included in the digitalized channel network of the Autonomous Province of Bolzano. Looking at the position of susceptible fans, the ones resulting from the Flow-R simulation (*Method 2*) match precisely those of the reference event. The unexpected susceptible cones are mainly located in zones where surrounding catchments have been already marked by historical debris flow events.

In total, the areas identified as susceptible to debris flow have an extension of almost 8.5 km^2, and cover the 11% of the valley.

The comparison with past debris flow events, indicates the inclusive behaviour of the model. All the historical debris flow events have been recognised as susceptible areas by Flow-R. The same happened for the debris flow events of August 2012 (Figure 2.8).

2.5.2.2 Sensitivity to the propagation parameters

As stated above, in the regional analysis we used the best propagation parameters obtained at a local scale. In particular, the CA01 case provided the maximum δ_m (Table 2.4), then adopted for the regional analysis.

The comparison between the inundated area over CA01 obtained from the regional scale simulation and from the local scale simulation, shows that the extension of the two propagations is very similar (Zoom 1 on Figure 2.8). The one obtained at a regional scale with a 10 m resolution has a wider spreading extension, but the runout distance is the same.

As to the regional scale, we additionally tested different routing parameters. We conducted 20 simulations within the following conditions:

- For the spreading calculation, we varied the x exponent of the Holmgren (1994) algorithm from 4 to 20.

- We also varied the runout function trying both travel angle and Perla function. In the case of the travel angle, we tested values from 10° to 12°. In the case of Perla function, we explored the field between M/D=30, μ=0.1 and MD=200, μ=0.02.
- Finally, we varied the flow velocity limit between 15 m/s and 20 m/s.

After every simulation, we counted the number of fans hit by debris flows. It has been obtained that the number of 56, resulting from the best simulation parameters (Table 2.5), varies of ± 10%. Furthermore, spreading deposition and runout distance show variations, with respect to the CA01 setting, of ± 25%. Based on the results, the propagation parameter setting, which was selected at the regional scale, has shown to be appropriate when coupled with *Method 2* to forecast the fans stroke by the event of August 2012.

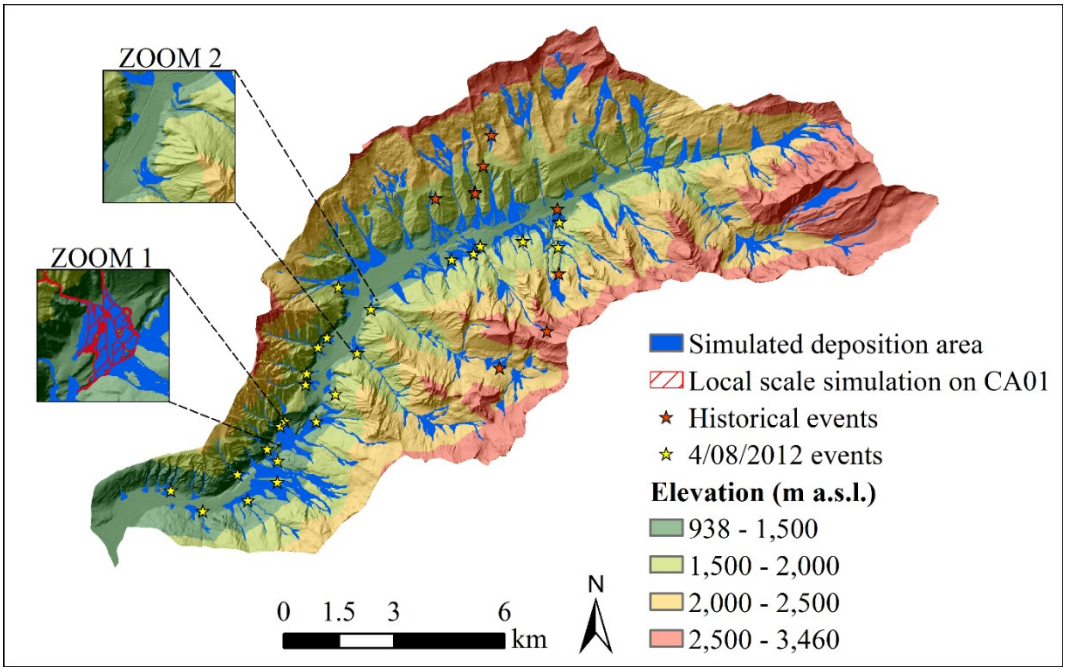

Figure 2.8: Final susceptibility map of the valley, with: (1) an overview of CA01 and its relative comparison with the simulated deposition at a local scale (zoom 1); (2) an overview of the two simulated deposition areas on Rio di Borgo and Rio di Montegrande (zoom 2).

Table 2.5: Comparison between the number of fans susceptible to debris flow obtained from Flow-R simulation, the historical analysis (ED30), the 4/08/2012 event (ED30) and the susceptibility map of the Province of Bozen.

Method 1 Flow-R	140
Method 2 Flow-R	56
Event of 2012	42
Susceptibility Map of the Province of Bozen	38
Historical events	12

2.6 Discussion

2.6.1 Single basin scale

At the single basin scale, the parameters that we wanted to identify were those for the computation of the spreading area and runout distance.

Even if Flow-R has been developed to work at a regional scale, the simulations made at the single basin scale showed good accuracy. The prediction quality at this local scale has been evaluated comparing the simulated propagation with the real deposition areas. We initially expected to find a set of spreading parameters like those used in previous studies. However, our results show that in this geographical area the simulation parameters are slightly different. For the computation of the spreading width, using the modified version of the Holmgren (1994) algorithm, previous authors suggested a value between 4 and 6 (i.e. Holmgren 1994; Claessens et al. 2005; Horton et al. 2008; Baumann et al. 2010). We found instead that a value of seven gave a better result. The accuracy value of CA01 using this exponent is the highest. The second important step is the choice between the SFLM model and the Perla et al. (1980) model for the computation of the runout. The two models gave similar results in all the three catchments, but the SFLM model, with a travel angle of 11° gave the best result. Another important parameter that we set is the velocity limit. Horton et al. (2013) suggested a value of 15 m/s, but we found that 20 m/s is the value that provides the simulated runout more like the real one. This highlights how a specific calibration of the velocity limit remains quite important to improve the Flow-R model performance.

2.6.2 Regional scale

At the regional scale, since the source areas are the most affecting factor on the resulting propagation, the main purpose was their correct identification.

The triggering mechanism is a part of the debris flow phenomenon not completely understood, especially in correspondence of areas characterized by moraines and loose debris (Rickenmann and Zimmermann 1993) as a great part of the upper zones of the Vizze Valley.

Method 1 can be defined as the default way for the identification of the source cells. Horton et al. (2011) evidenced that the morphological criteria derived from the DTM maps are the most important ones for the identification of the source areas. Whereas, the use of other input maps like for example land-use or geology helps to eliminate cells selected in correspondence of points that cannot be source areas (e.g. rocky outcrops). Considering that our land-use and geology maps had a low resolution, their implementation would not have influenced the output map. Therefore, we used as input maps: flow accumulation, terrain slope and planar curvature. The parameters that Flow-R uses for the analysis of these three input maps did not seem sufficiently sensitive, and too many cells were detected as possible triggering points, along the lateral sides of the valley (Figure 2.6).

In particular, the model analyses the flow accumulation map using one of the two implemented equations (i.e. Rickenmann and Zimmermann 1993; Heinimann 1998). In our case study, using these curves, the model identified source cells in all the gullies of the valley, without a good discrimination. Also Kappes et al. (2011) noted that Flow-R recognized the most part of the gullies as susceptible to debris flows.

With *Method 2*, we set as source cells those having a flow accumulation value higher than 0.1 km^2 and a slope angle higher than 15°. In this case, the cells selected as sources are more limited and focused on points with a stronger and more coherent connection with the channel network.

At this regional scale, the prediction quality has been evaluated comparing the resulted susceptibility map of the Vizze Valley with the historical debris flow events and the debris flows occurred on the 4th August 2012 event (Table 2.5). Flow-R (*Method 2*) recognized all the fans affected by past debris flow events as susceptible zones. The same happened also for the extreme debris flow event of 4th August 2012. Considering Table 2.5, we might conclude that the 2012 event, having a 300-year return period, is a good proxy of a quasi-maximum land susceptibility to debris flow hazard for the whole valley. Namely, a number of 56 fans resulted from the Flow-R (*Method 2*) application against 42 fans from the 2012 event and 38 from the susceptibility map of the Bozen Province. Furthermore, all comparisons between the modelling results and the above mentioned land information agree substantially in terms of spatial location of hazard-exposed fans. The goodness of these results benefits from the consistent assumption

of the triggering areas according to *Method 2*, as already outlined in the result section. Conversely, historical information could represent a view of near-to-minimal land susceptibility because only ¼ of the probable fans under hazard are reported (12 fans affected; Table 2.5) and none of these is novel in the Flow-R (*Method 2*) susceptibility map.

The possible involved fan areas have to be carefully analysed for the redaction of a hazard map. In fact, areas without registered events on the past still have a probability to be affected in the future (Suk and Klimánek 2011). Because people living on these zones have no memory of past events, they could have a wrong perception of no risk. On the other side, a poorly calibrated selection of the triggering source areas (*Method 1*) could bring to an exaggerated assumption of areas under risk and to a false need of protection.

Two catchments of the valley deserve a particular focus: Rio di Montegrande (Grossbergbach) and Rio di Borgo (Burgumerbach). These two basins are neighbours and are in the central part of the valley, on the left bank of Rio Vizze (Zoom 2 in Figure 2.8). They are the two largest catchments of the valley (9.1 km^2 for Rio di Borgo and 12.9 km^2 for Rio di Montegrande). Both streams suffered of a debris flow during the August 2012 event. On Rio di Montegrande, a significant debris flow that overflowed a filter check-dam was originated (volume of 90000 m^3) causing huge damages to the community of Fossa Trues (Fussendross). Whereas, on Rio di Borgo the debris flow volume had been of 50000 m^3. In both catchments, the model simulated several deposition areas in the upper and central part of the basins, but on the alluvial fans, the predicted deposits do not cover the real deposition areas of the 2012 event. The predicted runout distance is very similar to the real one, but the spreading width is thinner. Flow-R calculates the potential spreading only on a topographic base. In fact, using the Holmgren (1994) algorithm (Equation 2.2), the only significant variable is terrain slope (that is the elevation difference between two consecutive cells). Other variables, like for example flow velocity, volume of the debris surge, presence of control structures are ignored. All situations where large debris-flow volumes are in play in the reality could cause important under-prediction of flooded areas in terms of lateral spreading.

As to the model sensitivity to the setting of propagation parameters, the most effective and discriminating condition for the regional susceptibility remains the source areas assignation (*Method 2* in our case). The propagation conditions are significant, but they influence more the size of the inundated areas (e.g., runout distance, and spreading width), which are somewhat easier to control. To fulfill this issue, some local cases or historical documentation on the

studied region might be available or also some random geomorphic surveys could be undertaken in the field. Cases like CA02, where the local topography and morphology have been strongly modified by human actions, should be avoided.

Conversely, a complete and robust verification on the maximum land susceptibility at regional scale is more complicated, unless an extreme regional event is available like the case of 4th August 2012 in Vizze valley.

Method 2 has provided encouraging results but certainly merits further and deeper verification, because the two selected thresholds (upslope area and local slope) are likely - at least partially - sensitive to the catchment erodibility and soil permeability of the hillslopes. In any case, the availability of extreme and generalized debris-flow events at valley scale is quite rare within the step-mountain context and this pioneering verification could provide a first brick to our knowledge.

2.7 Conclusions

The creation of a susceptibility map with Flow-R seems an appropriate first step of analysis in a study of hazard and risk. In summary:

- Considering the complexity of debris flows, Flow-R enabled us to analyse the regional scale area with a minimum input data requirement and a short computation time;
- The simplicity of this model brings the disadvantage to ignore some important parameters. Therefore, the results have to be carefully analysed and compared with other data if possible;
- The back analysis using data from selected real events seems supportive to upscale the calibration carried out at local scale to the valley scale.
- Identifying the source areas separately from Flow-R, imposing at the same time a threshold of terrain slope and a threshold of flow accumulation area (*Method 2*), is a good alternative to the standard method of source identification of Flow-R (*Method 1*). The threshold of upslope contributing area that we set up with a GIS analysis seems a stronger discriminating factor than the upslope area-terrain slope relationship, in the case of alpine valleys characterized by an overall high slope gradient and geology, similar to Vizze Valley.

- All the streams interested by a past debris flow event have been recognized as susceptible areas and several streams not included in the digitalized channel network have been highlighted as susceptible areas;
- A topography-based model like Flow-R takes the advantage to generally overestimate the susceptible areas allowing to be more precautionary; nevertheless, for those basins producing large debris-flow volumes (e.g. >50.000 m^3) an additional spreading might be opportune to achieve a more realistic scenario in terms of flooded areas;
- The use of different triggering areas strongly affects the resulting propagation map. For this reason, we recommend that future studies will focus on the identification of the triggering areas and on their dependence on the geological conditions.

3 Correlation between the rainfall, sediment recharge and triggering of torrential flows in the Rebaixader catchment (Pyrenees, Spain)

3.1 Abstract

The debris flow (DF) and debris flood (DFD) activity in the Rebaixader catchment (Spanish Pyrenees) is analyzed in this study. The research is focused on how precipitation leads to the triggering of torrential floods and influences the sediment availability during the recharge period. Two kinds of correlations are studied: (1) the correlation between the rainfall features (intensity and kinetic energy) and the DF/DFD triggering and (2) the correlation between the hyetograph and the DF/DFD volumes. The tested hypothesis was that a greater amount of rainfall during the recharge period would produce a greater DF/DFD volume. The period between two consecutive DF/DFD events is processed using a variable, the erosion index, originally developed for the universal soil loss equation. This analysis considered the rainfall time series and 22 DF/DFD events registered during the period 2009-2015. The results show that the precipitation of the recharge period does not seem to have a strong influence on the mobilized volumes. In many cases, a second DF/DFD event was triggered soon after the previous event, which highlighted the role of the first event in creating an unstable state of the catchment. Additionally, a relationship between the erosion index and the maximum rainfall intensity for a 30-minute period seems a good criterion to discriminate between triggering and non-triggering rainfall events. The results show no clear trends with which to forecast the sediment-volume from precipitation, weakening the role of rainfall characteristics in determining the return period of mobilized sediment volumes in catchments like the Rebaixader torrent.

This chapter is an edited version of: Pastorello R, Hürlimann M, D'Agostino V. Correlation between the rainfall, sediment recharge and triggering of torrential flows in the Rebaixader catchment (Pyrenees, Spain). *Under review at Landslides.*

3.2 Introduction

Torrential flows such as debris flow (DF) and debris flood (DFD) are natural phenomena that affect mountain areas all over the planet (Hungr et al. 2013). Because of their characteristics, they are complicated events to forecast (Destro et al. 2017). They can occur with a range of magnitudes (Marchi and D'Agostino 2004), and they consequently cause considerable damage to human lives and infrastructures (Dowling and Santi 2014). Many studies demonstrated the fundamental role of precipitation in the triggering of a DF/DFD event, the rate of the available sediment and the total sediment volume delivered to the fan area (Deganutti et al. 2000; Bacchini and Zannoni 2003; Crosta and Frattini 2003, 2008; Borga et al. 2014; Abancó et al. 2016). A fundamental step to develop more efficient and reliable systems of prevention is to improve the understanding of the triggering mechanisms and to predict the mobilized volume and the recharge rate of sediments within the catchment. To this purpose, different catchments that are frequently subjected to DF/DFD events have been instrumented with meteorological stations and sensors. These sensors register the deposited volume and passed surges for a given cross section (Hürlimann et al. 2003; McArdell et al. 2007; Coe et al. 2008b; Berger et al. 2011; Comiti et al. 2014; Bel et al. 2017).

DF/DFD catchments can be divided into two different types: transport-limited (also named supply-unlimited) and weathering-limited (also named supply-limited) (Bovis and Jakob 1999; Jakob 2005). The transport-limited catchments are characterized by a high frequency of DF/DFD events, but they usually have, on average, a low magnitude because of their close sediment release. In these catchments, there is unlimited sediment availability, and so, a DF/DFD can be triggered every time the rainfall exceeds a defined threshold (e.g., intensity-duration, Guzzetti et al. 2008). The supply-unlimited basins usually have many erodible areas or "source areas" that are continuously prone to instability (D'Agostino and Bertoldi 2014). Therefore, other variables, in addition to sediment availability, play an important role in triggering the events and in the transport and deposition of the available sediment.

The second type of catchments, named supply-limited, has a limited sediment availability, and so, a DF/DFD event is triggered by rainfall only if the sediment quantity in a source area (channel network included) has reached or exceeded a defined threshold of accumulation (e.g., 50 years of sediment recharge due to weathering and water-driven transport processes since the last DF/DFD occurrence). In supply-limited basins, the frequency of the DF/DFD events is

usually lower compared to the supply-unlimited basins, but the magnitude of these events can be higher if the non-active periods are long. In these catchments, the time interval between two DF/DFD events is called the recharge period. In fact, during this rest time a catchment recharges itself with new loose debris. Often, after a DF/DFD event, source areas and channels have a smaller quantity of loose sediment that can be mobilized (Jakob 2005), so the recharge period is needed to accumulate new sediment. The length of this period depends on different factors, such as the presence of vegetation (Guthrie 2002), bedrock geology, meteorological characteristics, and the rate of erosional processes (Carrara et al. 2008; Dong et al. 2009). Conversely, Brayshaw and Hassan (2009) suggested that a substantial correlation of the timing and volume of a DF event with the following event might occur. In fact, in the period following a DF/DFD event, the catchment is more unstable and continues to promote the transportation of loose debris cover to the channel, which can facilitate the triggering of another event.

The key variable that leads to the triggering of a DF/DFD is the water runoff (Rickenmann and Zimmermann 1993; Berti and Simoni 2005; Gregoretti and Dalla Fontana 2008). This runoff is usually generated by intense rainfall events, and in fact, it has been demonstrated by many studies (Wieczorek and Glade 2005; Kappes et al. 2011, 2012; Reid et al. 2012; Cavalli et al. 2013) that the most common events causing debris flows are summer storms. These types of rainfall are usually characterized by a high intensity, i.e. a considerable amount of rainfall in a short time, capable of mobilizing the sediment cover. In other words, if the runoff is sufficiently intense, it can cause erosion and fluidization/mobilization of the debris cover and the consequent triggering of the DF/DFD (Berti and Simoni 2005; McCoy et al. 2010; Di Stefano et al. 2013).

To study a DF/DFD triggering area, the recharge rate of the basin (e.g., type, amount and location of loose sediment), the seasonal rainfall trend and other characteristics of the catchment must be known.

In a mountain territory with a high slope gradient and loose sediment, if rainfall conditions are sufficiently intense, debris flows are triggered with a variable frequency through time. The probability of occurrence depends on the morphological characteristics of the basins and the recharge rate during the intermediate period between two consecutive events (Jakob et al. 2005; Corominas and Moya 2008).

To briefly summarize the previous statements, it can be concluded that possible correlations between a DF/DFD volume and the duration of the recharge period, or as a proxy, the DF/DFD

timing with the amount of rain accumulated during the recharge period, are poorly investigated. The linkage between the return period of the DF/DFD volume and the physical characteristics of both the preparatory and triggering precipitation especially merits further investigation. The need for this knowledge is evidenced by the present approach to hazard map preparation and the design of protective structures against debris flows, since both tasks are very often based on the return period of the involved variables (e.g., critical rainfall intensities and subsequent transformation into runoff/sediment volumes).

In this study, we analyzed a small catchment named Rebaixader (Pyrenees, Spain) that has been equipped since the summer of 2009 with a monitoring system that records DF/DFD events and meteorological data (Hürlimann et al. 2014). In this supply-unlimited catchment, our research considers the following:

1. If the intermediate rainfall between two consecutive DF/DFD events affects the sediment recharge and consequently the mobilized volumes.
2. If the volume of DF/DFD events depends on (1) the intermediate rainfall (recharge period), (2) the triggering rainfall and/or (3) the critical rainfall kinetic energy linked to these rainfalls, similar to what Wischmeier and Smith (1978) have found in developing a universal soil loss equation (USLE).
3. If there are any triggering thresholds that are better performing than the classic intensity-duration thresholds. This could be a step forward from the traditional concept that the return period is related to the rainfall.

After the study area presentation, the materials and methods section illustrates how the rain data and information on DF/DFD volumes are used in the research. Correlations between the selected variables are shown in the results section. The discussion takes into consideration the results to fulfill the three research considerations described above and to highlight the elements of novelty in this approach. On Appendix 1 are presented the features of each DF/DFD event and are also supported the discussion and conclusion on the timing and agreement/disagreement between preparatory and generating precipitations and sediment volumes of the DF/DFD.

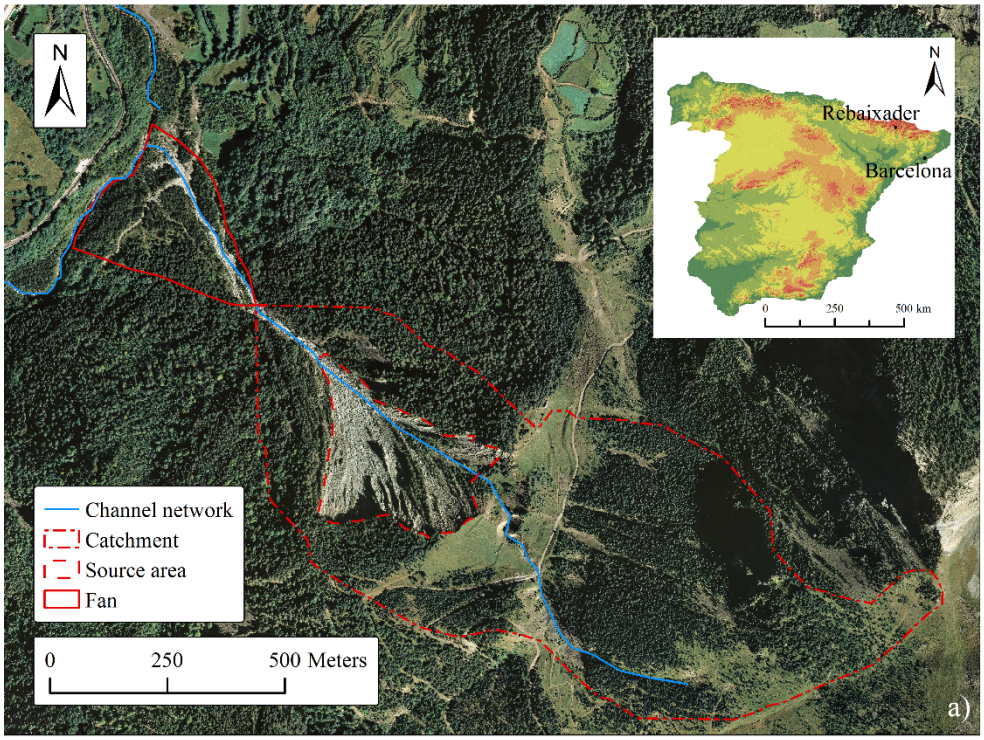

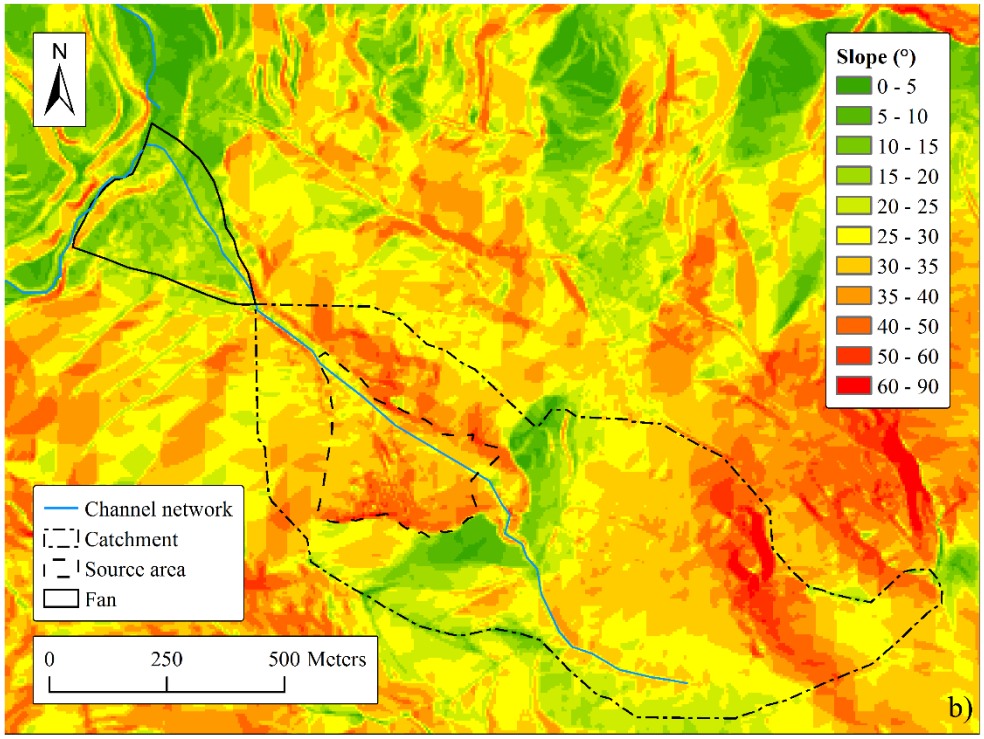

Figure 3.1: Map of the Rebaixader torrent catchment: a) orthophoto; (b) slope map.

3.3 Study area

The catchment analyzed in this study is crossed by the Rebaixader torrent and represents a typical high mountain watershed. It is in the Central Spanish Pyrenees, near the village of Senet, on the border between Catalonia and Aragon (Figure 3.1).

The catchment has a drainage area of 0.53 km^2 and an elevation that ranges between a maximum of 2310 m a.s.l. and a minimum of 1775 m a.s.l., the latter corresponding with the fan apex. The bedrock of the catchment is Paleozoic metamorphic rocks and mostly consists of Devonian slates and phyllites formed during the Hercynian orogeny (Munoz 1992). Colluvium and granular glacial deposits cover the bedrock. The large lateral moraine located between 1425 and 1710 m a.s.l. strongly affects the morphologic characteristics of the drainage basin and incorporates the source area of the DF/DFD events.

The catchment can be divided into two main zones: the upper part is characterized by the presence of forest and grassland. It includes steep slopes in the highest area and a flat area at approximately 1710 m a.s.l., which is associated with the upper limit of the lateral moraine. This upper part makes no significant contribution to the creation and accumulation of sediment. The lower part of the catchment is characterized by the presence of a large area covered by the loose debris of the lateral moraine, which is the source area of the DF/DFD events. The source area is linked to the fan by a short transport channel (Figure 3.1). Therefore, we can define this catchment as supply-unlimited, characterized by the presence of a unique, large source area.

The source area has an area of approximately 0.09 km^2, a mean slope angle of 35° with a maximum value of 61°, and an altitudinal gradient that ranges from 1709 m a.s.l. to 1400 m a.s.l. (the point where the transport channel originates). The loose sediment of the large lateral moraine that is frequently subjected to erosion characterizes this part of the catchment. These sediments range in size from sand/gravel to boulders with a diameter of several meters (for more details on the grain size distribution, see Hürlimann et al. 2012). An example of the morphology of the source area is shown in Figure 3.2, where the particular erosive pattern of a "badland-like" zone is evident and presents sparse and vegetated 'islands' of apparent stability. The steepness of the large source area and the availability of loose sediment have made the catchment very active, as confirmed by the occurrence of several DF and DFD events per year.

The transport channel is approximately 200 m long and has a width of approximatively 10 m. A fan forms the accumulation area of the catchment, and the Noguera Ribagorçana River bounds it.

In the summer of 2009, a monitoring station system was installed in the source area and transport zone. It comprises three main parts: (1) the meteorological station that includes other sensors and a rain gauge that registers rainfall with a 5-minute temporal resolution; (2) the station that has 8 geophones, an ultrasonic device, a radar sensor and a video camera to detect and characterize the flow dynamics of the events; and (3) the infiltration stations that include sensors to measure the soil moisture and water pressure. Detailed information on the monitoring system can be found in Hürlimann et al. (2014).

Between September 2009 and December 2015, a total of 29 events where registered, averaging more than four events per year.

The meteorological characteristics of the area are particularly influenced by the proximity of the Mediterranean Sea and the presence of the Pyrenees. The mean annual precipitation in this part of Catalonia ranges between 800 mm and 1200 mm (Hürlimann et al. 2016). The mean annual precipitation registered by the rain gauge of the monitoring station is 945 mm per year, with a minimum value of 700 mm and a maximum of 1100 mm.

Figure 3.2: A peculiar “badland-like” morphology located in the source area.

3.4 Materials and methods

The main data used in the analysis consist of two time series: (1) the rainfall data from September 2009 to December 2015, measured at a time step of 5 minutes, and (2) the volume of the DF/DFD events measured during the same period. The volume assessment for each DF/DFD was principally performed by the interpretation of the monitoring data and cross-checked by the post-event morphologic observations along the channel and on the fan. The duration, the flow velocity and the flow area of the DF/DFD events were determined by the data collected from the geophones, the ultrasonic sensor and the video camera. A detailed explanation of the volume assessment can be found in Hürlimann et al. (2014).

The time series registered by the rain gauge of the meteorological station were not complete because of functional problems of the instrument. Therefore, we used the data sets registered by a nearby rain gauge to fill the gaps in our time series. This second rain gauge is located at the hydropower dam of Baserca (approximately 3.2 km north of the Rebaixader catchment) and has a registration time step of 15 minutes.

The complete rainfall series of the Rebaixader rain gauge were analyzed with R software (R Development Core Team 2005). With a script that reads the date and time of every registered value, we were able to find all the gaps in the initial time series data. Once these gaps were identified, they were filled using the rainfall data registered by the rain gauge from Baserca. The final resolution of the resultant time series is 15 minutes for 2013 and 5 minutes for the other years.

The next step consisted of the identification of every rainfall event inside the time series registered by the rain gauge. From these time series, the rainfall events were defined by identifying a one-hour interval without precipitation before and after the event. This interval is similar to the ones used in companion studies (e.g., Deganutti et al. 2000; Badoux et al. 2009; Abancó et al. 2016). We excluded the events with a total precipitation of less than 4 mm. This limit was defined because the minimum triggering rainfall measured in the catchment was found to be 4.7 mm.

Using the extracted rainfall events, we calculated multiple variables related to the precipitation characteristics for each of the DF/DFD events: (1) total precipitation (P_{tot}), (2) total duration (D_{tot}), (3) maximum intensity within a 30 minute period during the event ($I_{30\,MAX}$), (4) maximum intensity within a 15 minute period during the event ($I_{15\,MAX}$), and (5) erosion index of the event

($EI_{\Delta t\ MAX}$) (Table 3.1). This last characteristic expresses the rain erosivity adopted by Wischmeier and Smith (1978) to calculate the soil loss for a given soil erodibility. This erosivity is calculated as the product of the total kinetic energy of the rainfall event (E) and the maximum intensity observed within a 30-minute period during the event. Originally, this index was created to study the temporal range of several years and rainfall time series with a temporal resolution from 5 to 60 minutes (Panagos et al. 2015). Nevertheless, we decided to use this index to study single rainfall events and specific time spans (recharge or triggering periods) because it allows us to summarize different characteristics of the rainfall event at the same time (intensity, duration, total rainfall and kinetic energy). Therefore, it is more physically significant than methods that consider only the rainfall depth/intensity. In the newer version of RUSLE (Kinnell 2010; Panagos et al. 2014, 2015), this calculation can be coupled with other factors. In our case, considering that the type of terrain topography analyzed here is extremely different from flat areas (the classic case study of the erosion index), we used the first version of the equation developed by USLE (Wischmeier and Smith 1978).

Hence, we made some changes to the initial assumptions of Wischmeier and Smith (1978) for defining the threshold for selecting erosive events. The original assumptions are as follows: (1) total rainfall depth higher than 13 mm and (2) at least 6 mm of rain within 15 minutes. Since we are working in a very steep environment, with a land cover of coarse-grained sediment, we decided to eliminate the lower limit to rain erosivity and use a total rainfall depth of at least 4.7 mm. The steps for the computation of the $EI_{\Delta t\ MAX}$ are as follows:

- Computation of the kinetic energy (e_k) of every time step during the event with the following equation (Wischmeier and Smith 1978):

$$e_k = 0.119 + 0.0873 \log_{10} i_{\Delta t} \quad (3.1)$$

  Where $i_{\Delta t}$ is the hourly intensity corresponding to the time step of computation.
- Calculation of the total kinetic energy of a single time step with the following equation:

$$E_k = P\ e_k \quad (3.2)$$

  where P is the rainfall registered in the considered time step.

– Finally, the erosion indices are calculated as follows:

$$EI_{\Delta t\ MAX} = I_{\Delta t\ MAX} \ \sum E_k \tag{3.3}$$

where Δt indicates the reference duration, either 30 or 15 minutes, for which the maximum intensity $I_{\Delta t\ MAX}$ occurred during the event (recharge event or triggering event) is computed ($I_{30\ MAX}$ or $I_{15\ MAX}$).

The $EI_{\Delta t\ MAX}$ values are used for two different analyses: the single $EI_{\Delta t\ MAX}$ values of every DF/DFD event from the triggering to the end of the flow are considered as the "triggering" values ($EI_{\Delta t\ TRIG}$). The sum of the $EI_{\Delta t\ MAX}$ values of all the rainfall events between two consecutive DF/DFD values are considered as the $EI_{\Delta t\ MAX}$ of the "recharge period" ($EI_{\Delta t\ RECH}$). The values of the $EI_{\Delta t\ TRIG}$ and the $EI_{\Delta t\ RECH}$ versus DF/DFD volumes are processed to verify if there is some correlation between the soil erosion caused by rainfall and the amount of mobilized volume. The $EI_{\Delta t\ TRIG}$ values indicate if the volume of the DF/DFD event is conditioned by the rain erosivity affecting the triggering area. The $EI_{\Delta t\ RECH}$ corresponds to the cumulated rainfall erosivity during the recharge period. As stated in the introduction, different authors (i.e., Bovis and Jakob, 1999; Brayshaw and Hassan, 2009) explain that there are two types of DF/DFD catchments: "supply-unlimited" catchments, where there is always available sediment, and "supply-limited" catchments, where the morphological characteristics are different so there is not always available sediment to trigger DF/DFD events. In supply-unlimited basins, there is a rainfall threshold that, if exceeded, leads to the triggering of DF/DFDs because there is always enough available sediment. However, in supply-limited catchments, there is not always enough available sediment for the triggering. Therefore, there is a period of time, named the recharge period, in which the basin recharges itself with newly available sediment. In this case, a rainfall threshold alone is not sufficient to generate a debris flow, there is a coupled sediment recharge threshold, and the DF/DFDs will be triggered if only both thresholds are exceeded.

We have no topographic measurements or data describing the sediment recharge in the period between two consecutives DF/DFD events. Therefore, we used the volume of the DF/DFD events as a proxy variable of sediment availability before each DF/DFD event. The initial assumption was that a greater recharging rainfall would correspond to a larger volume of the

following event. Therefore, we distinguished between recharging variables, which influence the recharge period and do not directly affect the triggering of the DF/DFD, and triggering variables, which directly concern the triggering precipitations. We carried out a back analysis considering the volume of the DF/DFD as an indirect measure of the sediment recharge that characterizes the recharge period before the DF/DFD occurrence. This is a simplified model because we are assuming that all of the sediment available to a DF/DFD event is mobilized when the rain threshold is exceeded. The purpose of this simplification is to understand if there is a direct correlation between the different energetic features of precipitation and sediment recharge.

Following the findings of the work of Abancó et al. (2016), we also analyzed how the 15- and 30-minute intensity and $EI_{\Delta t\ MAX}$ of the triggering event directly influence the volume of the torrential event, reducing the significance of the role of the recharge period.

Finally, the last analysis was conducted to verify if it is possible to extract a DF/DFD triggering threshold by coupling the 30-minute intensity ($I_{30\ MAX}$) with the $EI_{\Delta t\ TRIG}$.

Table 3.1: Parameters calculated for every DF/DFD event registered in the period between the summer of 2009 and December of 2015.

					Sediment recharge period parameters				Triggering event parameters			
Date	Antecedent 3 days rainfall (mm)	Type	Volume (m^3)	Recharge period (days)	P_{tot} (mm)	$I_{30\ MAX}$ (mm/h)	$I_{15\ MAX}$ (mm/h)	$EI_{30\ MAX}$ (MJ mm/ha h)	P_{tot} (mm)	$I_{30\ max}$ (mm/h)	$I_{15\ MAX}$ (mm/h)	$EI_{30\ MAX}$ (MJ mm/ha h)
01/09/2009	-	Flood	1000	-	-	-	-	-	46.20	26.00	44.00	276.86
25/03/2010	12.80	**Flow**	2100	205	442.60	20.60	24.00	763.28	21.20	13.00	18.00	50.60
11/07/2010	0	**Flow**	12500	108	128.30	14.20	25.60	169.24	21.20	59.80	65.20	1508.95
21/07/2010	0	Flood	1000	10	0	0	0	0	11.00	20.80	34.80	55.11
09/10/2010	21.00	Flood	1600	80	94.90	13.60	14.40	186.09	60.40	21.60	31.20	269.28
13/07/2011	0	Flood	700	277	409.50	15.60	24.80	405.21	12.00	18.40	36.00	51.47
05/08/2011	0	Flood	2800	23	0	0	0	0	13.80	27.60	47.60	98.67
05/08/2011	13.80	Flood	2500	0	0	0	0	0	15.6	29.80	45.60	117.43
07/08/2011	29.40	Flood	350	2	0	0	0	0	12.50	20.80	29.20	61.66
03/11/2011	5.60	Flood	600	88	126.00	13.40	49.20	200.56	63.60	18.80	28.00	225.61
27/06/2012	0	**Flow**	4000	237	240.60	13.80	17.20	282.46	17.70	25.60	39.60	104.30
04/07/2012	0	**Flow**	16200	7	0	0	0	0	17.30	28.80	48.80	119.78
05/07/2012	17.30	Flood	1000	1	0	0	0	0	4.70	8.40	15.60	8.29
05/06/2013	4.40	Flood	2100	335	426.20	20.20	33.60	404.19	21.80	14.00	16.00	61.78
17/06/2013	8.20	Flood	100	12	22.40	10.00	19.20	31.67	5.20	10.00	11.20	10.55
23/07/2013	16.20	Flood	600	36	74.80	19.20	35.20	154.30	17.80	29.60	48.80	128.86
27/07/2013	17.80	Flood	450	4	0	0	0	0	15.20	28.00	47.20	105.20
06/09/2013	0	Flood	941	41	135.20	24.00	46.40	326.32	6.90	12.20	20.40	18.40
20/07/2014	0	Flood	1000	317	427.50	18.20	23.60	599.76	12.90	21.80	30.40	64.77
25/07/2014	12.90	Flood	1150	5	0	0	0	0	12.60	23.00	34.00	68.35
13/08/2014	0	**Flow**	14000	19	0	0	0	0	18.50	19.80	26.80	76.39
31/07/2015	52.20	Flood	400	352	438.60	32.40	58.40	859.70	42.40	45.20	69.60	455.27

3.5 Results

3.5.1 Influence of the rainfall characteristics on the DF/DFD events

From the DFD events of the $EI_{\Delta t\ RECH}$ (i.e., the erosion index of the recharge period) versus volume in Figure 3.3, it can be observed that the volume does not follow a particular trend, and it seems completely independent from the erosion index during the recharge period. Similarly, for the DF events, the volume is not influenced by the $EI_{30\ RECH}$, and so, it seems that there is no correlation between the DF volume and the $EI_{30\ RECH}$. Nine of the DF/DFD events are located on the y-axis because for those events, there was no intermediate rainfall since the previous event; this is the reason why they have $EI_{30\ RECH}$ values equal to zero.

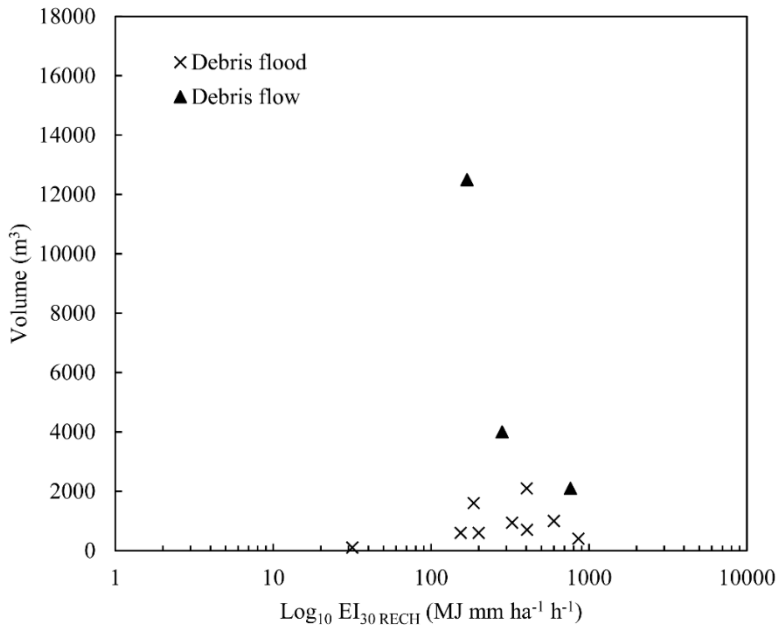

Figure 3.3: Correlation between the erosion index calculated for the recharge period and the volume of the corresponding DF/DFD event.

From observations of the $EI_{30\ TRIG}$ results (i.e., the erosion index of the triggering rainfall event), it can be noted that there is a somewhat positive correlation with the volume of the events (Figure 3.4). This result suggests that the "instability" caused by the triggering rainfall influences the magnitude of the event. This means that with greater the rainfall energy, the volume of the mobilized debris is greater. Moreover, the $EI_{30\ TRIG}$ is composed of both the

rainfall quantity and the rainfall intensity, so it simultaneously considers different rainfall characteristics. The range of the $EI_{30\ TRIG}$ is very close to the range of $EI_{30\ RECH}$; more precisely, the first varies from approximately 100 to 1000 MJ mm/ha/h and has a range slightly larger than that of the $EI_{30\ RECH}$ (Figure 3.3 and Figure 3.4).

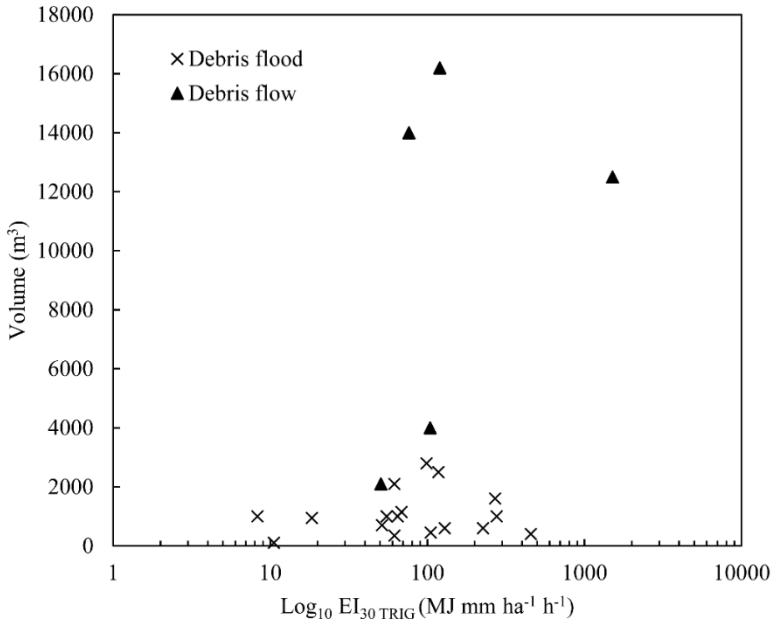

Figure 3.4: Correlation between the triggering erosion index and the volume of the corresponding DF/DFD event.

Considering the results, the behavior of a supply-unlimited catchment (Bovis and Jakob 1999) emerges. In fact, it seems that there is not a significant triggering threshold of rainfall, since there are some DF/DFD events that are triggered by the smallest rainfall events recorded. The minimal triggering rainfall occurred on 5/07/2012 and totaled only 4.70 mm with a total duration of 80 min (Table 3.1).

The variable that provides some correlation with volume is the rainfall intensity, in particular, $I_{\Delta t\ MAX}$ (Figure 3.5). For the DFD events, there is no correlation, since the volume data are sparse, as shown in Figure 3.5. However, for the DF events, it seems that a higher rain intensity corresponds to a greater flow volume. This link with the volume is slightly higher for $I_{15\ MAX}$ (a) than for $I_{30\ MAX}$ (b), and in both cases, we can conclude that the volume of the DFD events are below the upper limit of the DF volume (approximately 2000 m^3). Moreover, it is interesting to notice that the triggering intensities (Figure 3.5) of the DF events are not different from those

of the DFD events. This means that a rainfall event can trigger either a DF or a DFD and confirms our hypothesis that the switch from a DFD to a DF should be explained by other factors.

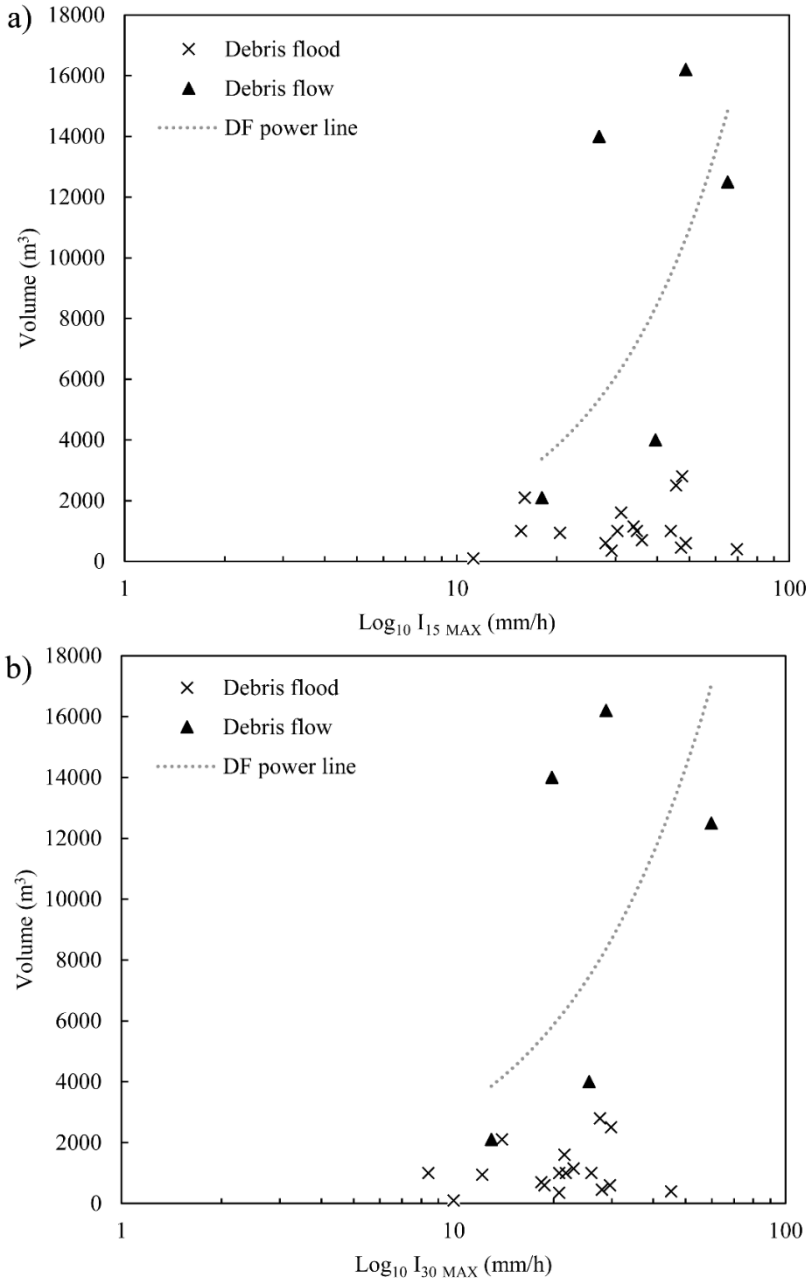

Figure 3.5: Correlation between the maximum intensity within 15 (a) and 30 (b) minutes and the volume of the corresponding DF/DFD event; fitting line for only the DFs.

An interesting correlation can be observed between the $EI_{30\ TRIG}$ and $I_{30\ MAX}$ in Figure 3.6. For the values of $EI_{30\ TRIG}$ lower than 8 MJ mm/ha/h (left part of Figure 3.6), there is no DF/DFD triggering. Whereas for the values of $EI_{30\ TRIG}$ greater than 8 MJ mm/ha/h, the graph can be divided in two parts by the power law relationship of the 95% triggering probability. Below the power law relationship there are five false negative predictions (4 DFD and 1 DF), whereas above it, the highest triggering probability exists: 18 true positive events against a total of 23 DF/DFD events (Table 3.2). Therefore, a specific value of the $EI_{30\ TRIG}$ is needed to trigger a DF/DFD event ($EI_{30\ TRIG} > 8$ MJ mm/ha/h). Moreover, the specific characteristics of the triggering storm (i.e., $I_{30\ MAX}$) are more capable of discriminating the triggering threshold: if $I_{30\ MAX}$ exceeds approximately 4 times the value of $EI_{30\ TRIG}^{0.37}$ (equation in Figure 3.6), the occurrence of a DF/DFD is almost certain. Conversely, if $I_{30\ MAX}$ does not reach this specific threshold (4 $EI_{30\ TRIG}^{0.37}$), a DF/DFD will not be triggered (Figure 3.6).

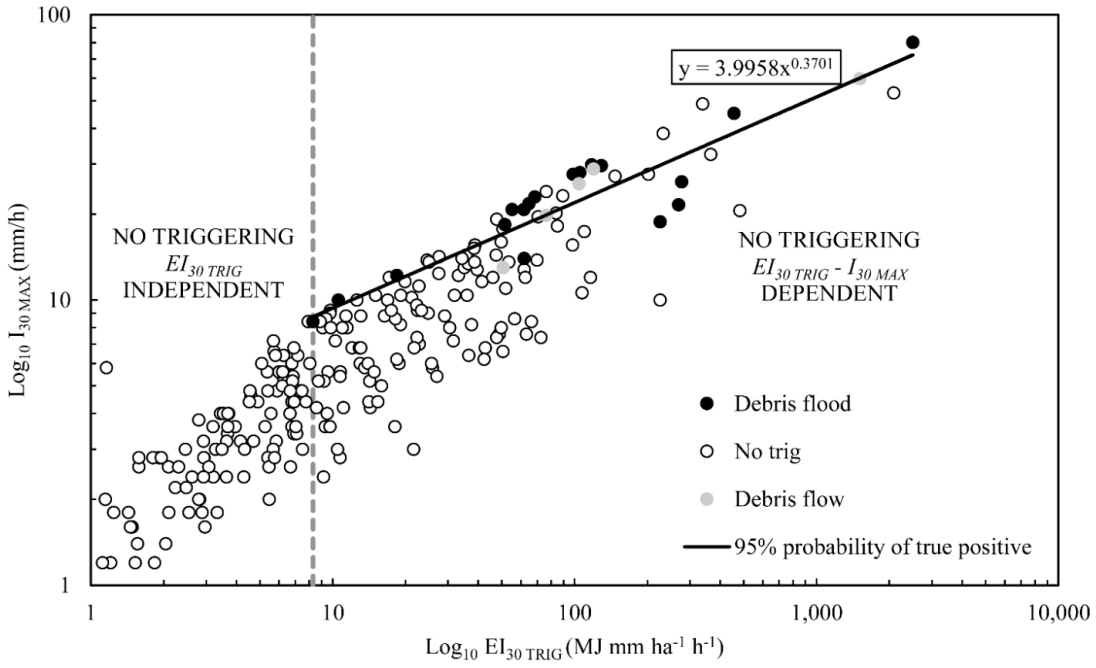

Figure 3.6: Differences between the rainfall events that triggered and did not trigger DF/DFD events. The "No trig" elements correspond to the rainfall events that did not triggered any torrential event. The "95% probability of true positive" power law relationship interpolates the DF and DFD events (equation shown inside the graph).

Table 3.2: Sensitivity analysis of the triggering and non-triggering events obtained from Figure 3.6.

	n°	%
TP	17	77.27
FP	12	5.41
TN	210	94.59
FN	5	22.73

3.5.2 Seasonal behavior of the catchment

Multiple variables contribute to the triggering mechanism: the antecedent DF/DFD volume, the triggering rainfall characteristics, and the length of the recharge period, among others. Therefore, it is important to describe the typical behavior of the Rebaixader catchment. Figure 3.7 shows an overview of the event history of the Rebaixader catchment during the years analyzed. The total amount of precipitation is compared with the total amount of sediment volume mobilized by the torrential flows between the summer of 2009 and the end of 2015. Generally, every year can be divided into four typical periods: (1) December to February (winter), (2) March to May (spring), (3) June to August (summer), and (4) September to November (autumn). Figure 3.7a shows that no DF/DFD events were triggered during the winter. During the spring, a single DF/DFD event was triggered (25/03/2010). Summer was the most active period, with 77% of all DF/DFD events occurring in that period. Finally, in the autumn, the number of triggered DF/DFD events was slightly lower (18%) than in the summer. From Figure 3.7b and c, it can be concluded that the mobilized sediment trend does not follow the same distribution as the precipitation. This means that the total rainfall amount during the recharge period is not enough to explain or predict the behavior of the sediment supply and mobilization. Therefore, to consider the seasonal behavior it is important to individually analyze every DF/DFD event. A summary of this description and a detailed examination can be found in the Appendix 1.

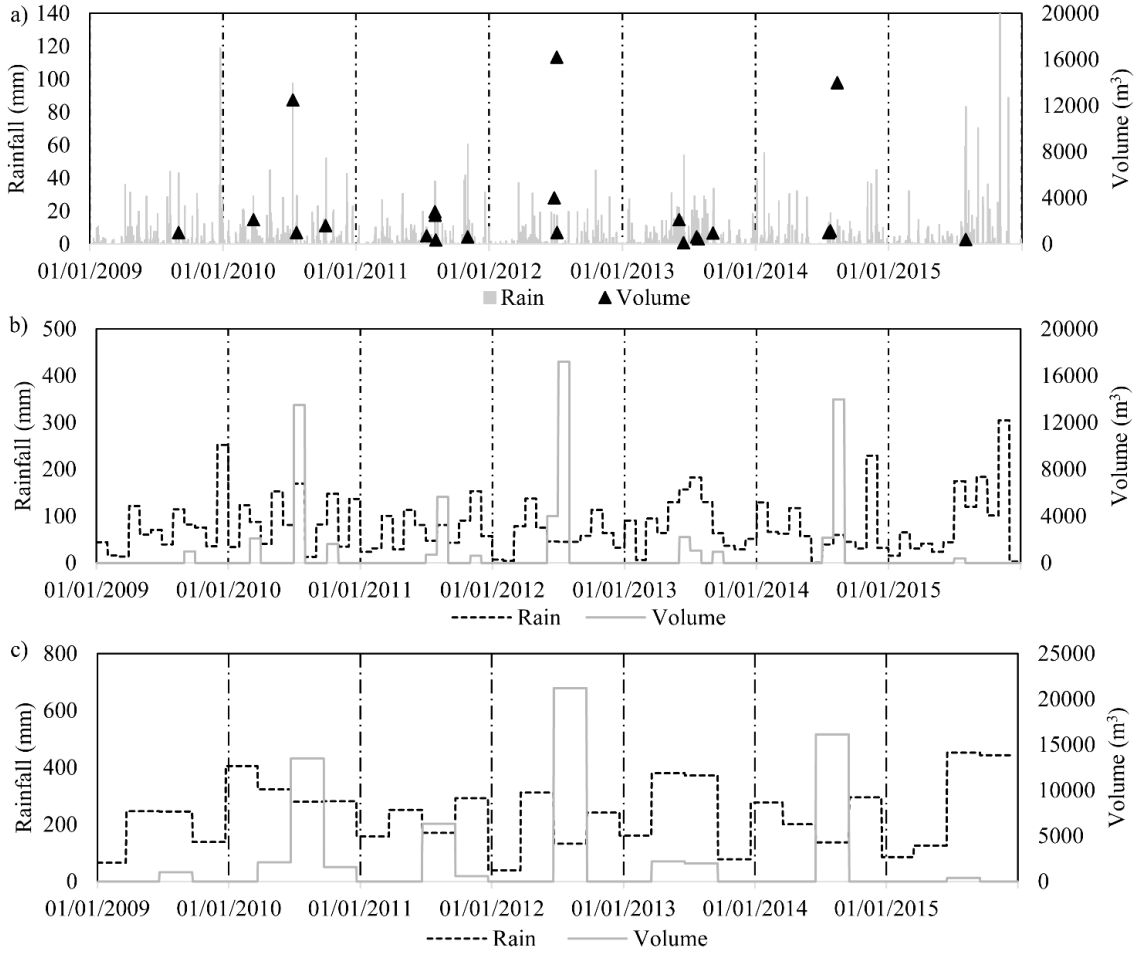

Figure 3.7: Distribution of the rainfall and volume of the DF/DFD events in the years of the analysis: a) daily rainfall versus volume of the single events, b) monthly rainfall versus cumulated monthly DF/DFD volume, and c) seasonal rainfall versus cumulated seasonal DF/DFD volume.

Another analysis of the influence of the recharge period on the event volumes can be seen in Figure 3.8. Here is shown the comparison between the volumes of two consecutive DF/DFD events, normalized by the corresponding $I_{30\ MAX}$ of the triggering phase. The event pairs that occurred less than 20 days from each other are reported; in the case of the occurrence of three close events, the intermediate one is plotted two times in Figure 3.8 as the second of the first couple of DF/DFD events and the first of the second couple of events. The general trend is that the normalized second event was smaller than the normalized first event, and in only two cases (numbers 4 and 9 in Figure 3.8), the second event was much larger than the first one.

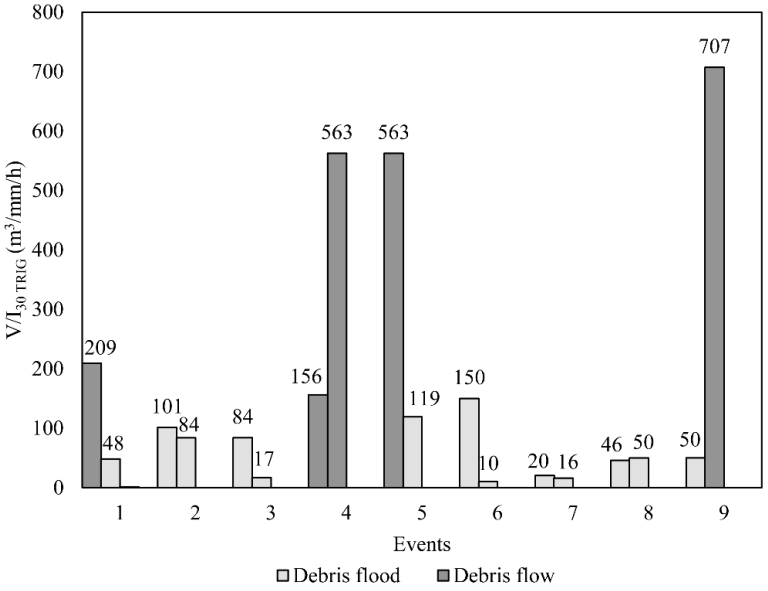

	1st EVENT	2nd EVENT
1	DF 11/07/2010	DFD 21/07/2010
2	DFD 05/08/2011	DFD 05/08/2011
3	DFD 05/08/2011	DFD 07/08/2011
4	DF 27/06/2012	DF 04/07/2012
5	DF 04/07/2012	DFD 05/07/2012
6	DFD 05/06/2013	DFD 17/06/2013
7	DFD 23/07/2013	DFD 27/07/2013
8	DFD 20/07/2014	DFD 25/07/2014
9	DFD 25/07/2014	DF 13/08/2014

Figure 3.8: Comparison between the normalized volume (normalized by $I_{30MAX\ TRIG}$) of a DF/DFD event and the subsequent DF/DFD event that occurred within a time span of less than 20 days. In the table are shown the data and type of event regarding the coupled events

3.6 Discussion

The first hypothesis to test of the present work was that a correlation between the rainfall during the recharge period and the volume of the next event existed. Moreover, we hypothesized that a greater rainfall amount during the recharge period would correspond to a greater available (and consequently mobilized) sediment load. To study this correlation, we analyzed all rainfall events using the $EI_{30\ MAX}$ variable. The $EI_{30\ MAX}$ incorporates the duration, the $I_{30\ MAX}$ and the total energetic contribution of the rainfall and it strongly expresses the rainfall characteristics and its capacity to produce sediment. The $I_{30\ MAX}$ plays the most important role. In fact, a rainfall event that not only has a short duration and relatively low total rainfall depth but also a high intensity can result in an $EI_{30\ MAX}$ index much higher than that of a rainfall event with very long duration and low intensity (Xie et al. 2016). This is a good feature of the selected indicator because we know that a DF/DFD is typically triggered by short and strong rainfall events (Floris et al. 2010), so it is clear that these are the events that more easily entrain and transport sediments downstream.

We expected to find some correlation between the $EI_{30\ RECH}$ and the volume of the following DF/DFD event, but no significant trend has been observed. It was noted in the results section

that there is not a positive correlation between the erosion index of the recharge period and the DF/DFD volume. This fact proves that basin preparation due to non-triggering rainfalls during rest periods has a small effect on future sediment volumes of DF/DFD events in situations comparable to that of the Rebaixader torrent. The lack of correlation demonstrates that other stochastic factors play a more important role in the preparation of new erodible material than rainfall during the recharge period.

It is worth stressing that our experimental basin is characterized by very frequent DF/DFD events, so the recharge periods are on the order of months. Therefore, the first events of every year are usually characterized by higher erosion indices because of the longer time since the last event and considerably greater volume of water input during the recharge period. A catchment with a recharge period on the order of tens to several tens of years (supply-limited type) would probably produce different results, and the erosive work of the precipitation could be more effective.

In contrast, a positive correlation between the $EI_{30\ TRIG}$ and the volume of the triggered flow is evidence of the dominance of the energetic/episodic impulse both on the triggering conditions (Figure 3.6) and on the volume magnitude (Figure 3.4). In any case, $I_{30\ MAX}$ and $I_{15\ MAX}$ of the triggering rainfall events (Figure 3.5) show a statistically insignificant correlation with the DF/DFD volume, confirming that the DF/DFD magnitudes remain weakly precipitation dependent. Other studies have already demonstrated the small role of the intensity in the magnitude estimation of the triggered event (e.g., Gartner et al. 2008). Our conclusion on this issue, in the case of the Rebaixader torrent catchment, is that using the triggering rainstorms of a given return period (i.e., derived from the hydrological statistics of rain data) to estimate the corresponding/equivalent return periods of expected DF/DFD volumes should still be done cautiously.

Since the rain intensity values, if used alone, are not capable of discriminating between the type of event (DF or DFD), the previous conclusion is corroborated and in accordance with the results found by Cannon et al. (2001). In the types of basins that behave like the typical supply-unlimited catchment (e.g., the Rebaixader torrent catchment), for which a single rainfall event intensity can trigger DF/DFD events with a range of magnitudes, a discriminatory criterion that is based on the precipitation pattern and intensity to forecast low-volume DFDs rather than high-volume DFs seems to be extremely difficult to construct. This last issue emerges clearly from the data of our study catchment, where a discrimination would have been useful if first

conditioned on the process type because of the difference in sediment volumes (DF or DFD in the Rebaixader catchment; Figure 3.3 and Figure 3.4). For example, a rainfall event with a very low intensity, such as the one triggered on 5/07/2012 (8.4 mm/h), was capable of triggering a DFD; conversely, events such as those that occurred on 11/07/2010, 23/07/2013 and 31/07/2015 were triggered by high rainfall intensities (Table 3.1).

Additionally, the results obtained by Theule et al. (2012) showed that the minimum rainfall intensity that causes the mobilization of sediments in the Manival torrent is not very high (7 mm/h), which is very similar to the minimum rainfall intensity measured in the Rebaixader catchment (Table 3.1). Furthermore, our results highlight that the same rainfall event can trigger, without discrimination, events with sediment volumes that range over at least one order of magnitude. For example, if the range of the triggering $I_{15\ MAX}$ rainfalls range from approximately 10 to 70 mm/h (Table 3.1), these similar rainfall events can trigger DF/DFD events from 2000 up to 14000 m^3. The same relationship can also be observed for greater $I_{15\ MAX}$ values.

Unlike the difficulty of forecasting process-type catchments, the threshold line from $I_{30\ MAX}$ and $EI_{30\ TRIG}$ (Figure 3.6) is highly capable of improving the distinction between triggering and non-triggering rainfall events. In fact, the results obtained by Abancó et al. (2016) using the classic intensity-duration graphics resulted in a value of false positive of 5.6%. In our case, this value is 5.4% (Table 3.2), with 17 events actually triggered out of a total of 22 predictions (true positive) and only 12 events out of a total of 222 predictions that plot above the line (false positive). The two regions in Figure 3.6 stress that first the triggering must be energetic enough ($EI_{30\ TRIG} > 8$ MJ mm/ha/h), and then, above this primary threshold, the $I_{30\ MAX}$ value is used to determine the DF/DFD occurrence. This response could be interpreted as the coexistence of a double condition for triggering: sufficient erosive work of the rain ($EI_{30\ TRIG}$) and a high enough overland flow rate to rapidly move and entrain the eroded particles (e.g., hillslope debris flow).

The record of temporal proximity between two or more DF/DFD events seems to add some additional information on the event sequence in the Rebaixader catchment. In fact, of a total of 22 events, in 9 cases the next event occurred less than 20 days after the previous one. In these cases, the recharge period was 0 days because the total rainfall in the interval between the two events is 0 mm (Table 3.1). Looking in particular at the DFD events, it seems that the "standard" scenario was that of a cleaning behavior, meaning that the second event was smaller than the first one, so it removed only a small volume of sediment left by the previous event. In only two

cases, the volume of the second event was much larger than the first one. This scenario seems to occur due to a kind of switch of the event magnitude, both in terms of the total solid volume (V) and normalized solid volume ($V/I_{30\ TRIGG}$), which obliterated the memory effect of the previous DF/DFD with much larger volumes of a DF event (and not a DFD; see also Figure 3.8). Therefore, these two event pairs partially confirm the behavior described by Brayshaw and Hassan (2009), in which the instability caused by the antecedent event could leave the catchment in a more unstable state, but the final response, which is a greater or larger volume than the expectation, remains uncertain. The relict presence of loose debris in the source area and in the transport channel could have facilitated the sudden triggering of a DF/DFD event. Such a scenario also explains why, in some cases, the triggering rainfall events had a low intensity and a low total precipitation (Table 3.1). This increment of basin susceptibility to DF/DFD events has also been described by Coe et al. (2008) for the Chalk Cliffs study area. In fact, they found that the period between two DF/DFD events can be very short and a DF/DFD is triggered, in some cases, by rainfall events that have a low return period. Conversely, Berger et al. (2011) found that in the Illgraben catchment, the channel segments recently incised by DF events have a lower probability of triggering another event in a short time, since right after the first event the area is relatively more stable.

In short, there is no definitive answer for the effect of torrential floods, but it may be concluded that, given a catchment with a high sediment supply, the second event response, when the triggering threshold is exceeded, appears contradictory: it generally tends to be lower or of the same order but is likely higher when a DF follows a DFD.

3.7 Conclusions

In this study, we analyzed a small catchment located in the Spanish Pyrenees and characterized by unlimited sediment supply. We tried to understand the correlation between the sediment accumulation during the recharge periods between consecutive events and the intermediate rainfalls during the same periods. We wanted to know if the mobilized volume was influenced by the intermediate rainfalls and/or by the triggering rainfalls. To reach this objective, we used some significant rainfall parameters (i.e., $I_{\Delta t\ MAX}$ and $EI_{\Delta t\ MAX}$), and the results brought us to the following conclusions:

- The volume of the DF/DFD events was not related to the intermediate rainfalls of the recharge period; namely, similar rainfall events were able to trigger DF/DFD events with very different magnitudes. In short, it seems inappropriate to link the volume of the DF/DFD events to the return periods of the triggering rainfall.
- The analyzed rainfall parameters ($I_{\Delta t\ TRIG}$ $EI_{\Delta t\ TRIG}$) were highly capable of discriminating between triggering and non-triggering of the DF/DFD events.
- Many DF/DFD events were triggered soon after the previous ones, showing that the susceptibility to DF/DFD triggering tends to increase, the amount of sediment volume of the second event was difficult to predict, and the process-type (DF or DFD) dominates the released volume.
- The calibration of a threshold relationship between $I_{30\ MAX}$ and $EI_{30\ TRIG}$ results is an excellent strategy to discriminate between triggering and non-triggering DF/DFD events. This type of calculation might be a good alternative and more robust than the classic intensity/duration analysis and merits further confirmation, particularly in those instrument-equipped DF/DFD basins where rain gauges and triggering areas are proximate.

4 Rainfall durations and corresponding dominant mechanism for the initiation of debris flows in three headwater basins characterized by different geomorphological settings

4.1 Abstract

This study is focused on the identification of the rainfall duration needed to reach the critical discharge for the initiation of debris flows in three different mountain catchments. Many studies deal with the theme of Intensity-Duration equations to discriminate between triggering and no-triggering of debris flows. These studies are usually considering only the triggering rainfall neglecting the corresponding critical discharge.

In this article, we put together the triggering rainfalls with the corresponding generated critical discharges, to study the behavior of three real case studies. Using the Flo-2D software we simulated different hydrological responses of the headwater basins to rainfall events extrapolated using some specific Intensity-Duration curves. The aim is to understand which is the rainfall duration needed to create a surface runoff that exceeds the critical discharge for the initiation of a torrential flow. To this purpose, a detailed morphological study of the headwater basins of the study areas has been conducted and in every study area, three control cross sections have been extracted with a GIS analysis.

Moreover, to consider also the possibility of a triggering mechanism due to shallow slope failure we also conducted a slope stability analysis in the three initiation areas.

The results show that the geomorphology of the catchments seem to have some influence to the triggering mechanism. Moreover, the rainfall durations needed to reach the critical discharges related to the debris flow initiation, are relatively short, making strongest rainfalls very dangerous for the capacity of the corresponding discharges to generate destructive debris surges.

This chapter is an edited version of: Pastorello R, Hürlimann M, D'Agostino V. Rainfall durations and corresponding dominant mechanism for the initiation of debris flows in three headwater basins characterized by different geomorphological settings. *In preparation for the publication on a peer-review journal.*

4.2 Introduction

Debris flows are mixed masses formed by rocks, mud, water and air that move with relatively rapid velocities inside steep channels in mountainous catchments, showing a characteristic wave form (Hungr et al. 2013). Because of the increasing expansion of human settlements in unstable mountainous areas, due to the economic development of the last century (Fuchs et al. 2008), this type of mass movement has become one of the most dangerous threats for alpine valleys (Cavalli and Grisotto 2006). Therefore, the studies on debris flows have become of crucial importance nowadays because of the economic and social losses that these phenomena can cause. In the recent years, many studies concentrated on the modelling of torrential flows (O'Brien et al. 1993; Burton and Bathurst 1998; Crosta and Frattini 2003; Armanini et al. 2009; Hungr and McDougall 2009; Horton et al. 2013; Gregoretti et al. 2016), and of particular importance is the focusing on the triggering part of the debris flow events. In fact, the triggering mechanism is a complex phenomenon depending on different variables. Many studies (Takahashi 1981; Rickenmann and Zimmermann 1993) stated that the three most important variables for the triggering of a debris flow are: slope gradient , sediment availability (Bovis and Jakob 1999; Brayshaw and Hassan 2009) and water input. Therefore, taking as case study a place in which the first two variables can easily exceed the triggering thresholds, the variable playing the most important role is the water input. This depends primarily on precipitations falling above the analyzed catchment (Wieczorek and Glade 2005). In fact, if the rainfall is strong enough, the water inside the channels can reach the critical discharge in which it starts the mobilization of sediments (Tognacca and Bezzola 1997; Cannon et al. 2004; Berti and Simoni 2005; Gregoretti and Dalla Fontana 2008).

Considering the hydrological response of the catchment to precipitations, two main types of debris flow triggering have been described: (1) channel-bed failure and (2) shallow slope failure. (1) The first one happens when the debris flow derives from the erosion of the channel bed and of the channel banks, caused by the superficial runoff (Tognacca and Bezzola 1997; Cannon et al. 2004; Berti and Simoni 2005; Gregoretti and Dalla Fontana 2008). Berti and Simoni (2005) stress that three different types of meteorological conditions can trigger a debris flow: short and intense thunderstorms following a relatively long dry period; less intense thunderstorms following a certain period of weak rainfall; or thunderstorms of low intensity following a long period of rainfall. Coe et al. (2008b) described also a sub-type of channel-bed

failure, which happens when the debris flow material does not derive from an erosional mechanism but derives from the mobilization of accumulated loose debris inside the channel (dam-break mechanism). (2) Shallow slope failure, when a shallow landslide, caused by a rapid infiltration of water in the superficial soil layers, develops in a debris flow. In fact, the subsurface water can saturate soil, taking the material near to its critical stability factor (Wu and Sidle 1995; Iverson et al. 1997; Reid et al. 1997; Lu and Godt 2008) and destabilizing the near to surface layers composed of loose sediments. These types of landslides can evolve into debris flows if the slope failure happens in a part of the basin connected to the channel network (Rickenmann 2016). For this analysis, it has been used the equations of Lambe and Whitman (1968), that is based on some geotechnical parameters (friction angle and cohesion of the material) and on some morphological characteristics (terrain slope).

Therefore, to understand how rainfall can generate critical runoff, it is of crucial importance to study the hydrology of the headwater basins. At this purpose, several models have been developed to simulate the water and sediment flow (e.g. Gregoretti et al. 2016) and in the present study, we used the software FLO-2D (O'Brien et al. 1993) to simulate the flood hydrograph on different study areas. In fact, FLO-2D allows to conduct hydrologic/hydraulic spatially distributed simulations, only considering runoff generation and routing (in this case sediment transport tool is turned off). Of particular relevance are the studies of the maximum rainfall intensity-duration equations that are related to the triggering of torrential flows. In fact, precipitations with intensity greater than the one described by these curves, can potentially initiate the sediment mobilization. A lot of studies carried out in the last decades, proposed different rainfall thresholds based on different study areas (e.g. Caine 1980; Innes 1983; Moser and Hohensinn 1983; Cannon and Ellen 1985; Wilson and Wieczorek 1995; Paronuzzi et al. 1998; Deganutti et al. 2000; Crosta and Frattini 2001; Bacchini and Zannoni 2003; Gregoretti and Dalla Fontana 2007).

From the other side, many studies concentrated on the analysis of the critical water discharge needed for the mobilization of sediments in channel (Gregoretti 2000; Tognacca et al. 2000; Gregoretti and Dalla Fontana 2008). Therefore, coupling these two aspects, we can obtain significant improvements on the conditions needed for the triggering of debris flows in real case study areas.

In the present work, we selected three different catchments: Rudan torrent (Mount Antelao) and Chiesa torrent (Col di Lana) in the eastern Italian Alps, and Rebaixader torrent in the Spanish

Axial Pyrenees. The catchments show different morphological and geological settings and so their response to the water input can be different. During the analysis, we concentrated on the headwater basins (Gregoretti and Dalla Fontana 2008; Borga et al. 2014; Kelleher et al. 2015; Gregoretti et al. 2016), that are the upper parts of the catchments, in which the source areas and the initiation points of the ephemeral gullies are located. These initiation zones are usually characterized by a very high slope gradient and the presence of loose and poorly cohesive debris that can be easily mobilized by running waters. The sediment recharge depends on the rock type and on the topography of the slope. The erosional processes that cause the recharge of material can be slow but continuous, causing a great annual accumulation, or in other cases there can be the presence of old non-consolidated deposits (Ancey 2001). In the initiation area, on the scree slopes at the base of steep rock faces (Gregoretti and Dalla Fontana 2008), are located also the channel heads, that are the points in which the gullies origin.

In the headwater basins, we did some hydrological simulations with the software FLO-2D, using different input rainfall events. Therefore, we selected some control cross sections in which we verified the reaching of the critical discharge for the initiation of torrential flows.

Then, to complete the analysis, we studied also the slope stability of the triggering areas using the geotechnical parameters of the soil. This second analysis allowed us to consider also the second triggering mechanism, which is the one related to the potential instability of the hillslope that can evolve into a shallow slope failure and consequently into a debris flow.

The main aim of this study consists of verifying at which extent the triggering conditions (in all senses) may change among basins with different geological and morphological conditions.

4.3 The study areas

4.3.1 The Rudan catchment

Rudan torrent is one of the main channels that flows down from the South side of Mount Antelao (3264 m a.s.l.) (Figure 4.1). It is located in the municipality of Vodo di Cadore (BL, North-Eastern Italy) and has an area of 2.71 km^2. The channel starts just below the peak of the mountain, inside a great source area named “Vallon dell’Antelao”, and flows down until the confluence with the Boite torrent. The catchment has a wide elevation range that goes from an elevation of 3229 m a.s.l to 788 m a.s.l (Bertoldi and D’Agostino 2014). The high Melton number (Table 4.1) shows its attitude to debris flows (Melton 1965). In the past, the catchment

has been stroke by very strong torrential events. Historical documentation talks about catastrophic debris flows that completely buried and destroyed ancient villages (D'Agostino et al. 2002). Also in the last decades, the catchment has suffered some debris flows that damaged the municipality and the national road "Alemagna". For this reason, in 2011, a filter check-dam with a storage basin has been built just above the street. Mainly dolomitic rocks characterize the geology of the basin, especially in the upper part. In fact, Mount Antelao is comprised in the Group of Marmarole one of the main groups of the Dolomites. The matrix of soil in the source area (that is the area of triggering) shown on Figure 4.1 is mainly composed of gravel and sand, whereas the finer material is present only in a little percentage (6.7%, Figure 4.4).

In the upper part of the basin, there are rock faces and talus slopes that continuously recharge the catchment with new sediment. For this reason, we can consider the Rudan torrent as a weathering-limited system (Bovis and Jakob 1999) in terms of solid responses. The most important source of sediment is the area named "Vallon dell'Antelao" that it is located between 2400 m a.s.l and 2000 m a.s.l (Figure 4.1). This zone is a steep talus cone covered by loose debris, with grain size that varies from silt to boulders of 5 m in size. This area is clearly an unlimited source of material, and the depth of the sediment thickness is evaluated in more than 20 meters (Bertoldi and D'Agostino 2014).

Table 4.1: Main characteristics of the three catchments

	Rudan	Chiesa	Rebaixader
Area (km^2)	2.71	0.95	0.82
Max Elevation (m a.s.l)	3229	2452	2297
Min Elevation (m a.s.l)	788	1465	1237
Mean Elevation (m a.s.l)	1784	1941	1738
Average slope (°)	47	36	31
Melton number	1.42	1.02	1.16

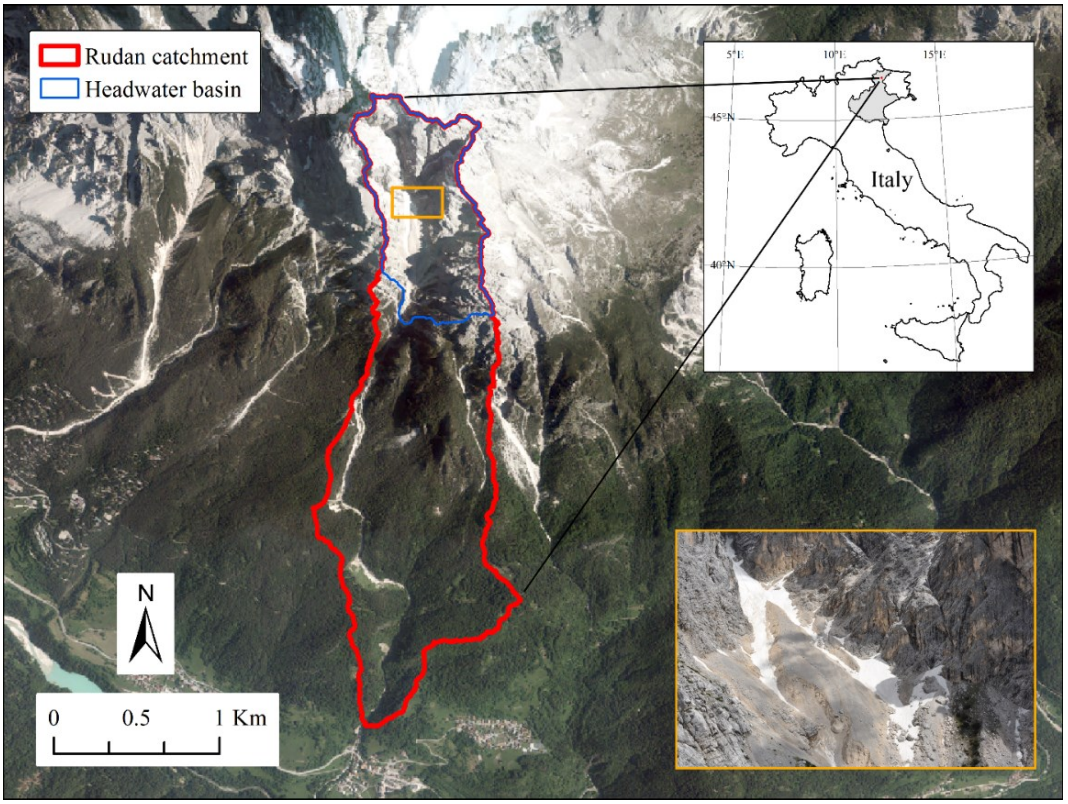

Figure 4.1: Map of the Rudan catchment with a zoom-in of the triggering area named "Vallon dell'Antelao".

4.3.2 The Chiesa catchment

Chiesa is a torrent that flows down on the south side of Col di Lana (2452 m a.s.l.) (Table 4.1). This mountain is inside the dolomitic territory, but it is characterized by a different geology compared to the Rudan basin. The main rock types consist of: (1) conglomerates, (2) volcanic rocks like hyaloclastites and tufas (Fernazza formation) and (3) especially in the lower part of the catchment we can also find calciculites and limestones (Livinallongo formation) (D'Agostino 2003). The soil composition is also different from the Rudan catchment: silt is present for the 22.6% and clay for the 9.4% (Figure 4.4), and so the finest part of the soil has a higher percentage compared to gravel and sand.

The main channel of the basin is named Chiesa torrent and it flows into the Cordevole river at 1175 m a.s.l., passing through the village of Pieve di Livinallongo (BL, North-Eastern Italy) (Figure 4.2). Right upstream of the National Road 48 "Delle Dolomiti", there is a filter check-dam, with a storage basin.

The source areas, where debris flows initiate, are eroded parts of the lateral sides of the head-slopes characterized by high slope gradient (about 35-45°) and they are not a loose debris-talus

cone surrounded by rock faces (Figure 4.2). In these eroded zones, the rocks and sediments emerge from a matrix mainly composed of silt and sand. Moreover, these triggering zones are not located exactly in the upper part of the catchment, but are placed between an elevation of about 2104 and 1800 m a.s.l. Here, the channel heads from which the stream flows down to the transport zone are also located. The upper part of the catchment that starts from the peak of the mountain is partly disconnected from the source areas. In fact, there is a flat zone just in the middle between these two parts (Cavalli et al. 2013).

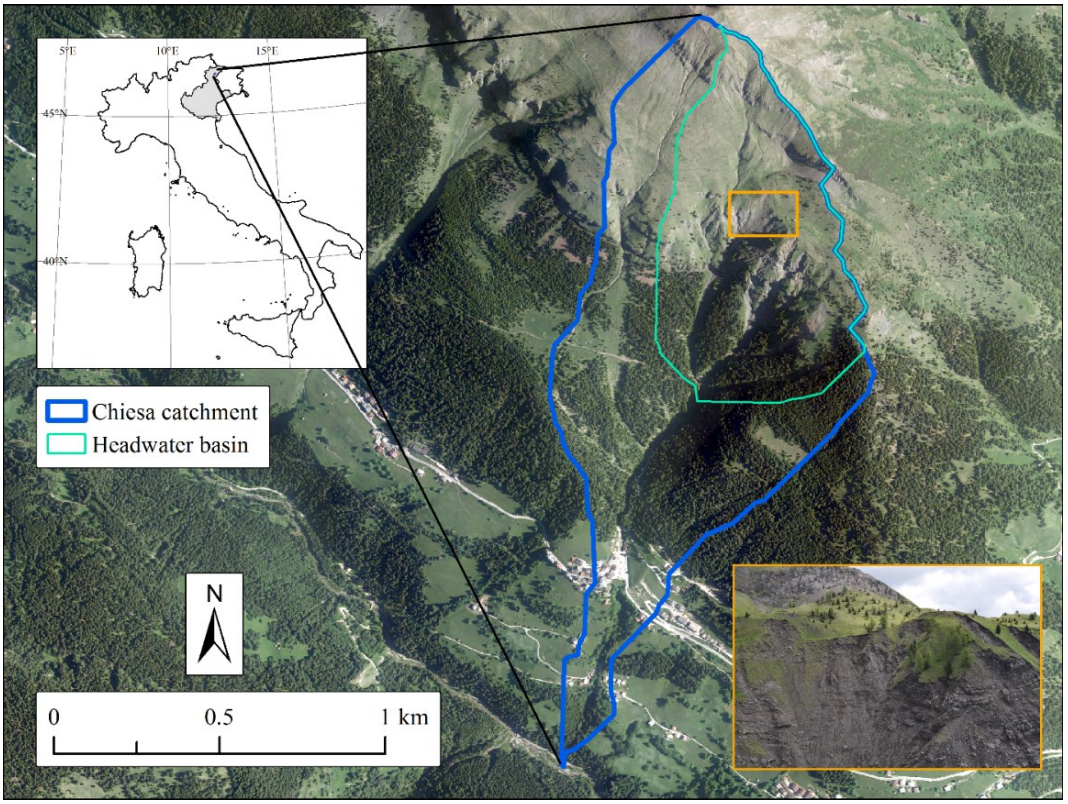

Figure 4.2: Map of the Chiesa catchment with a zoom-in of the source areas.

4.3.3 The Rebaixader catchment

This catchment is located in the Spanish Pyrenees, near the border between the regions of Catalonia and Aragon (Figure 4.3). The catchment area is relatively small (Table 4.1) and the channel is called Rebaixader torrent (Hürlimann et al. 2014). This is a very particular channel because it has a small extension and its shape is quite regular, evidencing the typical shape of a debris flow catchment: triggering area, transport zone and deposition area. The triggering

zone is a unique wide area characterized by a steep slope gradient and covered by an abundant loose debris cover. In the central part of this area, it can be observed some particular formations. They are a sort of bad-land areas where isolated zones at a higher elevation are bounded by micro-channels (rills). These zones are very steep and present unstable lateral sides (Figure 4.3). The estimated depth of this sediment cover reaches even tens of meters. For this reason, the catchment is often stroke by debris flow and debris flood events and it has been selected to install a monitoring station. In fact, the great activity allows to collect a lot of data in a relative short amount of time. The monitoring station has been installed in 2009, and in the first seven years of functioning, more than 30 events have been registered (Hürlimann et al. 2011; Abancó and Hürlimann 2014).

The transport zone is relatively short; the channel has a width of 8-10 m and a slope angle of 25° (Table 4.1). In the lower part of the catchment, there is a small fan, just before the intersection with the Noguera Ribagorçana River. The geology of the basin is composed of metamorphic rocks and in the triggering area (a lateral moraine with almost unlimited sediment supply, see Figure 4.3), we can observe blocks of different dimensions, going from clay and silt to large boulders. In this catchment, the composition of the matrix is similar to the one of the Rudan catchment, with the highest presence of gravel and sand and only 2% of silt and clay (Figure 4.4).

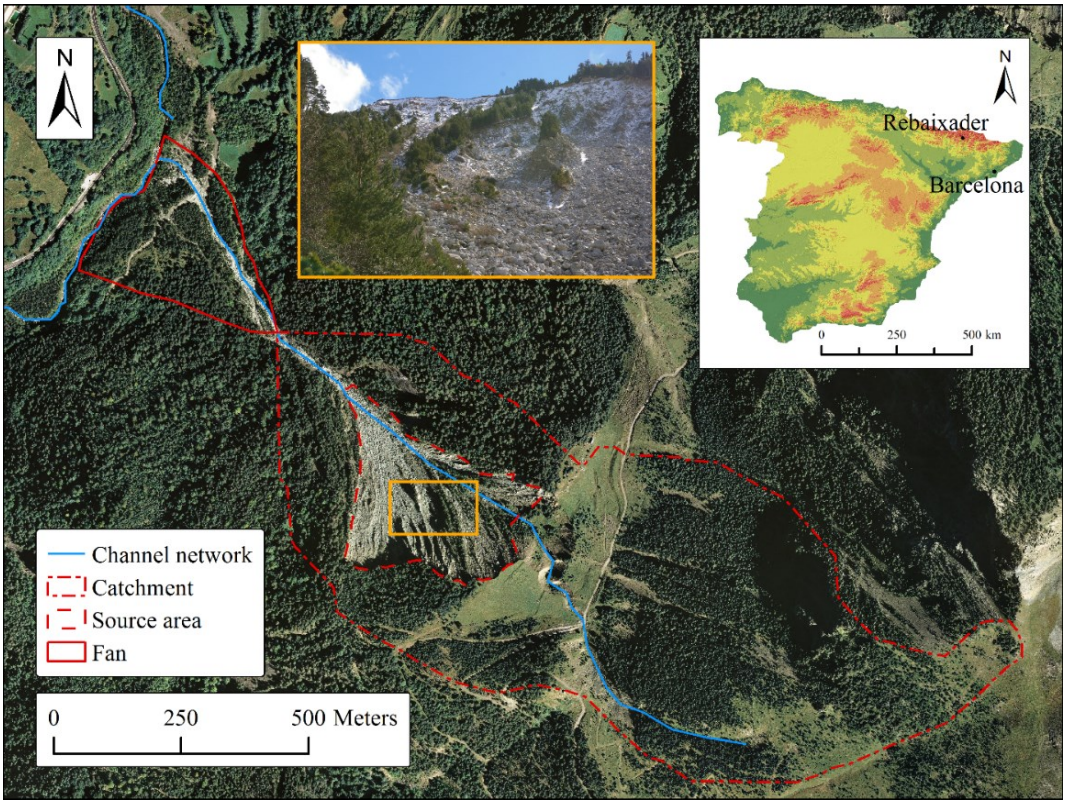

Figure 4.3: Map of the Rebaixader catchment with a zoom-in of the triggering area.

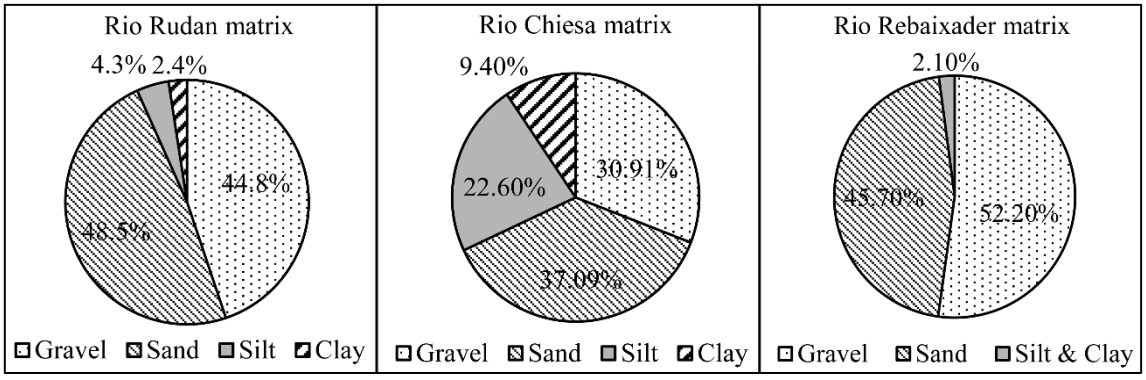

Figure 4.4: Grain size of the soil matrix in the three case study areas.

4.4 Materials and methods

4.4.1 The hydrological analysis

The aim of this part of the analysis was to identify the critical rainfall duration related to the critical water discharge capable of mobilize sediments, leading to the triggering of a debris

flow. First of all, in the three study areas, the headwater basins of debris flow initiation have been identified (Berti et al. 1999; Gregoretti and Dalla Fontana 2008). In fact, the hydrological analysis has been focused in the upper part of the catchments, in which the source areas are located.

Table 4.2: Main parameters of the control cross sections: d_m is the mean diameter of the considered headwater basin, S is the terrain slope, β is the slope angle, B is the section width and y is the hydraulic depth.

	Rio Rudan			Rio Chiesa			Rio Rebaixader		
	d_m = 0.15 m			d_m = 0.10 m			d_m = 0.10 m		
	Sec 1	Sec 2	Sec 3	Sec 1	Sec 2	Sec 3	Sec 1	Sec 2	Sec 3
S (m/m)	0.61	0.67	0.49	0.79	0.60	0.57	0.36	0.44	0.40
β (°)	31.38	33.82	26.10	38.48	31.10	29.88	19.56	23.45	21.96
B at y=1 m	3.51	6.18	11.5	12.49	11.56	4.86	7.56	11.61	5.51

In every headwater basin, we identified in the triggering area three cross-sections: two along the channel network and one in correspondence of the basin outlet (Figure 4.5, Figure 4.6, Figure 4.7). These sections have been extracted from the DTM maps and have been analysed using a Matlab tool to determine the main characteristics: channel flow width, wetted perimeter, area, hydraulic radius for different flow depths, and related, thalweg slope in a surrounding reach. In Table 4.2 width and bed slope of the cross sections are reported for 1 m of depth. .The choice of the quality of the topographic bases used for the three basins is as follows: 1 m cell resolution for Rudan catchment, and 5 m cell resolution for Chiesa and Rebaixader catchments. The DTM of Rudan torrent derives from a LiDAR survey made during 2015, whereas the DTMs of Chiesa and Rebaixader torrents derives from the technical cartography contour lines. For every cross section, we calculated the critical discharge per unit width, related to the initiation of a debris flow surge. Tognacca et al. (2000) proposed a first equation to calculate the critical runoff for the initiation of a debris flow. Nevertheless, their analysis has been carried on using a sample material made of sand and gravel. Whereas, Gregoretti and Dalla Fontana (2008), proposed a second equation using a similar methodology with samples composed only of gravel. Therefore, the diameter used in the formulas is strongly influenced by the different grain sizes in play , and for this reason we chose the equation of Gregoretti and Dalla Fontana (2008). In fact, the mean diameters of the three analysed basins are relatively high: 0.15 m for Rudan catchment, and 0.10 m for the two others (Table 4.2). These diameters, for Rudan and Chiesa

catchments, have been measured during the surveys made for the construction of the two filter check dams located in the two basins (D'Agostino et al. 2002; D'Agostino 2003). Whereas, for the Rebaixader catchment, the diameter information has been derived from the paper of Hürlimann et al. (2012).

The equation proposed by Gregoretti and Dalla Fontana (2008) is as follows:

$$q_c = 0.78 \frac{d_M^{1.5}}{\tan \beta^{1.27}} \quad (4.1)$$

Where d_M is the mean grain size of the terrain in the triggering zone (channel bed) and β is the channel-slope angle in correspondence of the cross section.

The second equation has been proposed by Whittaker and Jaggi (1986) and it has been developed to calculate the critical discharge capable of mobilize sediments (mainly composed of granular material) causing the destabilization of ramp slopes:

$$q_c = 0.257\ (s-1)^{0.5} g^{0.5} {d_M}^{1.5} S^{-1.17} \quad (4.2)$$

Where, s is the ratio of the sediment density to the density of water, g is the gravitational acceleration and S is the terrain slope (m/m) (Rickenmann 2016). In this second formula, the calculation regards the erosion of block ramps with large blocks, for this reason we tested two different grain sizes (d=0.3 m and d=0.5 m) to give a corresponding discharge range for the destabilization of the sparse boulders that are present on the channel bed and banks inside the source areas.

Using the real cross section width (B) extracted from the MATLAB analysis, for every cross section, we identified the corresponding critical water discharge with the formula:

$$Q = q\ B \quad (4.3)$$

The B value corresponds to the top width for a depth value (y) which is coherent with q. The stage-mean flow velocity relationship that has been assumed for such a calculation is the turbulent uniform flow equation, where the Manning's n used has a value of 0.1, according to the literature findings (Rickenmann 2016):

$$Q = A \frac{1}{n} (\sin \beta)^{1/2} R_h^{2/3} \quad (4.4)$$

Where A is the wetted area, n is the Manning coefficient, β is the slope angle and R_h is the hydraulic radius of the analysed section.

Using these data, we also calculated the shear stress τ (N/m^2) using the following equation:

$$\tau = \gamma R_h S \quad (4.5)$$

Where γ is the specific weight of water (this is a simplification made because we are considering the water runoff for the initiation of a debris flow and not a totally formed debris flow wave) and S is the slope gradient (m/m) (Table 4.2).

The application of equations (4.1)-(4.3) entails the Sections 1-2-3 for a global view. It is worth to say that Equations (4.1) and (4.2) are meaningful if they refer to a well confined flow at low flow stages. Therefore, the critical threshold values obtained at the Section 3 (basin outlet) are considered as the most reliable, occurring here a bounded flow concentration in all three basins.

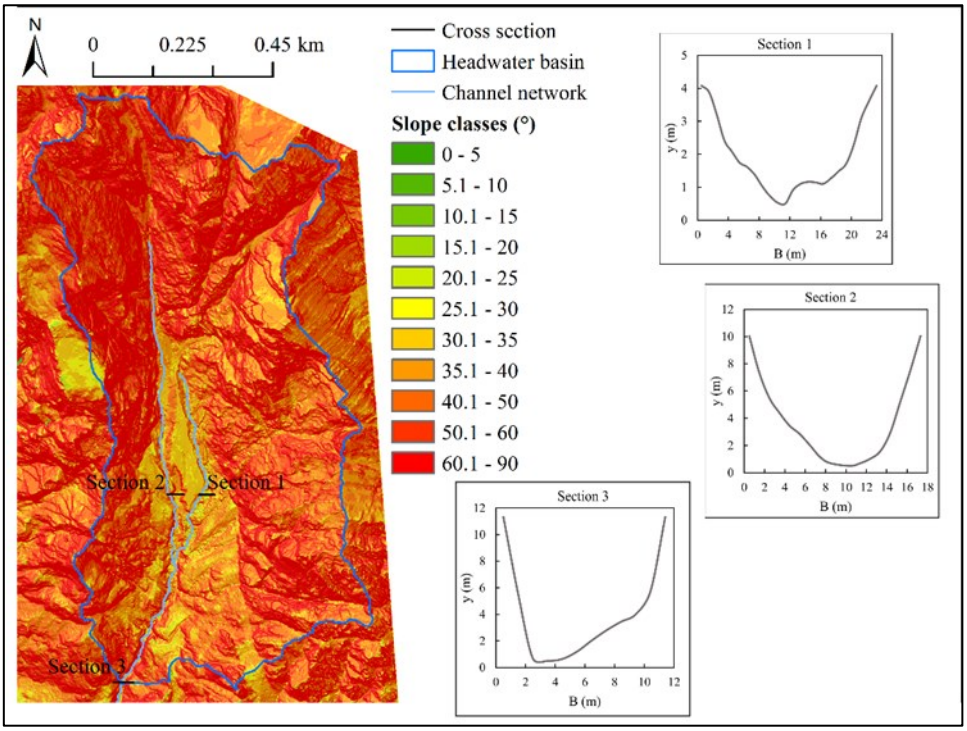

Figure 4.5: Location and shape of the three cross-sections of the Rudan catchment.

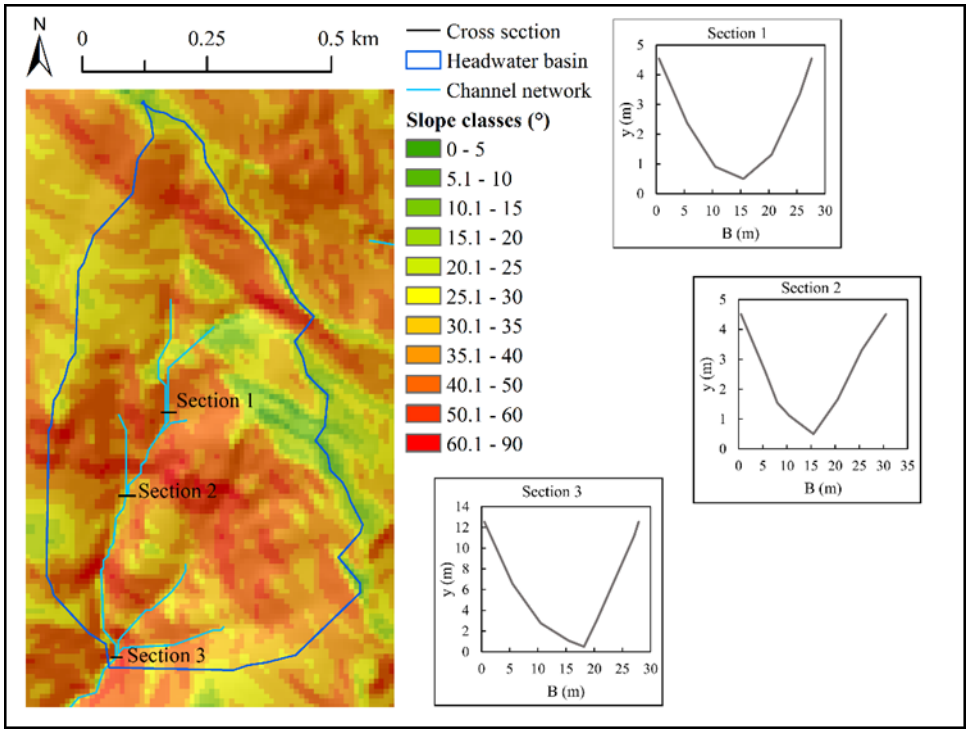

Figure 4.6: Location and shape of the three cross-sections of the Chiesa catchment.

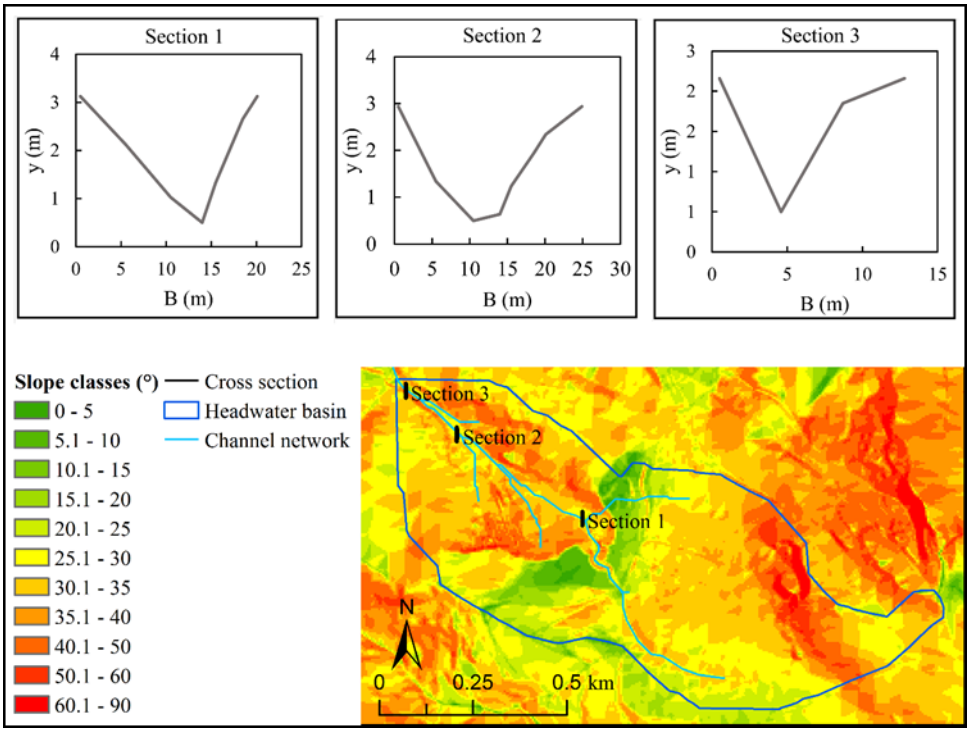

Figure 4.7: Location and shape of the three cross-sections of the Rebaixader catchment.

To create the hyetographs that will be used as input in the hydrological simulations with the software FLO-2D (O'Brien et al. 1993) we accounted for some empirical Intensity-Duration equations found in literature. In particular, we chose between three intensity-duration equations already used in other investigations: Cannon and Ellen (1985), Paronuzzi et al. (1998) and Gregoretti and Dalla Fontana (2007).To choose the equation more similar to the typical rainfall events of each basin, we analysed some real rainfall events registered in correspondence of the triggering of a torrential flow.

The selection of the appropriate equation has been carried on specifically for each basin:

1) For the Rudan catchment, we simply used the equation from Gregoretti and Dalla Fontana (2007):

$$I_M = 21\ D^{-0.55} \tag{4.6}$$

Where I_M is the mean hourly intensity and D is the duration. We choose this equation because Gregoretti and Dalla Fontana (2007), for the creation of this equation already used rainfall events registered in the Rudan catchment. Therefore, this equation has been set specifically for the dolomitic area that includes also our catchment.

2) For the Chiesa catchment, we selected four rainfall events that over the last 20 years triggered a torrential flow: 20/09/2000, 28/07/2003, 26/07/2006 and 8/08/2015. For every rainfall event, we extracted the strongest burst, characterized by a minimum precipitation of 1 mm in 5 minutes. For every burst, we calculated the corresponding medium hourly intensity for different durations: 5, 10, 20, 30 and 60 minutes. We reported these values in a graph together with the three Intensity-Duration equations from literature (Figure 4.8). Looking at the graph, it can be noticed that the majority of the real bursts points are located near the equation of Cannon and Ellen (1985):

$$I_M = 30.7\ D^{-0.45} \tag{4.7}$$

For this reason, we chose this equation to create the hyetographs for the hydrological simulations.

3) For the Rebaixader catchment, we made a similar analysis using four triggering rainfall events: 11/07/2010, 27/06/2012, 4/07/2012 and 31/07/2015. We extracted the bursts of these events and we compared the points with the empirical equations (Figure 4.9). Also in this case we selected the equation of Cannon and Ellen (1985). In fact, two events lies below and two events lies above this curve and so it seems the equation that on average can better represent the typical triggering rainfall events .

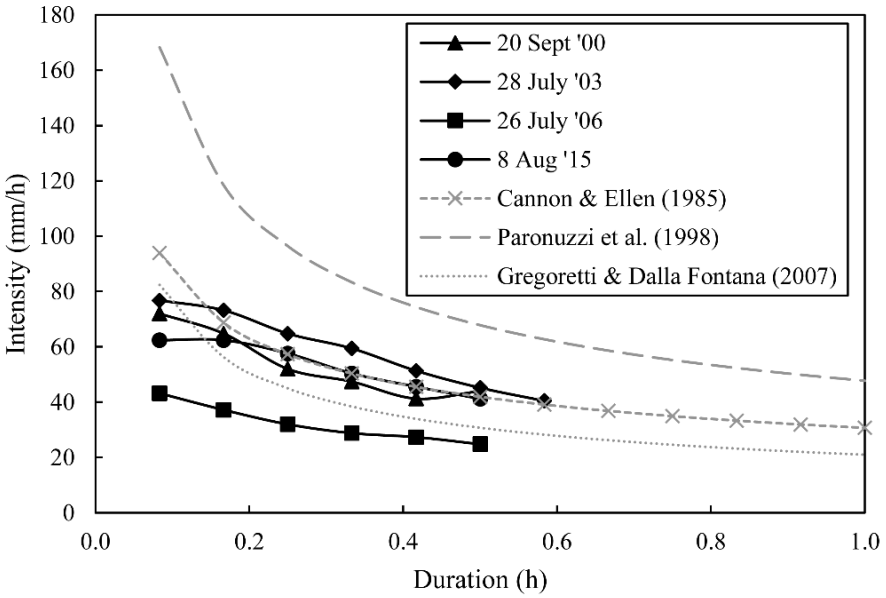

Figure 4.8: Comparison between the four bursts that triggered a debris flow in the Chiesa catchment and the equations of Cannon and Ellen (1985), Paronuzzi et al. (1998) and Gregoretti and Dalla Fontana (2007).

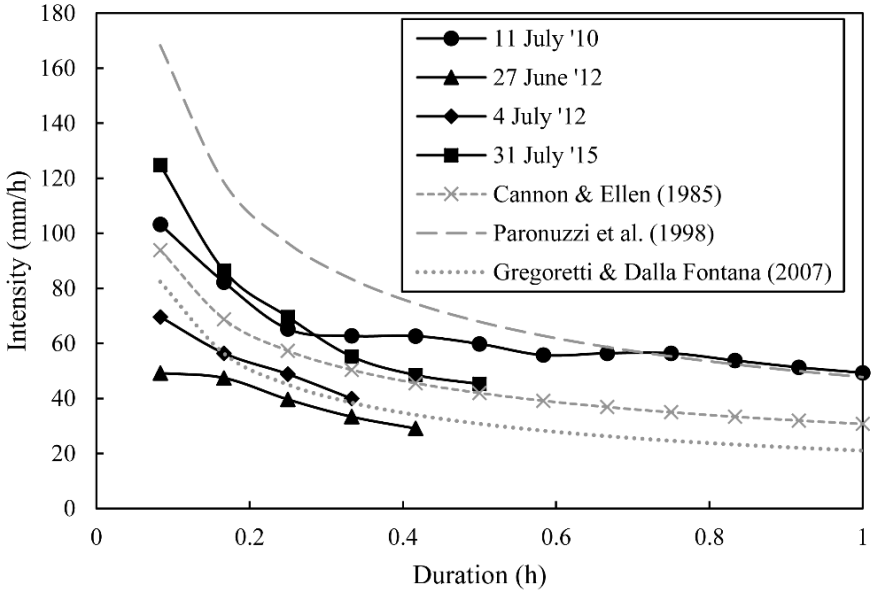

Figure 4.9: Comparison between the four bursts that triggered a debris flow in the Rebaixader catchment and the equations of Cannon and Ellen (1985), Paronuzzi et al. (1998) and Gregoretti and Dalla Fontana (2007).

Using Equations (4.6) and (4.7), we built four different hyetographs with constant rain intensity for four reference total durations: 15, 30, 60 and 120 minutes. These were base durations to address then in refining the final critical duration, which exactly generated the debris-flow triggering discharge at Section 3.

We used these hyetographs as input for the FLO-2D modelling software (O'Brien et al. 1993).

FLO-2D is a bidimensional numerical model created to simulate hydraulic fluxes. It is certified by FEMA (Federal Emergency Management, USA) and it is widely used to analyze the effects of floods on alluvial planes, fans, rivers and mountain torrents. The model works by means of the DTM maps of the analyzed basins. For each cell, the propagation of the flux is calculated on the quadratic matrix composed by itself and the neighboring cells and it is possible in all the eight directions. Two equations are used for the calculations: the dynamic equation (De Sant Vénant) and the equation of the mass conservation. The main parameters that influence the results are: (1) the grid dimension of the DTM cells used to create the floodplain, (2) the altitude, n-Manning and CN (Curve Number) coefficients of every cell, (3) the input hyetographs. We used this model because it allows to carry on different types of hydrological simulations using specific input parameters such as the rainfall hyetograph and the detailed characteristics of the area (n-Manning and CN value at the spatial resolution of the DTM grid and making also immediate the simultaneous extraction of predicted runoff in different selected cross sections).

For the hydrological simulations, we used a mean unique CN for each basin, rather than a distributed CN, being low the total catchment areas and after verifying that the distributed CN assignment does not vary significantly the results particularly for strong rainfall events. On Table 4.3 are shown the different areas of the headwater basins and the corresponding mean CN.

Table 4.3: Percentage of the superficial extent of the different land-use of the three headwater basins and calculated mean CN.

Rio Rudan		Rio Chiesa		Rio Rebaixader	
Land type	Area (%)	Land type	Area (%)	Land type	Area (%)
Shrubs	4	Woods	32	Woods	75
Pastures	10	Pastures	56	Pastures	16
Scree	10	Scree	3	Scree	9
Rocks	76	Rocks	9		
Mean CN = 78		**Mean CN = 75**		**Mean CN = 65**	

Regarding the initial abstractions, we used a value of 1 mm in all the simulations. In fact, many authors suggested that lower values of the initial abstractions give better simulation results than higher values in case of steep slopes catchments (e.g. Gregoretti and Dalla Fontana 2008; Hawkins et al. 2010; D'Asaro and Grillone 2012; Gregoretti et al. 2016).

We conducted the hydrological simulations, modelling the flood hydrograph originating from the input hyetographs. We analysed the resulting peak discharge in the three control cross sections, to verify if this peak discharge exceeds the critical discharge from Equations (4.1) and (4.2). Finally, we made some additional simulations, varying the duration of the rainfall event until we found the exact rainfall duration corresponding to the critical discharge for the mobilization of sediments in the studied channels.

4.4.2 The slope stability analysis

To take into consideration also the possibility of the triggering of a debris flow due to a concurrent shallow landslide, we performed a stability analysis of the triggering areas. The objective of this part was that of verifying at which elevation of the water table, the hillslope nearby the triggering area becomes unstable or prone to collapse. To carry out this analysis, we

firstly collected some samples of the soil matrix in the triggering areas. Then, a geotechnical analysis has been made by professional laboratories, to extract the soil characteristics (Table 4.4). The parameters that has been extracted are:

- Visual geotechnical classification of the soil;
- Computation of the Atterberg limits;
- Size classification (Figure 4.4);
- Direct shear test (Casagrande's apparatus).

Using these parameters, we conducted the infinite slope analysis of the three triggering areas, calculating the Stability factor (*FS*) with the equation proposed by Lambe and Whitman (1968):

$$FS = \frac{c' + (\gamma_s - m\gamma_w) z \cos\beta^2 \tan\emptyset}{\gamma_s z \cos\beta \sin\beta} \quad (4.8)$$

Where *c'* is effective cohesion, *z* is the height of the potential sliding plane, *m* is the water table parameter (the fraction of *z* where the water table is located), β is the hillslope gradient, γ_s is the saturated soil weight and γ_w is the water weight (9.81 kN/m^3). In particular, we extracted the hillslope gradient of the zones right above the channel heads in the three source areas.

If the safety factor (*FS*) is higher than one the hillslope is stable, whereas, when *FS* approaches one the hillslope becomes unstable and the possibility of a shallow landslides increases.

Table 4.4: Main geotechnical parameters of the three headwater basins.

	Rio Rudan*	Rio Chiesa*	Rio Rebaixader**
Soil unit weight (γ_s) (kN/m^3)	17.52	17.98	17.00
Soil friction angle (φ') (°)	42.50	36.50	45.00
Cohesion (c') (kPa)	10.00	12.00	5.00
Mean hillslope gradient (β) (°)	31	40	31

* GEODATA Laboratory (Ponte San Nicolò, Padova, Italy)

** Geomar Laboratory (Barcelona, Spain)

4.5 Results

4.5.1 Results of the hydrological analysis

Looking at the results of the analysis of the critical discharge, it can be seen from Table 4.5 that the critical discharges per unit width obtained using the equation of Gregoretti and Dalla Fontana (2008) are generally low. In fact, considering the three analyzed headwater basins, the range is between 0.03 and 0.12 $m^3/s/m$. Transposing this value to the real critical discharge for every analyzed cross section, using the real section width, the discharge ranges between 0.03 and 0.28 m^3/s. On Table 4.6 a sensibility analysis is reported on the bed-slope extraction approximation in correspondence of the three cross sections at the basins outlets. The slope of the thalweg profile used for the analysis -(computation of the critical discharge per unit width with equations (4.1) and (4.2) - has been calculated as the mean slope gradient on a close channel reach (cross section placed in the intermediate position) with the length of 30 m. To verify if the length taken for slope computation of the reach influences the slope values and consequently the critical discharge values, we computed the mean slope also on reaches of 10 meters and of 50 meters length. It can be seen from Table 4.6 that the critical discharge values only vary in a small range of -0.02 and +0.01 m^2/s.

It is interesting to notice that the value of τ_c, for Chiesa and Rebaixader catchments are very similar (between about 270 and 280 N/m^2), whereas in the Rudan basin the values are higher, but not so far (about 350-400 N/m^2) (Table 4.5).

Using the equation for block-ramps proposed by Whittaker and Jaggi (1986) with the two different diameters (Table 4.7), the critical discharge is obviously higher because the runoff needed for the mobilization of greater blocks is greater.

Table 4.5: Critical hydrological parameters derived from Gregoretti and Dalla Fontana (2008) (Equation 4.1) of the analysed cross sections. In bold-italic are evidenced the cross sections at the headwater basin outlet.

	Rudan			Chiesa			Rebaixader		
	Sec 1	Sec 2	**Sec 3**	Sec 1	Sec 2	***Sec 3***	Sec 1	Sec 2	***Sec 3***
q_c (m^2/s)	0.12	0.08	***0.09***	0.03	0.05	***0.05***	0.09	0.07	***0.08***
Q_c (m^3/s)	0.19	0.13	***0.16***	0.04	0.06	***0.03***	0.12	0.28	***0.07***
τ_c (N/m^2)	352.53	357.86	***413.37***	269.48	275.75	***261.02***	271.94	279.63	***276.47***

Table 4.6: Sensibility analysis of the slope extracted with different reach lengths for each cross section at the basin outlet. In italic are evidenced the values used for the hydrological analysis.

	Rudan			Chiesa			Rebaixader		
Reach length	10 m	*30 m*	50 m	10 m	*30 m*	50 m	10 m	*30 m*	50 m
S (m/m)	0.66	*0.61*	0.62	0.50	*0.57*	0.59	0.47	*0.40*	0.38
q_c *(m^2/s)*	0.08	*0.09*	0.09	0.06	*0.05*	0.05	0.06	*0.08*	0.08

Table 4.7: Critical hydrological parameters derived from Whittaker and Jaggi (1986) (Equation 4.2) of the analysed cross sections, using two diameters 0.3 m (value before the slash) and of 0.5 m (value after the slash). In bold-italic are evidenced the cross sections at the headwater basin outlet.

	Rudan			Chiesa			Rebaixader		
	Sec 1	Sec 2	**Sec 3**	Sec 1	Sec 2	***Sec 3***	Sec 1	Sec 2	***Sec 3***
q_c (m^2/s)	0.27/ 0.58	0.19/ 0.40	***0.21/ 0.45***	0.16/ 0.34	0.21/ 0.47	***0.23/ 0.50***	0.37/ 0.81	0.30/ 0.64	***0.33/ 0.71***
Q_c (m^3/s)	0.47/ 1.74	0.25/ 1.34	***0.43/ 1.03***	0.53/ 1.90	0.60/ 2.22	***0.35/ 1.17***	1.19/ 3.97	1.60/ 4.13	***0.64/ 2.14***
τ_c (N/m^2)	528.03/ 925.07	455.46/ 945.14	***661.61/ 1049.60***	692.95/ 1116.40	667.61/ 1088.50	***662.09/ 1044.10***	645.85/ 1037.10	675.88/ 1063.10	***645.10/ 1013.70***

As stated in the previous section we prepared four different hyetographs for the hydrological simulations under these hypotheses. Given the selected critical rain intensity-duration curve (Equations 4.6 and 4.7) and looking for the critical triggering discharges computed in Table 4.7 for Section 3, in the Rudan catchment, to build these hyetographs, we used the equation of the rainfall threshold for the initiation of debris flows proposed by Gregoretti and Dalla Fontana (2007) (Equation 4.6). Whereas, for the other two basins we used the equation proposed by Cannon and Ellen (1985) (Equation 4.7) because the analysis of some real triggering rainfall events showed that this second equation gives a better approximation of the real triggering rainfall events. Looking at the results (Table 4.8), it can be observed that the critical rainfall duration needed to reach the critical discharge for the debris flow initiation calculated using the equation of Gregoretti and Dalla Fontana (2008), ranges between 12 and 22 minutes in the three basins. In particular: Rudan catchment is characterized by a critical rainfall duration of 22 minutes, Chiesa catchment of 12 minutes and Rebaixader catchment of 22 minutes. Moreover, Rudan catchment shows the lower rainfall intensity, while Chiesa catchment shows the highest intensity and consequently the minimum rainfall duration to reach the critical value for the initiation of the sediment mobilization.

Table 4.8: Main parameters of the hyetographs used for the FLO-2D hydrological simulations, in the three basins and corresponding peak discharge resulting from the simulations in the outlet cross-section. In the last line, are evidenced in bold-italic the hyetographs that cause a hydrograph with a peak discharge similar to the critical discharge previously calculated with Equations (4.1) and (4.2).

Rio Rudan				Rio Chiesa				Rio Rebaixader			
D_{tot} (min)	P_{tot} (mm)	I_{max} (mm/h)	Q_{max} (m^3/s)	D_{tot} (min)	P_{tot} (mm)	I_{max} (mm/h)	Q_{max} (m^3/s)	D_{tot} (min)	P_{tot} (mm)	I_{max} (mm/h)	Q_{max} (m^3/s)
15	11.25	45.00	0.02	15	14.32	57.28	0.08	15	14.32	57.28	0.02
30	15.37	30.74	0.36	30	20.97	41.94	0.46	30	20.97	41.94	0.14
60	21.00	21.00	0.98	60	30.70	30.70	1.14	60	30.70	30.70	0.88
120	28.68	14.34	1.37	120	44.95	22.47	1.43	120	44.95	22.47	1.37
22	***13.36***	***36.43***	***0.13***	***12***	***12.61***	***63.05***	***0.04***	***22***	***17.68***	***48.21***	***0.07***

On Figure 4.10, Figure 4.11 and Figure 4.12 are shown the hydrographs corresponding to the section located at the headwater basin outlet. The Rudan catchment is characterized by the highest critical discharge between the three basins: 0.16 m^3/s (Table 4.5). Whereas, the values of Chiesa and Rebaixader catchments are lower 0.03 m^3/s and 0.07 m^3/s respectively. Probably, the higher value of the Rudan catchment derives from the higher slope gradient of the cross section, compared to the others. Consequently, in the Chiesa catchment, the rainfall duration needed to reach the critical discharge is lower (12 minutes, Table 4.8) and in fact the hydrograph corresponding to the 15 minutes rainfall duration already exceeds the critical threshold (Figure 4.11) of Gregoretti and Dalla Fontana (2008).

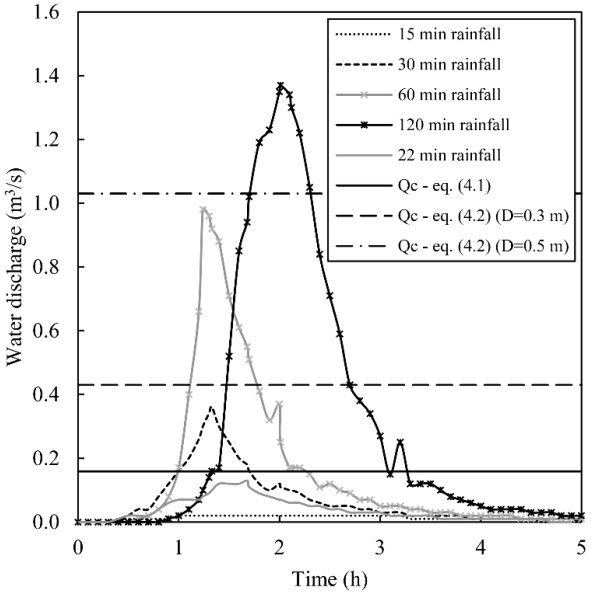

Figure 4.10 Hydrographs for the different simulated rainfall durations compared with the critical discharge for cross section 3 of Rudan headwater basin.

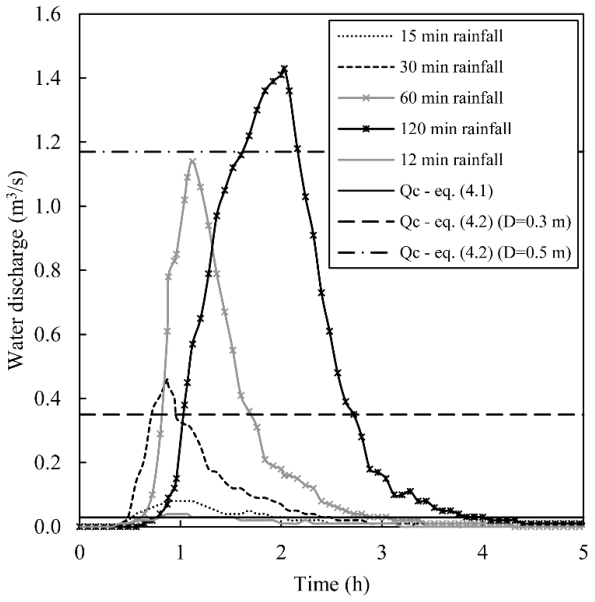

Figure 4.11: Hydrographs for the different simulated rainfall durations compared with the critical discharge for cross section 3 of Chiesa headwater basin.

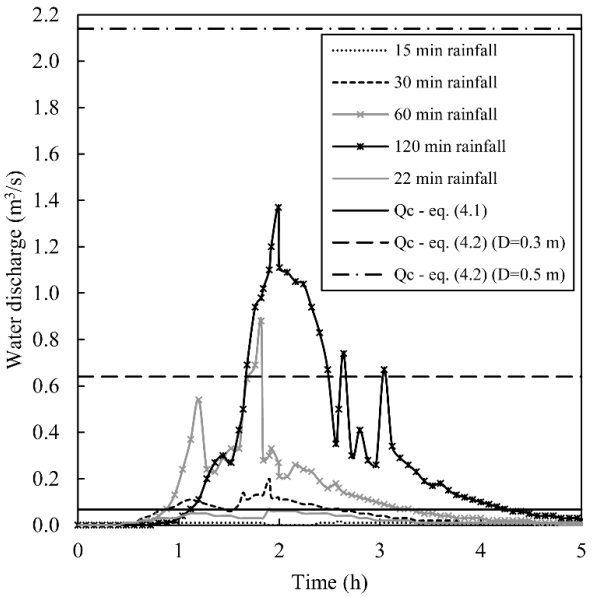

Figure 4.12: Hydrographs for the different simulated rainfall durations compared with the critical discharge for cross section 3 of Rebaixader headwater basin.

Finally, for the Rebaixader headwater basin, the critical discharge corresponding to the possible triggering of debris flows is of 0.07 m^3/s (Table 4.5), and so in between the values of the two other headwater basins. Nevertheless, in this case, the rainfall duration needed to reach this critical discharge at the headwater basin outlet is of 22 minutes (Table 4.8) in fact, the hydrograph resulting from the 15 minutes rainfall duration is really low (Figure 4.12).

Considering the critical runoff discharge obtained using the equation proposed by Whittaker and Jaggi (1986), we evidenced a range in between blocks of higher dimensions than the one considered with the formula of Gregoretti and Dalla Fontana (2008), can be mobilized. In this case, the intensities and durations needed to reach these critical discharge are higher and range between 0.25 and 2.14 m^3/s in the three study areas. Therefore, from the hydrological simulations we can see that generally the rainfall duration needed for the mobilization of boulders are between 30 and 60 minutes.

4.5.2 Results of the slope stability analysis

From the slope stability analysis, it can be seen that Rudan and Rebaixader catchments remain generally stable also for important depths of the potential sliding plane (Figure 4.13). These two basins, show hillslope slopes of about 31° and soil friction angle higher than 40° (Table

4.4), and so in both cases the slope of the area is lower than the friction angle. Whereas, in the case of the Chiesa basin, the hillslope slope is of about 40° and the soil friction angle is of 36.5° (Table 4.4). For this reason, it can be observed on Figure 4.13, that when the thickness of slipping is between 2 and 3 meters, the hillslope becomes unstable and the Stability factor reaches and goes below the stability threshold.

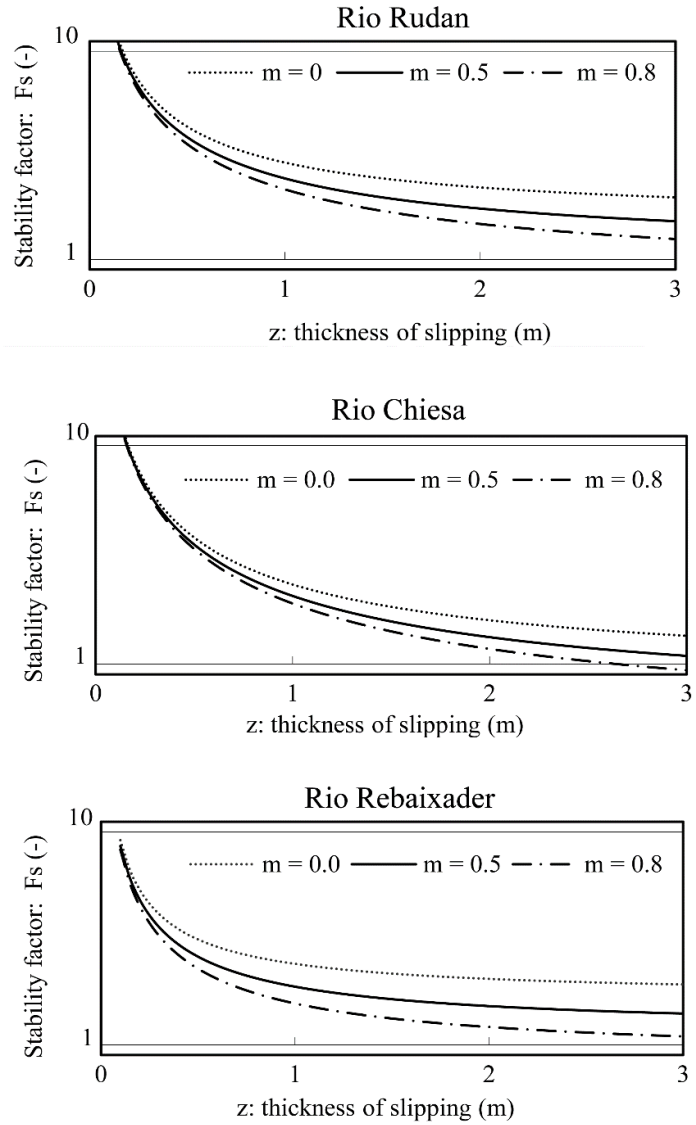

Figure 4.13: Stability factors for three possible water table height in the three study areas.

4.6 Discussion

In the present study, the analysis of the triggering phenomenon in the three study areas has been developed considering three different triggering mechanisms that can happen in the headwater basin. Tognacca and Bezzola (1997) already distinguished two main triggering mechanisms: shallow slope failure and channel bed failure. The third scenario that we considered in our analysis derives from the subdivision of channel bed failure in two different mechanisms: the first one studies the runoff generation starting from intense precipitations in the channels of the triggering areas (progressive erosion of the channel bed). Whereas, the second one considers the dam-break scenario (still considering the hydraulic behavior of the channel).

Finally, the third considered mechanisms is the shallow slope failure, which has been conducted comparing the stability of the triggering areas to that of an open hillslope partially saturated with water (D'Agostino et al. 2004).

To compute the critical water discharges in the control cross sections we used two different equations: the one proposed by Gregoretti and Dalla Fontana (2008) for the progressive erosion of the channel bed; the one proposed by Whittaker and Jaggi (1986) for the dam-break scenario. In fact, this second equation has been developed to study the possible destabilization of ramp-slopes. The critical discharges obtained with this second equation are likely corresponding to more powerful and destructive debris flows. In fact, the corresponding surges originating from these discharges have the possibility to mobilize and transport blocks and boulders of greater dimensions, leading also to mechanisms of clogging and dam-break inside the channels.

Considering the range of critical discharges resulting between Equation (4.1) and Equation (4.2), we can assume that inside this interval there is the maximum probability of debris flow triggering. From our analysis it can be noticed that the critical discharge for the initiation of debris flow is generally low (ranging between 0.02 and 0.16 m^3/s) and this discharge can be generated by short and intense rainfall events with a duration between about 10 and 20 minutes (Table 4.8, Figure 4.10, Figure 4.11 and Figure 4.12). The maximum hourly intensities that we empirically found with this approach are comparable with the ones measured in some Dolomitic headwater basins by Gregoretti et al. (2016). These rainfall intensities are undoubtedly a fundamental variable, but Guzzetti et al. (2007) stated that in mountainous areas the only duration can be itself a sufficient parameter leading to a potential debris flow triggering. Conversely, if the channel banks are characterized by the presence of blocks of dimensions

greater than 0.3 m armoring the bed bottom (critical discharge equation of Whittaker and Jaggi (1986)), it is needed a longer rainfall duration (30 – 60 minutes) for the mobilization of sediments, postponing the potential debris flow triggering.

In each considered catchment, the outlet cross section does not show the highest critical discharge among the three sections (Table 4.5). On Rudan basin, the highest critical discharge corresponds to the cross section 1 that is the one located in the left channel in the middle of the source area. This section is the widest and it is characterized by the lowest channel slope (Table 4.2 and Figure 4.5). On the Chiesa basin, the highest critical discharge corresponds to cross section 2 that is positioned in the central part of the gully and in this case, it is not the widest or the less steep one. Finally, in the Rebaixader basin, the highest critical discharge corresponds to cross section 2, that is located in the lower part of the source area. This is the widest section but also the steepest one. Therefore, it seems that generally, along the ephemeral gullies located inside the source areas, the critical runoff needed for the mobilization of sediments is higher than the ones resulting from the outlet sections. This means that also the rainfall intensities and durations needed to destabilize these zones of the source areas are slightly higher than the ones observed at the headwater basin outlets.

A top probability in terms of necessary flow rate for debris-flow initiation could be determined by selecting for every headwater catchment the maximum critical values among different control cross-sections where the process might take place. In our study cases, we found again a quite narrow range of triggering discharges and shear stresses, which vary from 0.03 to 0.28 m^3/s and from 269 to 413 N/m^2, respectively.

Moreover, the critical runoff discharge found in our study for the mobilization of sediments is comparable to the one found by Coe et al. (2008). In fact, they found a value of 0.15 m^3/s of in-channel runoff needed to start a debris flow and they also stated that for the debris flow initiation it is not required a high antecedent moisture level in the soil. The behavior in particular of the Rudan headwater basin can be compared to that of the Chalk Cliffs catchment: apparently, debris flows initiate because intense rainfall events fall on the rocky faces and couloirs above the source areas, generating a critical runoff that abruptly mobilize sediments. This typical triggering behavior has been already described by various authors in the last years (e.g. Berti and Simoni 2005; Gregoretti and Dalla Fontana 2008; Marchi et al. 2008; Gregoretti et al. 2016) and our simulated hydrological behavior highlights the strong capacity of water to initiate the mobilization of sediments. In a perspective of protection of the populations living near these

critical zones, it is important to understand this particular behavior. In fact, the high amount of material stored in the source areas, the generally low runoff discharge needed for the mobilization of sediments (Table 4.5 and Table 4.7), coupled with the frequency of intense and short thunderstorms during summer (Berti and Simoni 2005; Bertoldi and D'Agostino 2014; Abancó et al. 2016; Marra et al. 2016), makes these areas strongly susceptible to debris flows.

The critical shear stresses resulting from the control cross sections analysis are comparable between the three basins, meaning that similar erosive forces are needed to mobilize the sediments inside the channels. Nevertheless, the Chiesa and Rebaixader catchments, characterized by large steep eroded hillslopes, show slightly smaller critical shear stresses if compared to Rudan basin. This last one is characterized by the presence of a steep talus cone rich of large boulders surrounded by rock faces and it seems that this different morphology requires a higher stress to mobilize sediments in the channel bed.

Rudan and Rebaixader catchments are characterized by the presence of big blocks in the triggering areas (Hürlimann et al. 2012) and so, the second discharge initiation threshold derived with the formula of Whittaker and Jaggi (1986) assumes a quite important relevance in the comprehension of the triggering mechanism, but also of the following overall dynamics. The mobilization of these big blocks in fact is the consequence of a higher water discharge that could result in the generation of debris flows near to the maximal values in terms of both flow peaks and total volumes.

Nevertheless, the Chiesa and Rebaixader catchments show significant differences from the Rudan basin. In fact, as already stated, the first two catchments are characterized by open eroded hillslopes, without the presence of rock walls incised by couloirs (typical of the Rudan triggering area). The surface runoff generation in these two basins seems therefore linked to the saturation of the first soil layers that prevent water to infiltrate. In this perspective, it takes a great importance the second type of debris flow generation: the triggering mechanism by shallow slope failure. In fact, Rickenmann (2016) states that if the shallow landslides are sufficiently large and fluid and occur near the channel network, they can evolve into hillslope debris flows. Looking in particular at the Chiesa catchment case study (Figure 4.13), we can see that when the water table parameter exceeds the value of 0.5 (meaning that if the thickness of slipping is of 2 meters the water table is located at 1 meter of depth) we already move close to the instability limit. Analyzing the pore pressure data about the destabilization of the slope by shallow landslides, Genevois et al. (2000) found that this mechanism can be initiated also

when the water table is far below the terrain surface. This is in agreement with our findings, in fact especially in the Chiesa and Rebaixader catchments, the stability limit can be reached considering a water table still relatively distant from the total saturation of the terrain.

4.7 Conclusions

Considering the results obtained from this study, we can state that:

- Even if there are many Intensity-Duration curves already computed for the discrimination of the triggering of debris flows, it seems that a minimum rainfall duration is needed, so that below this limit the starting of a debris flow is very unlike to occur.
- The critical rainfall durations related to a high triggering probability are in the range between 12 and 22 minutes in the three headwater basins
- The critical discharges needed to initiate a debris flow surge are generally low (between 0.03 and 0.28 m^3/s) meaning that a relatively low water runoff is needed to mobilize sediments inside the channel.
- The range of critical discharges found between the two equations (Whittaker and Jaggi 1986; Gregoretti and Dalla Fontana 2008) highlights the interval in which the debris flow triggering is higher. In particular, in all the headwater basins, a 60 minutes rainfall with critical intensity is capable of generating a water peak discharge exceeding the threshold for the mobilization of boulders larger than 0.3 m (dam-break scenario). This means that real rainfall events with similar characteristics can possibly trigger torrential events of very high magnitude.
- The central parts of the source areas resulted as the zones needing the higher water discharge to be destabilized. This means that these reaches of the gullies require a higher rainfall duration to initiate the debris flow surge.
- The results of the slope stability analysis show that the Rudan catchment source area is relatively stable, whereas Chiesa and Rebaixader basins show values that goes near the critical stability factor with thickness of slipping between 2 and 3 meters.

- The different catchments morphologies influence the main triggering mechanism, meaning that on Rudan like basins, channel bed failure seems the dominant mechanism. Whereas in basins similar to Rebaixader and Chiesa, shallow slope failure mechanism or at least a mixed behavior between the two types is more likely to occur.

5 Epilogue

In the present thesis, we studied the triggering of debris flows and the corresponding initiation areas in which the phenomenon starts. We developed a composed analysis, considering the three main variables needed for the debris flow triggering, which are: 1) morphological characteristics (the terrain slope of the triggering areas); (2) water input, in terms both of the rainfall and of the corresponding discharge; (3) sediment availability. In each part of the thesis, we focused on one or more of the three variables using also different spatial scales. On Chapter 2 we conducted a regional scale analysis, focusing on the morphological and hydrological characteristics (variables 1 and 2) that discriminate between potential source areas and non-source areas. In Chapter 3, we moved to the local scale analysis, considering a single catchment. Here we made a detailed analysis about rainfalls and their influence on sediment availability (variables 2 and 3). Finally, on Chapter 4, we still worked on the single basin scale, coupling a hydrological analysis with a morphological analysis of the headwater basins (variables 1 and 2).

In the first part of the analysis, working on the Vizze Valley, we found that a limiting threshold of 0.1 km^2 of drainage area could identify the potential source areas along the valley hillslopes. Whereas, if we look to the upslope contributing areas of the source points that we considered in Chapter 4, these values are higher. In fact, on Rio Rudan catchment, the contributing area of the three cross sections, starting from number 1 (that is the one located at the basin outlet) are respectively of 0.82, 0.29 and 0.21 km^2. On Rio Chiesa catchment, starting from section 1, the values are respectively of 0.06, 0.23 and 0.95 km^2 (in this case the basin outlet corresponds to section 3). Moreover, on Rio Rebaixader catchment, starting from section 1, the values are respectively: 0.42, 0.62 and 0.67 km^2 (also in this case the basin outlet corresponds to section 3). This difference can be explained considering that the event of the Vizze Valley is an extreme one, triggered by rainfalls characterized by high intensities and high durations (72.8 mm in 6 hours), with an approximate return period between 200 and 300 years (Macconi et al. 2012). It seems that this strong rainfall event was capable of activate “new” source areas. These new collapsed zones were usually non-active areas and so there was not a historical memory of their possible destabilization. This hypothesis is also confirmed by the fact that we considered also a relatively low slope threshold (higher than 15°). Whereas, in the three analysed catchments,

the triggering areas are perfectly visible and known and we can consider them as "historical" source areas. These areas are always characterized by unstable conditions and for this reason they can be activated also with higher limiting thresholds, as the considered values of upslope contributing areas. Therefore, we can consider the limiting threshold of 0.1 km^2 as the extreme hydrological condition to activate the initiation areas and higher values of drainage area as the "normal" values for the activation of great and frequently active source areas.

Concerning the rainfall thresholds found in the study about Rio Rebaixader catchment (Chapter 3), we can couple the obtained results with the hydrological analysis made on Chapter 4. The correlation between the rainfall intensity and the event volume can be compared to the different thresholds of critical discharge calculated on Chapter 4 using the equations of Gregoretti and Dalla Fontana (2008) and Whittaker and Jaggi (1986). Looking at Figure 5.1 it can be observed that there is a first threshold of rainfall intensity above which the triggering mechanism is possible (about 10 mm/h of $I_{30\ MAX}$), and then there is a second intensity threshold (about 20 mm/h of $I_{30\ MAX}$) above which are triggered also events characterized by volumes with higher magnitudes. This reflects the two critical discharges thresholds described on Chapter 4, the first one related to a primary mobilization of sediments, the second one related to the potential mobilization of debris of coarser dimensions that can result in stronger and more destructive debris flow events. The typical behaviour of the catchments seems not to follow a continuous/regular increasing of the volume related to the increasing of rainfalls, but it seems that there is a kind of switch-like growth (Figure 5.1). This means that when a certain rainfall quantity is reached (and a corresponding water runoff) the mobilized volume abruptly increases moving from a small almost ordinary event (e.g., some hundreds/few thousands of cubic meters) to a big one (e.g., volume equal or greater than 10000-15000 cubic meters, in the case of the volume range of the Rio Rebaixader basin).

The Rio Rebaixader catchment is characterized by a higher frequency of torrential events. Looking at Figure 3.7 it can be noticed that on average this basin experiences four events per year (one event every year and a half considering only events of the debris flow type). From the historical analysis of Rio Chiesa and Rio Rudan catchments (D'Agostino et al. (2002) and D'Agostino (2003)), the first one resulted on a frequency of about one event every four years, whereas the second one has a frequency of about one event every eight years (one event every five years considering also the debris flood events). Therefore, the Rio Rebaixader catchment is undoubtedly a supply-unlimited type of basin with a high delivery-capacity to the basin

outlet. This is also demonstrated by the fact that relatively low rainfalls can activate the catchment and trigger a torrential flow. Moreover, the transport zone of this basin is short (length of about 200 m between the headwater basin outlet and the deposition starting point), and so every time that the source area is activated, the mobilized sediments reach the deposition area. Conversely, in the Rio Rudan catchment the transport zone is very long (distance of about 3 km between the headwater basin outlet and the deposition initiation point). Therefore, small magnitude events (hundreds of m^3) usually start and finish inside this zone of the basin without reaching the deposition area at the valley bottom. This characteristic makes the Rio Rudan catchment a supply-unlimited type with a low delivery-capacity to the basin outlet, meaning that it is potentially more dangerous than the Rio Rebaixader catchment. In fact, Bovis and Jakob (1999) stated that basins with lower frequencies are usually characterized by higher magnitudes due to an increasing sediment recharge in the torrent bed. The Rio Chiesa catchment has an intermediate situation because it is characterized by a frequency that is twice that of the Rio Rudan basin and it presents a transport zone of about 600 m long. Moreover, this catchment is mainly characterized by high terrain slope gradients also in the transport zone, meaning that every time that a debris flow is triggered, it would probably reach the deposition area.

The hydrological study made on Chapter 4 highlights that generally the hydrological conditions for the debris flow triggering are comparable (both in terms of critical discharge and of shear stress). Moreover, the maximum "first-level" triggering discharge (Figure 5.1, Equation 4.1) among the three basins is quite low (of the order of 150 l/s) and reflects an overall high susceptibility to the phenomenon, which doubles if we consider the "upper-level" critical discharge (Figure 5.1, Equation 4.2). Differently, the morphological conditions vary among the three initiation areas. In the Rio Rebaixader and in the Rio Chiesa catchments, the source areas are wide unstable portions of the hillslopes, inside which are located different initiation points that can be activated individually or simultaneously. Conversely, in Rio Rudan catchment the initiation zone seems more related to the channel network and to the "ephemeral gullies". In fact, the slope stability analysis showed that the talus cone inside the headwater basin is relatively stable. Moreover, considering that the entire torrent is characterized by high instability, with the channel bed and banks strongly affected by erosion, it is reasonable to assume that a great part of the sediment mobilized during a debris flow event is entrained inside the channel. For this reason, we can state that on basins more similar to Rio Rudan, the most probable triggering mechanism is that of channel bed failure (in the head zone mostly),

characterized by high erosion and deposition. Whereas on basins with morphological features similar to the ones of Rio Rebaixader and Rio Chiesa, the triggering mechanism is related to shallow or thin slope failures. Here we can observe a collapse of the first layers of the soil (e.g., 0.05-0.20 m). Therefore, the rainfall erosivity analysis seems more appropriate in these kind of catchments, in which the energy of precipitation can determine or not the collapse of the terrain.

The study of the Vizze Valley regards the typical triggering mechanism of an extreme meteorological event, with high intensities and durations. In this case, the destabilization can easily affect areas that are usually stable leading to the overall collapse/reactivation of new/sleeping source areas. For these circumstances the triggered events might be characterized by highly variable magnitudes in terms of volumes depending on the mass amount of the source areas under destabilization.

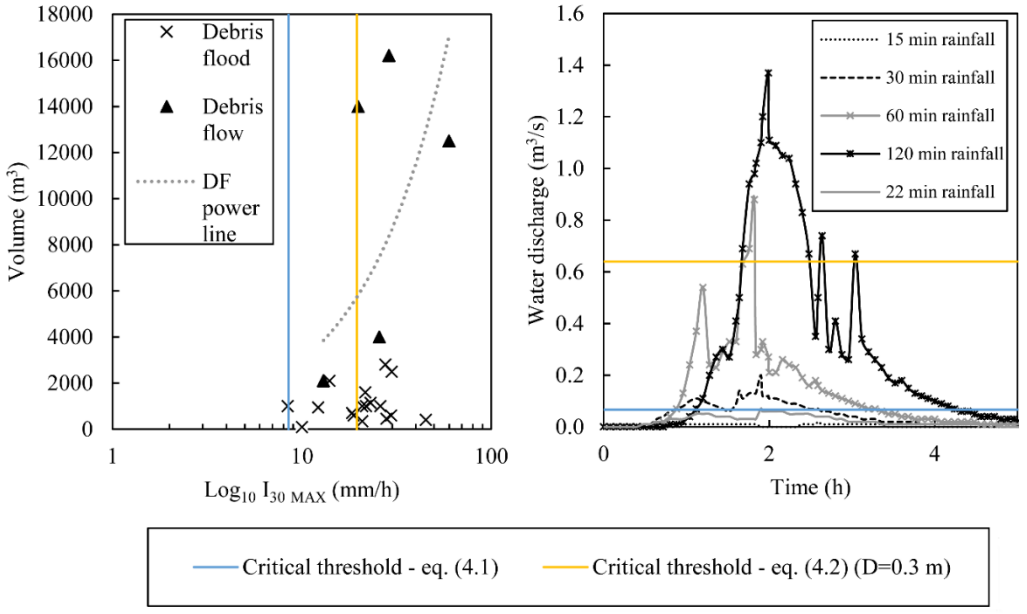

Rebaixader critical discharges	
Q_c eq. (4.1)	0.07 m³/s
Q_c eq. (4.2) (D=0.3 m)	0.64 m³/s

Range of critical discharges in the three headwater basins	
Q_c eq. $(4.1)_{MIN}$	0.03 m³/s
Q_c eq. $(4.1)_{MAX}$	0.16 m³/s
Q_c eq. $(4.2)_{MIN}$ (D=0.3 m)	0.35 m³/s
Q_c eq. $(4.2)_{MAX}$ (D=0.3 m)	0.64 m³/s

Figure 5.1: Comparison between rainfall thresholds and critical discharges in the Rebaixader catchment and range of critical discharges obtained in the three analysed headwater basins: Rudan, Chiesa and Rebaixader torrents.

Acknowledgements

I would like to thank “Fondazione Ing. Aldo Gini” which supported me with a scholarship, giving me the possibility to spend six months at BarcelonaTECH UPC (Spain), working with Prof. Marcel Hürlimann.

References

Abancó C, Hürlimann M (2014) Estimate of the debris-flow entrainment using field and topographical data. Nat Hazards 71:363–383. doi: 10.1007/s11069-013-0930-5

Abancó C, Hürlimann M, Moya J, Berenguer M (2016) Critical rainfall conditions for the initiation of torrential flows. Results from the Rebaixader catchment (Central Pyrenees). J Hydrol 541:218–229. doi: 10.1016/j.jhydrol.2016.01.019

Ancey C (2001) Debris Flows and Related Phenomena A Typology of Torrential Flows. Springer Berlin Heidelb 528–547.

Armanini A, Fraccarollo L, Rosatti G (2009) Two-dimensional simulation of debris flows in erodible channels. Comput Geosci 35:993–1006. doi: 10.1016/j.cageo.2007.11.008

Astori A, Venturini C (2012) Evoluzione quaternaria della media Val di Vizze - Pfitschtal (Vipiteno, BZ - Alpi Aurine). Gortania Geol Paleontol Paletnologia 33:63–92.

Bacchini M, Zannoni A (2003) Relations between rainfall and triggering of debris-flow: case study of Cancia (Dolomites, Northeastern Italy). Nat Hazards Earth Syst Sci 3:71–79. doi: 10.5194/nhess-3-71-2003

Badoux A, Graf C, Rhyner J, et al (2009) A debris-flow alarm system for the Alpine Illgraben catchment: Design and performance. Nat Hazards 49:517–539. doi: 10.1007/s11069-008-9303-x

Barbolini M (2008) Hazard mapping of extremely rapid mass movements in Europe. Deliv D31, Integr Risk Manag Extrem Rapid Mass Movements Sixht Fram:147.

Bardou E, Boivin P, Pfeifer H-R (2007) Properties of debris flow deposits and source materials compared: implications for debris flow characterization. Sedimentology 54:469–480. doi: 10.1111/j.1365-3091.2007.00855.x

Bathurst JC, Burton A, Ward TJ (1997) Debris Flow Run-Out and Landslide Sediment Delivery Model Tests. J Hydraul Eng 123:410–419. doi: 10.1061/(ASCE)0733-9429(1997)123:5(410)

Baumann V, Wick E, Horton P, Jaboyedoff M (2010) Debris flow susceptibility mapping at a regional scale along the National Road N7, Argentina. In: Proceedings of the 14th Pan-American Conference on Soil Mechanics and Geotechnical Engineering. Toronto, Ontario, Canada,

Bel C, Liébault F, Navratil O, et al (2017) Rainfall control of debris-flow triggering in the Réal Torrent, Southern French Prealps. Geomorphology 291:17–32. doi: 10.1016/j.geomorph.2016.04.004

Berger C, McArdell BW, Schlunegger F (2011) Sediment transfer patterns at the Illgraben catchment, Switzerland: Implications for the time scales of debris flow activities. Geomorphology 125:421–432. doi: 10.1016/j.geomorph.2010.10.019

Berti M, Genevois R, Simoni A, Tecca PR (1999) Field observations of a debris flow event in the Dolomites. Geomorphology 29:265–274.

Berti M, Simoni A (2005) Experimental evidences and numerical modelling of debris flow initiated by channel runoff. Landslides 2:171–182. doi: 10.1007/s10346-005-0062-4

Bertoldi G, D'Agostino V (2014) Colate detritiche: dinamiche degli apporti di sedimento a scala integrata di bacino. Padova

Bettella F, D'Agostino V (2012) Reologia e dinamica di propagazione delle colate detritiche: analisi e modellazione a diversa scala. Università degli Studi di Padova

Beverage JP, Culbertson JK (1964) Hyperconcentrations of suspended sediment. J Hydraul Div 90:117–128.

Blahut J, Horton P, Sterlacchini S, Jaboyedoff M (2010) Debris flow hazard modelling on medium scale: Valtellina di Tirano, Italy. Nat Hazards Earth Syst Sci 10:2379–2390. doi: 10.5194/nhess-10-2379-2010

Borga M, Stoffel M, Marchi L, et al (2014) Hydrogeomorphic response to extreme rainfall in headwater systems: Flash floods and debris flows. J Hydrol 518:194–205. doi: 10.1016/j.jhydrol.2014.05.022

Bovis MJ, Jakob M (1999) The role of debris supply conditions in predicting debris flow activity. Earth Surf Process Landforms 24:1039–1054. doi: 10.1002/(SICI)1096-9837(199910)24:11<1039::AID-ESP29>3.0.CO;2-U

Brayshaw D, Hassan M a. (2009) Debris flow initiation and sediment recharge in gullies. Geomorphology 109:122–131. doi: 10.1016/j.geomorph.2009.02.021

Breien H, De Blasio F V., Elverhøi A, Høeg K (2008) Erosion and morphology of a debris flow caused by a glacial lake outburst flood, Western Norway. Landslides 5:271–280. doi: 10.1007/s10346-008-0118-3

Burton A, Bathurst JC (1998) Physically based modelling of shallow landslide sediment yield at a catchment scale. Environ Geol 35:89–99. doi: 10.1007/s002540050296

Caine N (1980) The rainfall intensity - Duration control of shallow landslides and debris flows. Geogr Ann Ser A, Phys Geogr 62:23–27.

Cannon SH, Bigio ER, Mine E (2001) A process for fire-related debris flow initiation, Cerro Grande fire, New Mexico. Hydrol Process 15:3011–3023. doi: 10.1002/hyp.388

Cannon SH, Ellen S (1985) Rainfall conditions for abundant debris avalanches, San Francisco Bay region, California. Calif Geol 38:267–272.

Cannon SH, Gartner JE, Rupert MG, Michael J a (2004) Emergency assessment of debris-flow hazards from basins burned by the Grand Prix and Old Fires of 2003, Southern California.

Capart H, Young DL, Zech Y (2001) Dam-Break induced debris flow. Part gravity Curr 149–156.

Carrara A, Crosta G, Frattini P (2008) Comparing models of debris-flow susceptibility in the alpine environment. Geomorphology 94:353–378. doi: 10.1016/j.geomorph.2006.10.033

Cavalli M, Grisotto S (2006) Individuazione con metodi GIS delle aste torrentizie soggette a colate detritiche: applicazione al bacino dell'Alto Avisio (Trento). Quad di idronomia Mont 26:1–12.

Cavalli M, Trevisani S, Comiti F, Marchi L (2013) Geomorphometric assessment of spatial sediment connectivity in small Alpine catchments. Geomorphology 188:31–41. doi: 10.1016/j.geomorph.2012.05.007

Claessens L, Heuvelink GBM, Schoorl JM, Veldkamp A (2005) DEM resolution effects on shallow landslide hazard and soil redistribution modelling. Earth Surf Process Landforms 30:461–477. doi: 10.1002/esp.1155

Coe J a., Cannon SH, Santi PM (2008a) Introduction to the special issue on debris flows initiated by runoff, erosion, and sediment entrainment in western North America. Geomorphology 96:247–249. doi: 10.1016/j.geomorph.2007.05.001

Coe JA, Kinner DA, Godt JW (2008b) Initiation conditions for debris flows generated by runoff at Chalk Cliffs, central Colorado. Geomorphology 96:270–297. doi: 10.1016/j.geomorph.2007.03.017

Comiti F, Marchi L, Macconi P, et al (2014) A new monitoring station for debris flows in the European Alps: first observations in the Gadria basin. Nat Hazards 73:1175–1198. doi: 10.1007/s11069-014-1088-5

Corominas J, Moya J (2008) A review of assessing landslide frequency for hazard zoning purposes. Eng Geol 102:193–213. doi: 10.1016/j.enggeo.2008.03.018

Costa JE (1984) Physical geomorphology of debris flows. Dev Appl Geomorphol 268–317.

Costa JE, Williams GD (1984) Debris flow dynamics.

Coussot P, Meunier M (1996) Recognition, classification and mechanical description of debris flows. Earth-Science Rev 40:209–227.

Crosta G, Frattini P (2001) Physically based distributed modelling for shallow landslide Hazard Zonation. In: Proceedings 3rd EGS Plinius Conference. Baja, Sardinia, Italy, pp 463–487

Crosta GB, Frattini P (2003) Distributed modelling of shallow landslides triggered by intense rainfall. Nat Hazards Earth Syst Sci 3:81–93.

Crosta GB, Frattini P (2008) Rainfall-induced landslides and debris flows. Hydrol Process 22:473–477. doi: 10.1002/hyp.6885

Cruden DM, Varnes DJ (1996) Landslides types and processes. Special Report 247, Washington D.C.

D'Agostino V (1996) Analisi quantitativa e qualitativa del trasporto solido torrentizio nei bacini montani del Trentino Orientale. Scr dedicati a Giovanni Tournon, Assoc Ital di Ing Agrar Idrotec Ital 111–123.

D'Agostino V (2013) Assessment of Past Torrential Events Through Historical Sources. In: Schneuwly-Bollschweiler M, Stoffel M, Rudolf-Miklow F (eds) Dating Torrential Processes on Fans and Cones in Advances on Global Change Research 47. Springer Netherlands, pp 131–146

D'Agostino V (2003) Progetto n° 647: Realizzazione di barriere fermaneve elastiche e di opere di miglioramento del deflusso idraulico, Comune di Livinallongo del Col di Lana (BL). Belluno

D'Agostino V, Bertoldi G (2014) On the assessment of the management priority of sediment source areas in a debris-flow catchment. Earth Surf Process Landforms 39:656–668. doi: 10.1002/esp.3518

D'Agostino V, Degetto M, Marchi L, et al (2002) Individuazione e definizione delle soluzioni tecnico-realizzative maggiormente idonee alla messa in sicurezza del torrente Rudan a ridosso dell'abitato di Vodo di Cadore (loc. Peaio).

D'Agostino V, Marchi L, Coali R (2004) Fenomeni di colata detritica alla testata di un bacino dolomitico. In:

Internationales Symposion interpraevent 2004. Riva/Trient, pp 81–92

D'Asaro F, Grillone G (2012) Empirical Investigation of Curve Number Method Parameters in the Mediterranean Area. J Hydrol Eng 17:1141–1152. doi: 10.1061/(ASCE)HE.1943-5584.0000570

Deganutti AM, Marchi L, Arattano M (2000) Rainfall and debris-flow occurrence in the Moscardo basin (Italian Alps). In: Wieczorek GF, Naeser ND (eds) Debris flow Hazards Mitigation: Mechanics, Prediction, and Assessment; Proceedings of the 2nd International DFHM Conference. Taipei, Taiwan, pp 67–72

DeGraff JV (1997) Geologic investigation of the Pilot Ridge debris flow, Groveland Range District, Stanislaus National Forest.

Destro E, Marra F, Nikolopoulos EI, et al (2017) Spatial estimation of debris flows-triggering rainfall and its dependence on rainfall return period. Geomorphology 278:269–279. doi: 10.1016/j.geomorph.2016.11.019

Dhakal AS, Sidle RC (2003) Long-term modelling of landslides for different forest management practices. Earth Surf Process Landforms 28:853–868. doi: 10.1002/esp.499

Di Stefano C, Ferro V, Pampalone V, Sanzone F (2013) Field investigation of rill and ephemeral gully erosion in the Sparacia experimental area, South Italy. Catena 101:226–234. doi: 10.1016/j.catena.2012.10.012

Dong J-J, Lee C-T, Tung Y-H, et al (2009) The role of the sediment budget in understanding debris flow susceptibility. Earth Surf Process Landforms 34:1612–1624. doi: 10.1002/esp.1850

Dowling CA, Santi PM (2014) Debris flows and their toll on human life: A global analysis of debris-flow fatalities from 1950 to 2011. Nat Hazards 71:203–227. doi: 10.1007/s11069-013-0907-4

Ellen, Fleming (1987) Mobilization of debris flows from soil slips, San Francisco bay Region. Eng Geol 7:31–40.

Fannin RJ, Wise MP (2001) An empirical-statistical model for debris flow travel distance. Can Geotech J 38:982–994. doi: 10.1139/cgj-38-5-982

Fischer L, Rubensdotter L, Sletten K, et al (2012) Debris flow modeling for susceptibility mapping at regional to national scale in Norway. In: Eberhardt et al. (eds) (ed) Landslides and Engineered Slopes: Protecting Society through Improved Understanding. Taylor & Francis Group, London, UK, pp 723–729

Floris M, D'Alpaos A, Squarzoni C, et al (2010) Recent changes in rainfall characteristics and their influence on thresholds for debris flow triggering in the Dolomitic area of Cortina d'Ampezzo, north-eastern Italian Alps. Nat Hazards Earth Syst Sci 10:571–580. doi: 10.5194/nhess-10-571-2010

Fryirs K (2013) (Dis)Connectivity in catchment sediment cascades: a fresh look at the sediment delivery problem. Earth Surf Process Landforms 38:30–46. doi: 10.1002/esp.3242

Fuchs S, Kaitna R, Scheidl C, Hübl J (2008) The Application of the Risk Concept to Debris Flow Hazards. Geomech und Tunnelbau 1:120–129. doi: 10.1002/geot.200800013

Gamma P (2000) dfwalk - Ein Murgang Simulationsprogramm zur Gefahrenzonierung. Bern

Gartner JE, Cannon SH, Santi PM, Dewolfe VG (2008) Empirical models to predict the volumes of debris flows generated by recently burned basins in the western U.S. Geomorphology 96:339–354. doi: 10.1016/j.geomorph.2007.02.033

Genevois R, Tecca PR, Berti M, Simoni A (2000) Pore pressure distribution in the initiation area of a granular debris flow. In: Bromhead E, Dixon N, Ibsen M (eds) Proceedings of the 8th International Symposium on Landslides. Cardiff, UK, pp 615–620

Ghilardi P, Natale L, Savi F (2001) Modeling Debris Flow Propagation and Deposition. Phys Chem Earth, Part C Solar, Terr Planet Sci 26:651–656. doi: 10.1016/S1464-1917(01)00063-0

Gregoretti C (2000) The initiation of debris flow at high slopes: Experimental results. J Hydraul Res 38:83–88. doi: 10.1080/00221680009498343

Gregoretti C, Dalla Fontana G (2008) The triggering of debris flow due to channel-bed failure in some alpine headwater basins of the Dolomites: Analyses of critical runoff. Hydrol Process 22:2248–2263. doi: 10.1002/hyp.6821

Gregoretti C, Dalla Fontana G (2007) Rainfall threshold for the initiation of debris flows by channel-bed failure in the Dolomites. Debris-Flow Hazards Mitig Mech Predict Assesment 11–21.

Gregoretti C, Degetto M (2012) Modello di innesco di una colata detritica originata dall'erosione di sedimenti per deflusso superificiale e dell'idrogramma solido-liquido. In: XXXIII Convegno Nazionale di Idraulica e Costruzioni Idrauliche. Brescia,

Gregoretti C, Degetto M, Bernard M, et al (2016) Runoff of small rocky headwater catchments: Field observations and hydrological modeling. Water Resour Res 52:8138–8158. doi: 10.1002/2016WR018675

Guthrie RH (2002) The effects of logging on frequency and distribution of landslides in three watersheds on Vancouver Island, British Columbia. Geomorphology 43:273–292. doi: 10.1016/S0169-555X(01)00138-6

Guzzetti F, Peruccacci S, Rossi M, Stark CP (2007) The rainfall intensity–duration control of shallow landslides and debris flows: an update. Landslides 5:3–17. doi: 10.1007/s10346-007-0112-1

Hawkins RH, Ward TJ, Woodward E, Van Mullem J a (2010) Continuing evolution of rainfall-runoff and the curve number precedent. 2nd Jt Fed Interag Conf 2–12.

Heim A (1932) Bergsturz und Menschenleben. Vierteljhareszeitschrift der Naturforschenden Gesellschaft Zurich 30:

Heinimann H (1998) Methoden zur Analyse und Bewertung von Naturgefahren, Bundesamt für Umwelt, Wald und Landschaft. Bundesamt für Umwelt, Wald und Landschaft (BUWAL), Bern, Switzerland

Helvey JD (1980) Effects of a north central Washington wildfire on runoff and sediment production. Water Resour Bull 16:627–634.

Holmgren P (1994) Multiple flow direction algorithms for runoff modelling in grid based elevation models: An empirical evaluation. Hydrol Process 8:327–334. doi: 10.1002/hyp.3360080405

Horton P, Jaboyedoff M, Bardou E (2008) Debris flow susceptibility mapping at a regional scale. In: Locat, J., Perret, D., Turmel, D., Demers, D., et Leroueil S (ed) Proceedings of the 4th Canadian Conference on Geohazards: From Causes to Management. Presse de l'Université Laval, Québec, pp 399–406

Horton P, Jaboyedoff M, Rudaz B, Zimmermann M (2013) Flow-R, a model for susceptibility mapping of debris

flows and other gravitational hazards at a regional scale. Nat Hazards Earth Syst Sci 13:869–885. doi: 10.5194/nhess-13-869-2013

Horton P, Jaboyedoff M, Zimmermann M, et al (2011) Flow-R, a model for debris flow susceptibility mapping at a regional scale - some case studies. In: Casa Editrice Università La Sapienza (ed) Proceedings of the 5th International Conference on Debris-Flow Hazards Mitigation: Mechanics, Prediction and Assessment - Italian Journal of Engineering Geology and Environment. Padova, Italy, pp 875–884

Huggel C, Kaab A, Haeberli W, et al (2002) Remote sensing based assessment of hazards from glacier lake outbursts: a case study in the Swiss Alps. Can Geotech J 39:316–330. doi: 10.1139/t01-099

Hungr O, Leroueil S, Picarelli L (2013) The Varnes classification of landslide types, an update. Landslides 11:167–194. doi: 10.1007/s10346-013-0436-y

Hungr O, McDougall S (2009) Two numerical models for landslide dynamic analysis. Comput Geosci 35:978–992. doi: 10.1016/j.cageo.2007.12.003

Hürlimann M, Abancó C, Moya J, et al (2011) Debris-Flow Monitoring Stations in the Eastern Pyrenees . Description of Instrumentation , First Experiences and Pre- Liminary Results. Ital J Eng Geol Environ 553–562. doi: 10.4408/IJEGE.2011-03.B-061

Hürlimann M, Abancó C, Moya J (2016) Debris-Flow Monitoring for the Set-Up of a Warning and Alarm System - Experiences from the Pyrenees -. Int J Eros Control Eng 9:107–113. doi: http://doi.org/10.13101/ijece.9.107

Hürlimann M, Abancó C, Moya J (2012) Rockfalls detached from a lateral moraine during spring season. 2010 and 2011 events observed at the Rebaixader debris-flow monitoring site (Central Pyrenees, Spain). Landslides 9:385–393. doi: 10.1007/s10346-011-0314-4

Hürlimann M, Abancó C, Moya J, Vilajosana I (2014) Results and experiences gathered at the Rebaixader debris-flow monitoring site, Central Pyrenees, Spain. Landslides 11:939–953. doi: 10.1007/s10346-013-0452-y

Hürlimann M, Copons R, Altimir J (2006) Detailed debris flow hazard assessment in Andorra: A multidisciplinary approach. Geomorphology 78:359–372. doi: 10.1016/j.geomorph.2006.02.003

Hürlimann M, Rickenmann D, Graf C (2003) Field and monitoring data of debris-flow events in the Swiss Alps. Can Geotech J 40:161–175. doi: 10.1139/t02-087

Imaizumi F, Sidle RC, Tsuchiya S, Ohsaka O (2006) Hydrogeomorphic processes in a steep debris flow initiation zone. Geophys Res Lett 33:n/a-n/a. doi: 10.1029/2006GL026250

Innes J (1983) Debris flows. Prog Phys Geogr 7:469–501. doi: 10.1177/030913338300700401

Iverson RM, Denlinger RP (2001) Mechanics of debris flows and debris-laden flash floods. In: Research U (ed) Seventh Federal Interagency Sedimentation Conference. Reno, Nevada, USA, pp 1–8

Iverson RM, Reid ME, Lahusen RG (1997) Debris flow mobilization from landslides. Annu Rev Earth Planet Sci 25:85–138. doi: 10.1146/annurev.earth.25.1.85

Jakob M (2005) A size classification for debris flows. Eng Geol 79:151–161. doi: 10.1016/j.enggeo.2005.01.006

Jakob M, Bovis M, Oden M (2005) The significance of channel recharge rates for estimating debris-flow magnitude and frequency. Earth Surf Process Landforms 30:755–766. doi: 10.1002/esp.1188

Johnson AM, Rodine JR (1984) Debris flow. Slope Instab 257–361.

Kappes MS, Gruber K, Frigerio S, et al (2012) The MultiRISK platform: The technical concept and application of a regional-scale multihazard exposure analysis tool. Geomorphology 151–152:139–155. doi: 10.1016/j.geomorph.2012.01.024

Kappes MS, Malet J-P, Remaître A, et al (2011) Assessment of debris-flow susceptibility at medium-scale in the Barcelonnette Basin, France. Nat Hazards Earth Syst Sci 11:627–641. doi: 10.5194/nhess-11-627-2011

Kelleher C, Wagener T, McGlynn B (2015) Model-based analysis of the influence of catchment properties on hydrologic partitioning across five mountain headwater subcatchments. Water Resour Res 51:4109–4136. doi: 10.1002/2014WR016147

Kinnell PIA (2010) Event soil loss, runoff and the Universal Soil Loss Equation family of models: A review. J Hydrol 385:384–397. doi: 10.1016/j.jhydrol.2010.01.024

Klock, Helvey (1976) Debris flows following wildfires in north central Washington. In: Proceedings of the Third Federal Inter-Agency Sedimentation Conference. Denver, Colorado, pp 91–96

Lambe TW, Whitman RV (1968) Soil Mechanics. John Wiley & Sons, New York

Lari S, Crosta GB, Frattini P, et al (2011) Regional-scale debris flow risk assessment for an alpine valley. In: 5th International Conference on Debris-Flow Hazards Mitigation: Mechanics, Prediction and Assessment. pp 933–940

Legg NT, Meigs AJ, Grant GE, Kennard P (2014) Debris flow initiation in proglacial gullies on Mount Rainier, Washington. Geomorphology 226:249–260. doi: 10.1016/j.geomorph.2014.08.003

Lin CW, Shieh CL, Yuan BD, et al (2004) Impact of Chi-Chi earthquake on the occurrence of landslides and debris flows: Example from the Chenyulan River watershed, Nantou, Taiwan. Eng Geol 71:49–61. doi: 10.1016/S0013-7952(03)00125-X

Lu N, Godt J (2008) Infinite slope stability under steady unsaturated seepage conditions. Water Resour Res 44:1–13. doi: 10.1029/2008WR006976

Macconi P, Formaggioni O, Sperling M (2012) Report Annuale ED30 2012. Bolzano

Marchi L, D'Agostino V (2004) Estimation of debris-flow magnitude in the Eastern Italian Alps. Earth Surf Process Landforms 29:207–220. doi: 10.1002/esp.1027

Marchi L, Dalla Fontana G, Cavalli M, Tagliavini F (2008) Rocky Headwaters in the Dolomites, Italy: Field Observations and Topographic Analysis. Arctic, Antarct Alp Res 40:685–694. doi: 10.1657/1523-0430(07-037)[MARCHI]2.0.CO;2

Marra F, Nikolopoulos EI, Creutin JD, Borga M (2016) Space-time organization of debris flows-triggering rainfall and its effect on the identification of the rainfall threshold relationship. J Hydrol 541:246–255. doi: 10.1016/j.jhydrol.2015.10.010

McArdell BW, Bartelt P, Kowalski J (2007) Field observations of basal forces and fluid pore pressure in a debris flow. Geophys Res Lett 34:2–5. doi: 10.1029/2006GL029183

McCoy SW, Kean JW, Coe JA, et al (2010) Evolution of a natural debris flow: In situ measurements of flow dynamics, video imagery, and terrestrial laser scanning. Geology 38:735–738. doi: 10.1130/G30928.1

Megahan WF (1983) Hydrologic effects of clearcutting and wildfire on steep granitic slopes in Idaho. Water Resour Res 19:811–819.

Melton M (1965) The geomorphic and paleoclimatic significance of alluvial deposits in southern Arizona. J Geol 73:1–38.

Michelini T, Pastorello R, D'Agostino V (2014) Modellazione morfo-energetica delle colate detritiche per la definizione della suscettibilità al pericolo. In: Editore Z (ed) XXXIV Convegno di Idraulica e Costruzioni Idrauliche. Bari, Italy, pp 701–702

Michoud C, Derron MH, Horton P, et al (2012) Rockfall hazard and risk assessments along roads at a regional scale: Example in Swiss Alps. Nat Hazards Earth Syst Sci 12:615–629. doi: 10.5194/nhess-12-615-2012

Miller DJ, Burnett KM (2008) A probabilistic model of debris-flow delivery to stream channels, demonstrated for the Coast Range of Oregon, USA. Geomorphology 94:184–205. doi: 10.1016/j.geomorph.2007.05.009

Montgomery DR, Dietrich WE (1988) Where do channels begin? Nature 336:232–234.

Montgomery DR, Dietrich WE (1994) A physically based model for the topographic control on shallow landsliding. Water Resour Res 30:1153–1171. doi: 10.1029/93WR02979

Montgomery DR, Foufoula-Georgiou E (1993) Channel network source representation using digital elevation models. Water Resour Res 29:3925. doi: 10.1029/93WR02463

Moser M, Hohensinn F (1983) Geotechnical aspects of soil slips in Alpine regions. Eng Geol 19:185–211. doi: https://doi.org/10.1016/0013-7952(83)90003-0

Munoz JA (1992) Evolution of a continental collision belt: ECORS-Pyrenees crustal balanced cross-section. Thrust Tectonics 235–246. doi: 10.1007/978-94-011-3066-0_21

O'Brien JS, Julien PY, Fullerton WT (1993) Two-Dimensional water flood and mudflow simulation. J Hydraul Eng 119:24–261. doi: 10.1061/(ASCE)0733-9429(1993)119:2(244)

O'Callaghan JF, Mark DM (1984) The extraction of drainage networks from digital elevation data. Comput Vision, Graph Image Process 27:247. doi: 10.1016/S0734-189X(84)80047-X

Panagos P, Ballabio C, Borrelli P, et al (2015) Rainfall erosivity in Europe. Sci Total Environ 511:801–814. doi: 10.1016/j.scitotenv.2015.01.008

Panagos P, Meusburger K, Van Liedekerke M, et al (2014) Assessing soil erosion in Europe based on data collected through a European network. Soil Sci Plant Nutr 60:15–29. doi: 10.1080/00380768.2013.835701

Park D, Lee S, Nikhil N V, et al (2013) Debris flow hazard zonation by probabilistic analysis (Mt. Woomyeon, Seoul, Korea). Int J Innov Res Sci Eng Technol 2:2381–2390.

Paronuzzi P, Coccolo A, Garlatti G (1998) Eventi meteorici critici e debris flow nei bacini montani del Friuli.

L’acqua 6:39–50.

Perla R, Cheng TT, McClung DM (1980) A two-parameter model of snow-avalanche motion. J Glaciol 26:197–207. doi: 10.1017/S002214300001073X

Petrakov D a, Krylenko I V (2007) Debris flow hazard of glacial lakes in the Central Caucasus. Debris-Flow Hazards Mitig Mech Predict Assesment 703–714.

Pierson TC (1986) Flow behavior of channelized debris flows, Mount St. Helens, Washington. Hillslope Process 269–296.

Pierson TC, Costa JE (1987) A rheologic classification of subaerial sediment-water flows. In: Costa JE, Wieczorek GF (eds) Debris Flows/Avalanches. Geological Society of America,

Quinn P, Beven K, Chevallier P (1991) The prediction of hillslope flow paths for distributed hydrological modelling using digital terrain models. Hydrol Process 5:59–79. doi: 10.1002/hyp.3360050106

R Development Core Team (2005) R: A language and environment for statistical computing. Vienna, Austria

Reid ME, Lahusen RG, Baum RL, et al (2012) Real-Time Monitoring of Landslides.

Reid ME, LaHusen RG, Iverson RM (1997) Debris-Flow Initiation Experiments Using Diverse Hydrologic Triggers. In: Cheng-Iung C (ed) Debris-Flow Hazards Mitigation: Mechanics, Prediction and Assessment. American Society of Civil Engineers (ASCE), San Francisco, California, pp 1–11

Rickenmann D (1999) Empirical Relationships for Debris Flows. Landscape 19:47–77. doi: 10.1023/A:1008064220727

Rickenmann D (2016) Methods for the quantitative assessment of channel processes in torrents (steep streams). CRC Press, Taylor and Francis Group, Leiden, Netherlands

Rickenmann D, Laigle D, McArdell BW, Hübl J (2006) Comparison of 2D debris-flow simulation models with field events. Comput Geosci 10:241–264. doi: 10.1007/s10596-005-9021-3

Rickenmann D, Zimmermann M (1993) The 1987 debris flows in Switzerland: documentation and analysis. Geomorphology 8:175–189. doi: 10.1016/0169-555X(93)90036-2

Santi PM, DeWolfe VG, Higgins JD, et al (2008) Sources of debris flow material in burned areas. Geomorphology 96:310–321. doi: 10.1016/j.geomorph.2007.02.022

Santi PM, Mathewson CC (1988) What happens between the scar and the fan? In: Fragaszy RJ (ed) 24th Annual Symposium on Engineering Geology and Soils Engineering. Washington D.C., pp 73–78

Santos R, Menéndez Duarte R (2006) Topographic signature of debris flow dominated channels: implications for hazard assessment. WIT Trans Ecol Environ 90:301–310. doi: 10.2495/DEB060291

Sassa K, Wang GH (2005) Mechanism of landslide-triggered debris flows. In: Jakob M, Hungr O (eds) Debris-Flow Hazards and Related Phenomena. pp 81–104

Scheidl C, Rickenmann D (2010) Empirical prediction of debris-flow mobility and deposition on fans. Earth Surf Process Landforms 35:157–173. doi: 10.1002/esp.1897

Sidle RC, Pearce AJ, O’Loughin CO (1985) Hillslope stability and land use. American Geophysical Union Water

Resources, Washington

Suk P, Klimánek M (2011) Creation of the snow avalanche susceptibility map of the krkonoše mountains using gis. Acta Univ Agric Silvic Mendelianae Brun 59:237–246. doi: 10.11118/actaun201159050237

Swanson FJ (1981) Fire and geomorphic processes. Washington D.C.

Swanston DN, Swanson FJ (1976) Timber harvesting, mass erosion, and steepland forest geomorphology in the Pacific Northwest. Geomorphol Eng 199–221.

Takahashi T (1981) Estimation of potential debris flows and their hazardous zones; soft countermeasures for a disaster. J Nat Disaster Sci 3:57–89.

Takahashi T (2000) Initiation and flow of variuos types of debris flow. In: Wieczorek GF, Naeser (eds) Debris-Flow Hazards Mitigation: Mechanics, Prediction, and Assessment. Rotterdam, pp 15–25

Takahashi T (2007) Debris Flow: Mechanics, Prediction and Countermeasures. Taylor and Francis/Balkema, Leiden, Netherlands

Theule JI, Liébault F, Loye a., et al (2012) Sediment budget monitoring of debris-flow and bedload transport in the Manival Torrent, SE France. Nat Hazards Earth Syst Sci 12:731–749. doi: 10.5194/nhess-12-731-2012

Tognacca C, Bezzola GR (1997) Debris-flow initiation by channel-bed failure. Debris-Flow Hazards Mitigations, Mech Predict Assess 44–53.

Tognacca C, Bezzola GR, Minor H-E (2000) Threshold criterion for debris-flow initiation due to channel-bed failure. In: Wieczorek GF, Naeser (eds) Debris-Flow Hazards Mitigation: Mechanics, Prediction, and Assessment. pp 89–97

VanDine DF (1996) Debris Flow Control Structures for Forest Engineering. British Columbia

Vanzetta A (1987) Relazione tecnica riguardante i lavori di sistemazione idraulico-forestale da eseguirsi nei rivi Riva e Avenes, affluenti del torrente Vizze in comune di Prati di Vizze. Bolzano

Varnes DJ (1954) Landlside types and processes. National Academy of Sciences, Washington D.C.

Varnes DJ (1978) Slope movement types and processes. National Academy of Sciences, Washington D.C.

Whittaker J, Jaggi M (1986) Blockschwellen. Versuchsanstalt für Wasserbau, Hydrologie und Glaziologie, Zurich, Switzerland

Wieczorek GF, Glade T (2005) Climatic factors influencing occurrence of debris flows. In: Jakob M, Hungr O (eds) Debris-flow Hazards and Related Phenomena. Springer Berlin Heidelberg, pp 325–326

Wilson RC, Wieczorek GF (1995) Rainfall Thresholds for the Initiation of Debris Flows at La Honda, California. Environ Eng Geosci I:11–27. doi: https://doi.org/10.2113/gseegeosci.I.1.11

Wischmeier W, Smith DD (1978) Predicting rainfall erosion losses-A guide to conservation planning.

Wu W, Sidle RC (1995) A Distributed Slope Stability Model for Steep Forested Basins. Water Resour Res 31:2097–2110. doi: 10.1029/95WR01136

Xie Y, Yin S qing, Liu B yuan, et al (2016) Models for estimating daily rainfall erosivity in China. J Hydrol

535:547–558. doi: 10.1016/j.jhydrol.2016.02.020

Zimmermann M, Mani P, Gamma (1997) Murganggefahr und Klimaänderung - ein GIS-basierter Ansatz. Schlussbericht Hochschulverlag and der ETH, Zurich, Switzerland

Appendix 1 (of Chapter 3)

Supplementary data: description of the DF/DFD events

- DFD 1/09/2009: this is the first event of the series so we do not have information about previous DF/DFD events.
- DF 25/03/2010: this is the first event of the year; for this reason, the erosion index of the recharge period is relatively high (763.28 MJ mm/ha/h), but the corresponding event volume is not so large (2100 m^3). This can be explained because of the relatively low triggering erosion index (50.6 MJ mm/ha/h).
- DF 11/07/2010: this is one of the events with the largest volume of sediment (12500 m^3); however, the erosion index of the recharge period is not so high (169.24 MJ mm/ha/h), whereas the triggering erosion index is the highest ever calculated among the dataset: 1508.95 MJ mm/ha/h. In this case, the recharge period before the event is 4 months. This is a relatively long time compared with the typical recharge behavior of this catchment. However, the recharge erosion index cannot explain the large mobilized volume. In this case, it seems that the role of the triggering erosion index is more important than the rainfall of the recharge period. Most likely, this is the normal behavior of a catchment characterized by unlimited sediment availability from the source areas.
- DFD 21/07/2010: this event occurred only ten days after the previous one, which mobilized a very large volume. There is no rainfall registered during the recharge period, so the recharge erosion index is 0, although the triggering erosion index is 55.11 MJ mm/ha/h, a value that is high enough for repeated mobilization of sediment in this catchment. Different studies (Bovis and Jakob 1999; Brayshaw and Hassan 2009) concluded that debris flow events leave the catchment in a very unstable state, with a great amount of loose debris along the channel banks and in the triggering zone. For this reason, the triggering of a DF/DFD is more probable immediately after an event, and the triggering probability decreases as the time from the previous event increases. Therefore, the unstable state caused by the previous event, matched with a strong enough rainfall event, resulted in the triggering of this event.
- DFD 9/10/2010: this event is characterized by a relatively small volume (1600 m^3) and relatively low recharge erosion index (186.09 MJ mm/ha/h). Therefore, it follows a

normal trend. Additionally, in this case, it seems that the triggering erosion index plays the most important role and has a value of 269.28 MJ mm/ha/h, which is higher than the recharge index.

- DFD 13/07/2011: this is the first event of the year, so the recharge period is longer than the mean; the consequent recharge erosion index is high, 405.21 MJ mm/ha/h, but the volume of the event is small, 700 m^3. In this case, the triggering can also be explained with the triggering erosion index of 51.47 MJ mm/ha/h, which is however relatively low.
- DFD 5/08/2011: on this day, two different DF/DFD events were registered. In both cases, the recharge erosion index is 0 days because there is no intermediate rainfall since the previous event. Nevertheless, the two triggering erosion indices calculated from the two rainfall events that triggered the two flows are relatively high, 98.67 and 117.43 MJ mm/ha/h, respectively; moreover, the corresponding volumes of these two events are 2800 and 2500 m^3, respectively. In this case, the triggering parameters are more important than the parameters of the recharge period.
- DFD 7/08/2011: this is the typical case in which there is no rainfall since the last event ($EI_{\Delta t\ RECH} = 0$), but the $EI_{\Delta t\ TRIG}$ is 61.66 MJ mm/ha/h and was sufficient to trigger a small debris flood of 350 m^3. In this case, a small volume corresponded to a low erosion index.
- DFD 3/11/2011: in this case, the volume is small (600 m^3), whereas both the recharge and the triggering erosion index are high: 200.56 and 225.61 MJ mm/ha/h, respectively. The small mobilized volume can be explained because of the numerous events that had already occurred in the last months, so there was not much loose debris to trigger a larger event.
- DF 27/06/2012: this is the first event of the year and is characterized by a volume of 4000 m^3, which is not so large considering that the triggering erosion index was 104.3 MJ mm/ha/h. In addition, the recharge erosion index is relatively high, 282.46 MJ mm/ha/h, but this can be explained by the fact that this is the first event of the year so the recharge period was longer than the mean.
- DF 4/07/2012: this is the largest event registered in the catchment, with a volume of 16200 m^3. The recharge erosion index is equal to zero, and this again demonstrates the low importance of the intermediate rainfall. The triggering erosion index is 119.78 MJ

mm/ha/h, which is nearly the mean and thus not as high as could be expected considering the volume. An explanation of this discrepancy can also be the proximity in time with the previous event. Most likely, the last event left the catchment in an unstable state, and at the first strong rainfall event, all the available sediment was mobilized, even if this rainfall event was not one of the strongest.

- DFD 5/07/2012: we have already seen that the typical behavior of this catchment is to have several DF/DFD events in short periods. In this event, the mobilized volume is 1000 m^3, and there is basically no recharge period to identify because the previous event was just the day before and the triggering erosion index is very low at 8.29 MJ mm/ha/h. The only explanation is the existence of unstable conditions following the previous DF/DFD event.
- DFD 5/06/2013: this is the first event of the year, and it has a high recharge erosion index (404.19 MJ mm/ha/h). The triggering rainfall index is relatively low (61.78 MJ mm/ha/h), and this corresponds to a volume of 2100 m^3. Therefore, we can say that this event is average, like the most typical events of the basin.
- DFD 17/06/2013: this event is characterized by a small volume (100 m^3) and has a low recharge and triggering erosion indices: 31.67 and 10.55 MJ mm/ha/h, respectively.
- DFD 23/07/2013: this event is also characterized by a small volume (600 m^3), but this time, the recharge erosion index is 154.3 MJ mm/ha/h, which is relatively high. However, this does not follow a positive correlation with the mobilized sediment, as with all the other debris flood events.
- DFD 27/07/2013: this event occurs only a few days after the previous one and is the third event in less than one month. Therefore, it seems that in this period, the catchment was characterized by a general instability, which caused small and frequent events instead of one single larger event. This event also has a small volume of 450 m^3, and the triggering erosion index is 105.20, which is higher than the identified threshold between triggering and non-triggering.
- DFD 6/09/2013: this is one of the few cases in which the intermediate rainfall of the recharge period plays a more important role than the triggering rainfall. In fact, the recharge erosion index is 326.32 MJ mm/ha/h, showing a great amount of erosive rain processes in the short period since the last event (approximately 40 days). However, the triggering erosion index is very low: 18.4 MJ mm/ha/h.

- DFD 20/07/2014: as every first event of the year, it is characterized by a high recharge erosion index (599.76 MJ mm/ha/h). Nevertheless, the triggering erosion index is 64.77 MJ mm/ha/h, which explains the small volume of the event (1000 m^3).
- DFD 25/07/2014: this event occurs only 5 days after the previous one and has a recharge rainfall index of 0 mm. The triggering erosion index and the volume are similar to the mean values (68.35 MJ mm/ha/h and 1150 m^3, respectively).
- DF 13/08/2014: this is one of the most powerful events, with a volume of 14000 m^3. There is no recharge erosion index because of the lack of precipitation since the last event. The triggering rainfall index is 76.39 MJ mm/ha/h, which is slightly low. Most likely, the previous events that occurred 15-20 days before contributed to "prepare" the catchment for this larger event by mobilizing the sediment, and a great debris flow was triggered the first time that it rained after the earlier events.
- DFD 31/07/2015: this is the only event registered during 2015. Therefore, the recharge erosion index is high, 859.7 MJ mm/ha/h, but the mobilized volume is only 400 m^3. In addition, the triggering erosion index is high: 455.27 MJ mm/ha/h.

  Most likely, considering the lack of other events (that is not the typical behavior of this catchment); this had been a year with a scarcity of available loose sediment, and for this reason, only a very strong rainfall event triggered a torrential event, which was, however, characterized by a small volume.